The Dissertation Committee for Chung-Hsuan Kao
Certifies that this is the approved version of the following dissertation

Growth-regulated Hsp70 phosphorylation regulates stress responses and prion maintenance

APPROVED BY
SUPERVISING COMMITTEE:

Tanya Paull, Supervisor

Jon Huibregtse

Hung-Wen Liu

Andreas Matouschek

Martin Kevorkian

GROWTH-REGULATED HSP70 PHOSPHORYLATION REGULATES STRESS RESPONSES AND PRION MAINTENANCE

by

Chung-Hsuan Kao

Dissertation

Presented to the Faculty of the Graduate School of

The University of Texas at Austin

in Partial Fulfillment

of the Requirements

for the Degree of

Doctor of Philosophy

The University of Texas at Austin

May 2020

Dedication

I dedicate his dissertation to my family (Ching-Hui Kao, Hang-Fen Cheng, George Kao, Freda Chou) and my wife (Yu-Fang Cheng).

Acknowledgements

First, I would like to thank Tanya for her continual support and advice. She has been the most influential mentor and inspiration in my PhD career. I have learned how to become a great researcher from her.

I also want to thank my dissertation committee members: Dr. Jon Huibregtse, Dr. Hung-Wen Liu, Dr. Andreas Matouschek, and Dr. Martin Kevorkian for their valuable comments on my research over the years.

I would also like to thank all past and present members of the Paull lab: Ji-hoon, Rajashree, Nodar, Mike, Suting, Sucheta, Yi, Tanya, Logan, Seung, May, Samantha, Min, Caleb, Oshadi, Yizhi, Lisa, and Julie for being the greatest colleagues. Their suggestions on my project are extremely helpful. I enjoyed every day and every second working with all of you.

Last but not least, I would like to thank my family and friends for their encouragement and support. Without them, I would not have been able to finish this journey. I want to particularly thank my father for being a great life guidance who encouraged me to chase what I like, my mother for teaching me how to face all kinds of situations that happened in our daily life, my brother and sister-in-law for taking great care of my parents while I am not around, and my wife for being a great listener and support in many ways.

GROWTH-REGULATED HSP70 PHOSPHORYLATION REGULATES STRESS RESPONSES AND PRION MAINTENANCE

Chung-Hsuan Kao, Ph D

The University of Texas at Austin, 2020

Supervisor: Tanya Paull

Maintenance of protein homeostasis in eukaryotes during normal growth and stress conditions requires the functions of Hsp70 chaperones and associated co-chaperones. Here we investigate an evolutionarily-conserved serine phosphorylation that occurs at the site of communication between the nucleotide-binding and substrate-binding domains of Hsp70. Ser151 phosphorylation in yeast Hsp70 (Ssa1) is promoted by cyclin-dependent kinase (Cdk1) during normal growth and dramatically affects heat shock responses, a function conserved with HSC70 S153 phosphorylation in human cells. Phospho-mimic forms of Ssa1 (S151D) also fail to relocalize in response to starvation conditions, do not associate *in vivo* with Hsp40 co-chaperones, Ydj1 and Sis1, and do not catalyze refolding of denatured proteins *in vitro* in cooperation with Ydj1 and Hsp104. S151 phosphorylation strongly promotes survival of heavy metal exposure and reduces Sup35-dependent *[PSI$^+$]* prion activity, however, consistent with proposed roles for Ssa1 and Hsp104 in generating self-nucleating seeds of misfolded proteins. Taken together, these results suggest that Cdk1 downregulates Hsp70 function during periods of active

growth, reducing propagation of aggregated proteins despite potential costs to overall chaperone efficiency.

Table of Contents

List of Tables

List of Figures

CHAPTER1: INTRODUCTION

Protein homeostasis is an important system maintaining the functionality of proteins within the cellular environment (1). After nascent polypeptides are synthesized by ribosomes, they are folded into a specific 3-dimensional structure to enable them to execute their biological functions. Mammalian protein biosynthesis, however, may produce incorrectly folded proteins. It is estimated that 30-50% of mammalian proteomes are in metastable states with partially ordered structure (2). Such proteins can accumulate as aggregates with amorphous, oligomeric, or fibrillar structures that are toxic to cells (2). In order to maintain efficient protein folding and prevent protein aggregation, cells have evolved a network of chaperone proteins as a surveillance system for proteome integrity. Disruption of such networks can contribute to the pathology of a number of human diseases, including Alzheimer's, Parkinson's, and prion-related disorders (3).

Molecular chaperones are classified into Hsp70, Hsp90, Hsp110, Hsp40, and small HSP families. The canonical functions of Hsp70s and Hsp90 chaperones are to recognize unfolded protein clients, promote correct folding, and release them after the completion of protein folding. Protein folding requires an ATP/ADP exchange cycle and the assistance of co-chaperones (4). Two major co-chaperones, Hsp110 (nucleotide exchange factors, NEFs) and Hsp40 (DNAJ-related proteins), cooperate with Hsp70s and regulate the exchange between ATP-bound and ADP-bound states (Figure 1.1) (5).

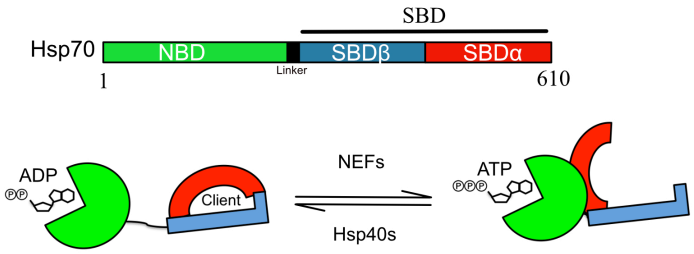

Figure 1.1 Hsp40 and NEF proteins modulate the Hsp70 catalytic cycle.

In the ADP-bound state, the nucleotide-binding domain of Hsp70 (NBD, green) is loosely connected to the substrate binding domain (SBD, red: alpha-helical lid; blue: beta-sheet pocket) via a flexible linker (Protein Data Bank (PDB) code: 3HSC). Hsp70 has a high affinity to the clients. In the ATP-bound state, the NBD interacts with the SBDβ domain that triggers a dramatic conformational change in Hsp70 (PDB: 1DKZ). Hsp70 has a low affinity to the clients.

Hsp70 proteins are highly conserved in all species (6) (Figure 1.2). In *Saccharomyces cerevisiae,* there are four functionally and structurally redundant Hsp70 proteins: Ssa1-4. While Ssa1 and Ssa2 are constitutively expressed similar to human Hsc70, Ssa3 and Ssa4 are induced by heat shock and other forms of stress similar to human Hsp70 (7). Removal of Ssa1-4 is lethal in yeast, but constitutive expression of any single gene can rescue this lethality (8, 9) .

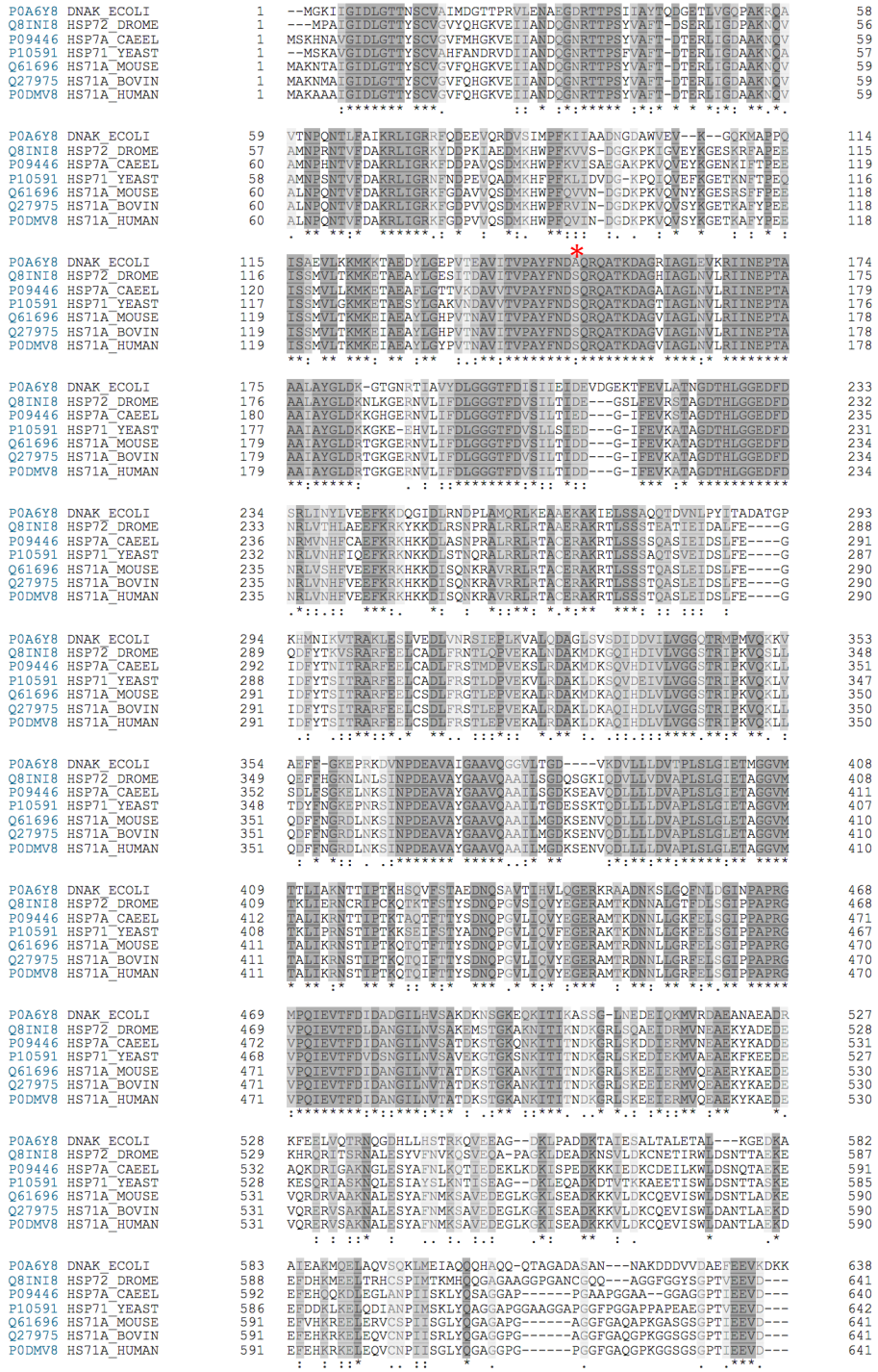

Figure 1.2 Alignment of Hsp70 in different species

Comparison of Hsp70 protein sequences between Escherichia coli (Chaperone protein DnaK, UniProt ID: P0A6Y8), Drosophila melanogaster (Major heatshock 70kDa protein

Ba, UniProt ID: Q8INI8), Caenorhabditis elegans (Heat shock 70kDa protein A, UniProt ID: P09446), Saccharomyces cerevisiae (Heat shock protein SSA1, UniProt ID: P10591), Mus musculus (Heat shock 70kDa protein 1A, UniProt ID: Q61696), Bos taurus (Heat shock 70kDa protein 1A, UniProt ID: Q27975), and Homo sapiens (Heat shock 70kDa protein 1A, UniProt ID: P0DMV8) from UniProt alignment tool (www.uniprot.org/help/sequence-alignments). The gradient of gray color represents the level of similarity.

Hsp70 orthologs in eukaryotes are targets of many post-translational modifications, including several phosphorylation events (10). Yeast Ssa1 has two phosphorylation hotspots: one in the N-terminal nucleotide binding domain (NBD) and C-terminal substrate binding domain (SBD) (Figure 1.3). Some of these phosphorylation events have been characterized and shown to regulate HSP70/SSA-dependent functions including heat shock responses, polysome association, protein refolding, and protein disaggregation (11). There have also been numerous other post-translational modifications observed in HSP70 proteins in eukaryotes (10). Although less well characterized, they may further adjust Hsp70 functionality.

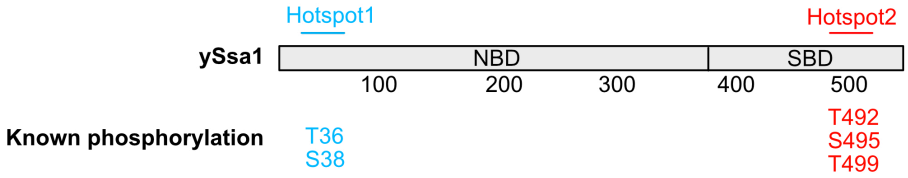

Figure 1.3 Phosphorylation hot spots of Hsp70

Enrichment analysis based on 11 species indicates two phosphorylation hot spots in Hsp70. In yeast Ssa1, there are 4 known phosphorylation sites representing two hot spot regions (11).

Heat Shock Protein 70

Hsp70 was first discovered in drosophila by FM Ritossa (12). One of his lab members accidentally treated the fruit flies with heat shock and observed a puffing pattern in salivary gland polytene chromosomes, indicating significantly increased transcription of an unknown protein under heat stress (13). This phenomenon was later described as the "heat shock" response, which involves increased production of Hsp70 proteins as well as other chaperones. A shift to higher temperature triggers cells to turn on the expression of heat shock genes, while other genes are turned off (14, 15). Hsp70 synthesis is the major cellular event after heat shock, and Hsp70 has been shown to have an essential role in thermotolerance (16, 17). Further studies indicate that Hsp70 can also be induced by ethanol or heavy metals, suggesting a role of Hsp70 in stress responses other than heat (18, 19). The induction of Hsp70 is also important for the tolerance to a variety of stress responses. For example, a mild treatment of ethanol can increase tolerance to later exposure of ethanol and heat stress (20–24). In addition to the role of Hsp70 in stress

responses, the enzyme and its isoforms are also involved in protein homeostasis in the absence of exogenous stress. Eukaryotic Hsp70 is generally classified into two types: heat-inducible Hsp70 and constitutively expressed Hsp70. Different classes of eukaryotic Hsp70s are expressed in specific organelles to perform specific functions (25).

In *Saccharomyces cerevisiae,* there are four major cytosolic Hsp70s: Ssa1-4, as well as organelle-specific Hsp70 proteins such as Ssb in ribosomes and Ssc and Ssq in the mitochondria. While Ssa1 and Ssa2 are constitutively expressed, Ssa3 and Ssa4 are induced by heat shock and other forms of stress (7). The deletion of Ssa1 and Ssa2 leads to slow growth and hypersensitivity at 37°C, indicating that constitutively expressed Hsp70s are able to maintain protein stability under non-stressed conditions. Interestingly, Ssa3/4 are not able to fully complement the deficiency of Ssa1/2 although Ssa3/4 are highly similar to Ssa1/2 in protein sequence and function (8). This indicates that constitutively expressed Ssa1/2 may have additional functions other than heat shock responses (26).

Ssb1 and Ssb2 are the two major Hsp70s localized to ribosomes and are identical to each other functionally (27). Their major role is thought to be cotranslational folding, by participating in the formation of the ribosome-associated complex (RAC) (28). The complex is located next to the ribosomal exit tunnel that is important for Ssb proteins to stabilize and fold nascent polypeptides (29).

In mitochondria, Ssc1, Ssc3, and Ssq1 are three major Hsp70s responsible for the translocation and protein folding of mitochondrial proteins. Ssc1 directly cooperates with the transporter inner membrane complex (TIM) to promote precursor protein movement

from the transporter outer membrane complex (TOM) to the mitochondrial matrix. Previous studies have shown that Ssc1 is associated with Tim44 and promotes substrate translocation (30). Ssc3 is highly similar to Ssc1 in protein sequence. However, Ssc3 functions only partially overlap with the Ssc1 functions, and Ssc3 has an additional function in cell wall formation that is not characterized (31, 32). Ssq1 is another mitochondrial Hsp70 homolog that is 52% identical to Ssc1. Ssc1 and Ssq1 have overlapping functions in cold shock resistance since Ssc1 can partially rescue the cell growth of Ssq1-deleted cells exposed to cold shock (33). However, Ssq1 fails to rescue Δ*ssc1* in cell growth and protein translocation under the nonpermissive temperature (34). The defects might be due to that Ssq1 is not able to associate with Tim44. Surprisingly, Ssq1 has been proven to be important in iron biogenesis in budding yeast (35). From this and other evidence, it is clear that Hsp70 isoforms are critical for stress but also play important roles under nonstressed conditions. The structure and regulation of Hsp70 isoforms provide valuable insights into Hsp70 functions, as discussed below.

Heat Shock Transcription Factor

In response to heat shock, the induction of heat shock proteins is transcriptionally regulated by heat shock transcription factor (Hsf). With many stress conditions such as heat shock or oxidative stress, cells are able to transcriptionally induce more cytosolic chaperones (Human Hsp70 and yeast Ssa3-4) to protect protein conformation and decrease protein aggregation (7). While there is a family of four Hsf proteins in vertebrates and plants, *Saccharomyces cerevisiae* and other invertebrates only have one Hsf (Hsf1). The DNA-binding domain (DBD), leucine zipper (LZ), and carboxy-terminal

transactivation domain (CTA) are three conserved domains of Hsf1 in different species. In yeast, there is an additional transcriptional activation domain at the N-terminus (NTA) (Figure 1.4A) (36). The main function of Hsf1 is to bind to heat shock elements (HSEs) composed of inverted pentameric repeats with the sequence of xGAAx (x represents any nucleotide) and promote downstream heat shock gene expression (37, 38).

The regulation of Hsf1 activity is also different between species. For metazoan and human Hsf1, the activation requires trimerization, nuclear translocation, DNA binding, and posttranslational modifications. In budding yeast, Hsf1 constitutively binds to HSEs in a trimer architecture under non-stressed conditions and both transactivation domains (NTA and CTA) are bound and inhibited by Ssa1/2. Heat shock generates misfolded proteins that compete with Hsf1 for the binding of Ssa1/2, which releases Hsf1 to transcribe HSE-driven genes that generate higher levels of Ssa3/4 as well as the repression of ribosomal proteins (39–41) (Fig 1.4B).

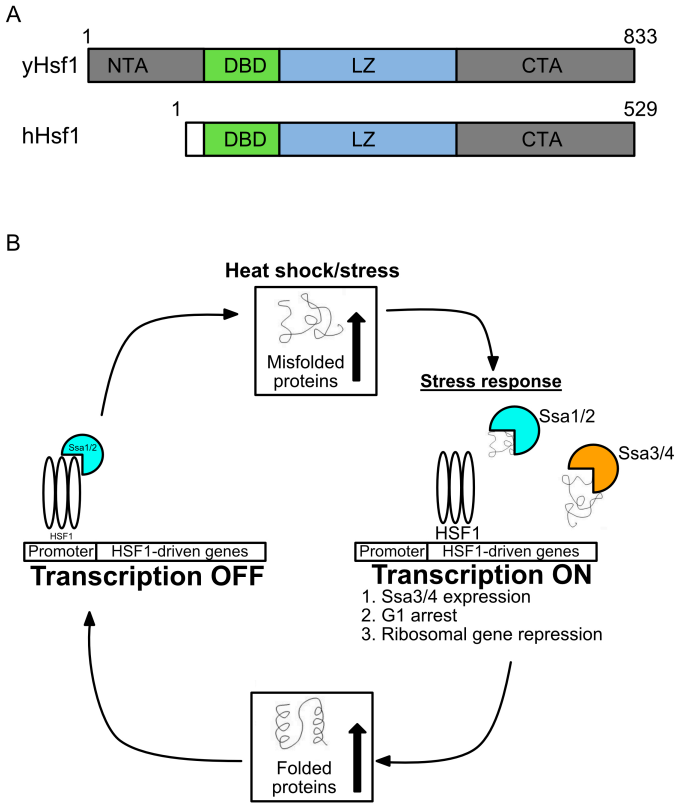

Figure 1.4 Domain structure and functions of heat shock transcription factor.

A. Schematic of the domain structure of yeast and human Hsf1 monomer. B. Diagram of the role of Hsf1 in the stress response. Increased misfoled proteins draw away the binding of Ssa1 on Hsf1 trimer that promotes HSF1-driven genes expression. Ssa1 binds to Hsf1 trimer to inhibit the transcription when the concentration of misfolded proteins is decreased.

Hsp70 Domains

There are many conserved Hsp70 isoforms in different species, and they share similar domains that perform ATP hydrolysis-dependent protein folding. Hsp70 includes 3 major

domains: the N-terminal nucleotide binding domain (NBD), a linker region, and the C-terminal substrate binding domain (SBD) (Figure 1.1).

The NBD is a ~ 40 kDa V-shaped structure, similar in shape to a cleft, that functions in nucleotide binding. It has 2 lobes and each lobe has 2 subdomains named IA, IB, IIA, and IIB (42). The two arms in the V-shaped structure are composed of IA-IB and IIA-IIB separately. Different subdomains are responsible for specific interactions with the α-phosphate, β-phosphate, and γ-phosphate from the ATP nucleotide. Previous crystallography results indicate that the structure orientation in Hsp70 NBD is similar to actin (43–48) (Figure 1.5).

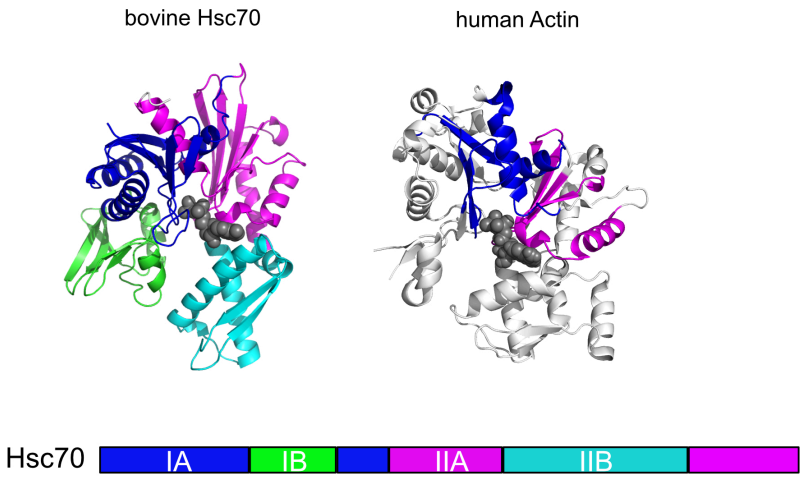

Figure 1.5 Structures of nucleotide binding domain in actin and Hsc70

Compare the structure orientation of nucleotide binding domain between ADP-bound bovine Hsc70 (PDB code: 3HSC) and ADP-bound human Actin (PDB code: 4PKH) (49, 50). Each subdomain of bovine Hsc70 is indicated in blue (IA subdomain), green (IB subdomain), magenta (IIA subdomain), and cyan (IIB subdomain). The color in human Actin corresponds a conserved motif to the subdomain in bovine Hsc70 with similar structure orientation. ADP is indicated in gray color for both proteins.

The hydrophobic linker region consists of a highly conserved 10-12 residues between the Hsp70 NBD and SBD domains. The conserved sequence has a characteristic D/E-V/I/L-L-L-D-V-*-P as observed in different species (51). The region is not only the bridge between NBD and SBD, but also important in transferring the allosteric signal of Hsp70 conformational change from NBD to SBD. Previous studies have shown that the presence of conserved linker sequence dramatically affects ATP hydrolysis efficiency and SBD mobility (52, 53).

The SBD is a ~ 25 kD basket-shaped structure composed of 2 subdomains: the alpha-helical lid (SBDα) and the beta-sheet pocket (SBDβ), which function in potential client protein docking (42, 54, 55) (Figure 1.6). The SBDβ pocket within 2 antiparallel β-sheets surrounds protein clients and displays a high affinity for 5- to 7- amino acid motifs enriched in hydrophobic residues such as Leucine (2, 56). The SBD also includes the SBDα lid which cooperates with the SBDβ pocket and constructs the "open" and "closed" states for the release of protein clients and binding in Hsp70 (Figure 1.6). The open and closed states in the SBD are controlled by the nucleotide binding state of the NBD. Since the distance between the NBD and the SBD is more than 50 Å, the allosteric communication between the nucleotide binding cleft in the NBD and the substrate binding cleft in the SBD becomes critical in protein refolding (54). In order to fully understand the allosteric mechanism in Hsp70 functional cycle, we will further discuss recent discoveries of Hsp70 structure in the next section.

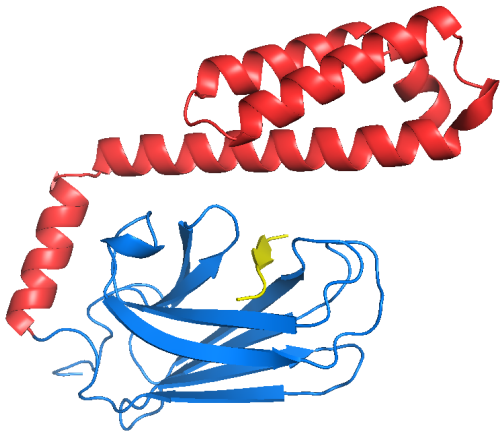

Figure 1.6 Structures of substrate binding domain in DnaK

Substrate binding domain of bacterial Hsp70 is composed SBDβ pocket (blue) and SBDα lid (red). Substrate peptide (NLLLTG) is indicated by yellow color (PDB code: 1DKZ) (56).

Hsp70 Structure

In order to understand how allosteric communication between NBD and SBD regulates the functionality of Hsp70, structural analysis can be used to study its dynamic orientation. Yet, there are several technical issues when using X-ray crystallography, nuclear magnetic resonance (NMR), and other biophysical techniques to study the structure of Hsp70. Some of challenges involve the tendency of ATP-bound Hsp70, ADP-bound Hsp70, and Hsp70 without protein clients to aggregate. Other challenges are due to the limitations of the techniques. For NMR, Hsp70 with multiple domains is classified as a "large" protein that exceeds the capability of NMR. For X-ray crystallography, the dynamic nature of Hsp70 conformations also hampers the crystallization step. One of the most interesting questions for an allosteric regulation is

the interaction between different domains, and thus requires observation of both domains at the same time. With all the challenges mentioned above, researchers were initially only able to analyze isolated SBD and NBD domains (47, 56–61). A decade ago, there were a few Hsp70 structures reported that included both NBD and SBD; however, the proteins were either mutated or truncated (62–64). A breakthrough happened in 2009, as Zuiderweg's group solved the structure of ADP-bound Hsp70 with the peptide NRLLLTG by a combined analysis including X-ray crystallography and NMR (65). Consistent with previous studies, all results indicated an absence of communication between NBD and SBD in the ADP-bound state (53, 65, 66) (Figure 1.7). The interaction between NBD and SBD, therefore, might exist in the ATP-bound state.

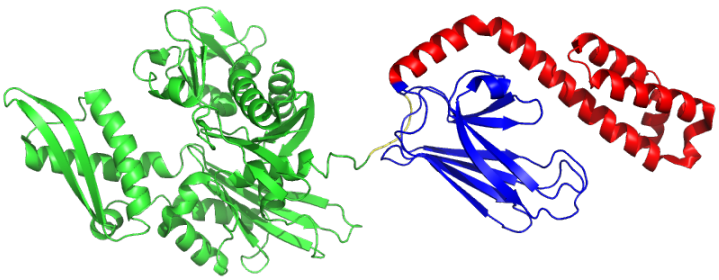

Figure 1.7 Three-dimensional structure of ADP-bound bacterial Hsp70

ADP-bound DnaK has less communication between the NBD (green) and the SBD (Red: lid domain, Blue: pocket domain). (PDB code: 2KHO) (65). The linker is indicated in yellow color.

The first evidence of domain interaction is in fact from the structure of Sse1 (67) (*S. cerevisiae* homologue of mammalian Hsp110) which functions as a yeast co-chaperone

(Nucleotide exchanged factor, NEF). In addition to the role as NEF, Sse1is also a "holdase" that binds to unfolded peptides in order to maintain their stability by preventing misfolding or aggregation (68). According to the evolutionary relationship between Hsp70 and Hsp110/Sse1, their functions have diverged but the protein similarity has preserved. The structural analysis from Hendrickson and colleagues indicates that the conformation of Sse1 NBD with ATP is highly similar to Hsc70 NBD with ATP (67). However, the structural conformation of Sse1 SBD with ATP is dramatically different from DnaK SBD in the ADP-bound state that binds to heptapeptide NRLLLTG. Multiple domain interactions: NBD-Linker, NBD-SBDβ, and NBD-SBDα have been discovered in the structural analysis of Sse1 with ATP. It is suggested that the structure of Hsp110/Sse1 with ATP might be used to approximate the structure of Hsp70 with ATP. (67).

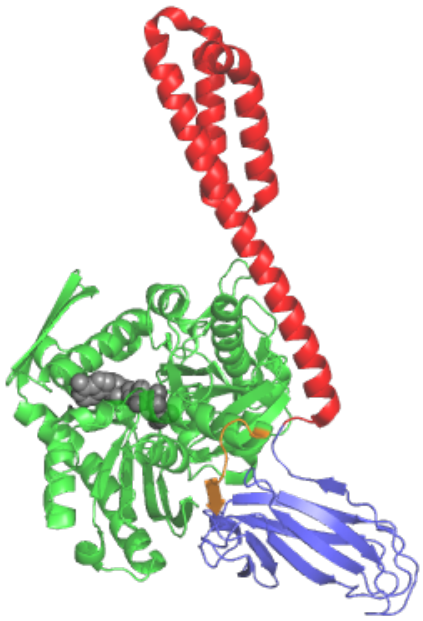

Figure 1.8 Three-dimensional structure of ATP-bound bacterial Hsp70

The NBD domain of Hsp70 (green) with ATP (gray) interacts with both lid (red) and pocket (blue) regions of SBD domain (PDB code: 4B9Q) (69).

In 2012, Mayer's group first discovered the structure of ATP-bound DnaK (*E. coli* homologue of mammalian Hsp70) by disulfide-stabilized conformation (69) (Figure 1.8). The structure clearly shows that SBD docks with the NBD where the complex has low affinity for its clients and the interacting surface between the NBD and the SBD is only ~3 Å away. Other groups further confirmed the interaction between NDB and the SBD of ATP-bound Hsp70 by methyl transverse relaxation optimized spectroscopy (methyl TROSY) NMR and ATP-deficient mutants (70, 71). Such recent structural discoveries explain the dynamic allosteric mechanism of Hsp70 such that ATP-binding by Hsp70 forces drastic conformational changes by increasing the interaction between

NBD, linker region, and SBD. ADP or ATP is mainly bound to NBD between IB and IIB subdomains that coordinate the structure orientation of the rest of subdomains. Previous NMR studies have proven that ATP-bound NBD triggers the re-orientations in NBD and results a new interaction surface between linker region and subdomain IIA of the NBD (52). In addition, the highly dynamic lid domain of SBD is detached from the pocket domain of SBD and further associates with the NBD (72). Among the pocket domains of SBD, β5, β7, and β8 are proven to be central hub regulating allosteric orientation in the βSBD by NMR perturbation studies (73). ATP-bound NBD promotes the disassociation within β5/β7/β8 that triggers a change from a high substrate binding affinity conformation to a low substrate binding affinity conformation (69, 70, 74). The binding of ATP establishes a catalytic cycle dependency on the nucleotide binding. Furthermore, the cycle is further regulated by 2 groups of co-factors: J-domain containing proteins (Hsp40s) and nucleotide-exchange factors (NEFs). Both regulators provide the specificity and variability in Hsp70 function that are similar to GTPase-activating proteins (GAPs) and Guanine nucleotide exchange factors (GEFs) in G-protein function (7) (Figure 1.9).

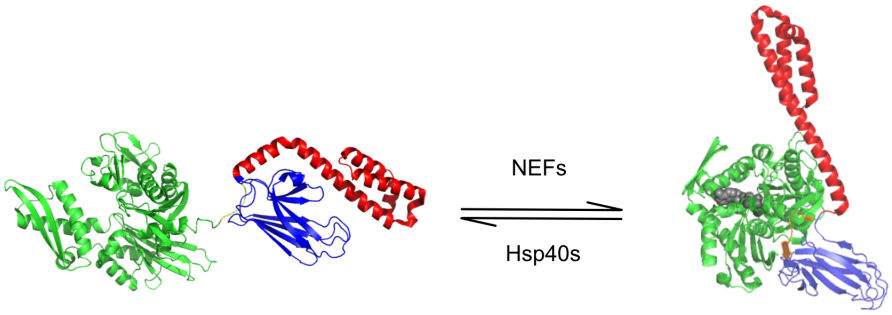

Figure 1.9 Hsp40 and NEF proteins modulate the Hsp70 catalytic cycle.

In the ADP-bound state, the nucleotide-binding domain of Hsp70 (NBD, green) is loosely connected to the substrate binding domain (SBD, red: alpha-helical lid; blue: beta-sheet pocket) via a flexible linker (PDB: 2KHO) (65). In the ATP-bound state, the NBD interacts with the SBDβ domain that triggers a dramatic conformational change in Hsp70 (PDB: 4B9Q) (69).

Heat Shock Protein 40

The important functions of the Hsp40 family in the catalytic cycle of HSP70 enzymes are their roles in escorting clients to Hsp70 and accelerating HSP70 ATP hydrolysis (75–77) (Fig 1.1). All members of the Hsp40 family have similar molecular masses of around 40kDa and contain J-domain modules, as first discovered in DnaJ (*E. coli* homologue of mammalian Hsp40) (5). J-domain modules include 4-helix bundles and an invariable histidine-proline-aspartic acid (HPD) motif which plays a critical role in the interaction with Hsp70 (78). Further study indicates that the HPD motif of J-domain inserts into the Hsp70 NBD and promotes the necessary conformational changes for substrate binding (79) (Figure 1.10).

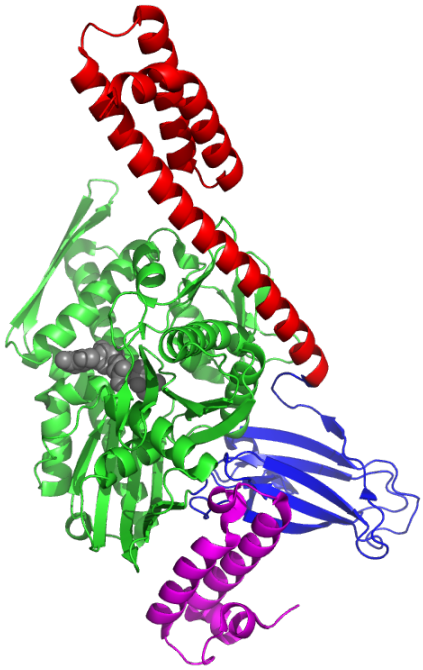

Figure 1.10 The interaction between ATP-bound Hsp70 and Hsp40

DnaJ (magenta) interacts with the NBD and the βSBD of ATP-bound DnaK (PDB code: 5NRO) (80).

In bacteria, DnaJ is the only Hsp40 which recognizes different types of substrates for Hsp70. The number of Hsp40 proteins is significantly increased in eukaryotes, in addition to the diversification of the family members, presumably in order to recognize a wide variety of substrates. In yeast cells, there are 13 cytosolic Hsp40s and each contains conserved domain architecture. Different Hsp40s have their independent downstream clients and also have some overlapped clients. Ydj1, Sis1, Caj1, Djp1, Xdj1, and Apj1 bind to many clients, but Jjj1, Jjj3, Cwc23, and Swa2 only bind to selective clients. Interestingly, Zuo1 and Hlj1 don't bind to clients (81). Among the family of Hsp40

enzymes, Ydj1 and Sis1 are the most abundant and well-studied Hsp40s in yeast cells (82). They both share similar functional modules: the J-domain, Gly-Phe-rich region (G/F), carboxyl-terminal domains (CTDs), and dimerization domain (83, 84) (Figure 1.11). The major function of the CTD domain in J proteins is substrate binding. The deletion of CTDs in Ydj1 or Sis1 can be tolerated, while the deficiency of CTDs in both proteins is lethal. An additional role of CTDs is to maintain the stability of Hsp40 dimerization (85). Similar to all other Hsp40s, Ydj1 and Sis1 form dimers by the dimerization domain in order to promote Hsp70 functions. Major differences between Ydj1 and Sis1 are that Ydj1 has a zinc-finger like region (ZFR) inserted in CTD domain while Sis1 has a Gly-Met-rich region (G/M) (86). ZFR has been proven to be important in modulating substrate transfer to Hsp70 (87), while the G/M region in Sis1 has a redundant role of G/F region related to prion propagation and maintenance (88). Previous studies have shown that Ydj1 and Sis1 have distinct substrate preferences and different stimulatory mechanism with Hsp70 proteins. They compare the substrate binding and refolding activity of Hsp70 in two chimeras that contained substrate binding domains of Sis1 and Ydj1 exchanged with each other. The results indicate that the substrate binding profiles are significantly different in these two chimeras (89–91). It is thus suggested that Ydj1 and Sis1 are responsible for different classes of clients and that have important roles in substrate recognition in the Hsp70 catalytic cycle.

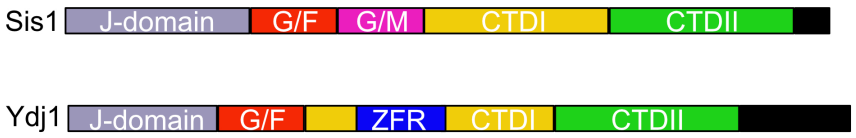

Figure 1.11 Schematic comparison of yeast Sis1 and Ydj1

Sis1 and Ydj1 both include conserved J-domains (light blue), as well as G/F (red), CTDI (yellow), CTDII (green), and dimerization motifs (black). The G/M (magenta) is a unique domain for Sis1 and the ZFR (blue) is a unique domain for Ydj1 (85).

In human cells, there are ~50 Hsp40 genes, classified into A and B classes (2). The difference between these two classes is similar to the difference between yeast Ydj1 and Sis1. In addition to their roles in direct regulation of Hsp70, the co-chaperone system has built a cooperative network between different Hsp40s to enhance protein disaggregation efficiency (92). For example, Bukau's group used recombinant human proteins in an *in vitro* system to show that the heterodimer of class A and B Hsp40s can enhance reactivation of denatured luciferase by 2.5 ~ 3 fold with Hsp70 and Hsp110, when compared to class A or class B Hsp40 added independently to Hsp70/Hsp110.

Nucleotide Exchange Factors (NEFs)

NEFs complete the catalytic cycle of Hsp70 by promoting the exchange of ADP to ATP that drives the conformational change of Hsp70 from the substrate-binding state to the substrate-releasing state (Figure 1.1). GrpE is the only NEF for DnaK in bacteria; however, there is no direct homologue in eukaryotes (47, 93). Instead, eukaryotic cells

have several structurally unrelated NEFs including Hsp110, HsBP1, and Bcl-2-asociated athanogene (BAG) domain proteins (Figure 1.12).

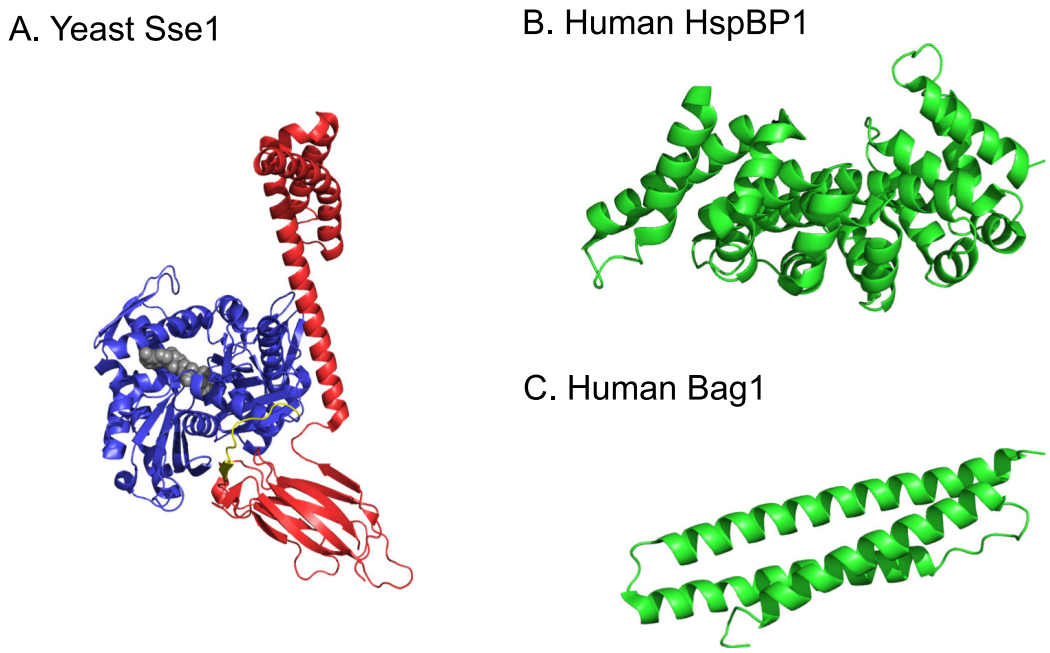

Figure 1.12 Structure of nucleotide exchange factors

A. Yeast Sse1 has similar domains and structure as Hsp70. In ATP (gray)-bound Sse1, the NDB (blue) also interacts to SBD (red) similar to ATP-bound Hsp70 (PDB code: 3D2F) (94). B. and C. Human HspBP1 (PDB code: 1XQS) and Bag1 (PDB code: 1HX1) both have very different structures compared to yeast Sse1 or to each other (44, 45).

The Hsp110 family includes 2 Hsp70 homologs in budding yeast: Sse1 and Sse2. HSPH1 and HSPH2 are the corresponding homologues in human cells. The structure of Sse1/2 is highly similar to Hsp70 except for the insertion region in the SBD and the

extension region at the C-terminus (67). The function of NEFs, however, is quite different from that of Hsp70 proteins.

Although Sse1/2 can bind ATP, ATP hydrolysis is significantly lower than the activity in Hsp70 (Raviol, 2006). The mutants that abolish ATPase activity (D8N, K69Q, D174N, D203N) can still complement the temperature sensitivity in cells lacked of Sse1 and lethality in cells lacked of both Sse1 and Sse2 (Lance Shaner, JBC, 2004), thus the catalytic cycle of Sse1 may not be critical in yeast cells. In addition, Hsp110s can prevent denatured proteins from aggregating but they fails to perform refolding activity. Hsp70 requires nucleotide to trigger substrate binding and refolding, while Sse1/2 is a holdase that maintains substrates in a state for further refolding (95).

Although budding yeast Sse1 and Sse2 are 70% identical to each other, their protein expression patterns are quite different. Sse1 is constitutively expressed and 10-fold more abundant than Sse2 under normal conditions (82). In contrast, Sse2 is highly induced under stress conditions, including heat shock and starvation (96). Both Sse1 and Sse2 are present in heterodimeric complexes with Ssa1 and Ssb1 (97, 98). Further studies have identified and characterized the binding interface between Sse1 NBD and Hsp70 (46, 94, 99–101). The interaction moves IIb subdomain of NBD and opens up the nucleotide cleft for ADP/ATP exchange (47, 94, 100). Fes1 (*S. cerevisiae* NEF homologue of mammalian HspBP1) and Snl1 (*S. cerevisiae* NEF homologue of mammalian Bag1) are also important NEFs. They can also interact with Hsp70s and promote substrate release (102–104).

Heat Shock Protein 100

The Hsp100 chaperone family is responsible for remodeling disordered or misfolded proteins and toxic aggregates (e.g., amyloids). This process also involves different classes of heat shock proteins through formation of a disaggregase complex (105). Hsp100 proteins have been discovered in multiple species, including bacterial ClpB, plant Hsp101, and budding yeast Hsp104; yet there are no clear homologs identified in humans and metazoans. In the absence of a powerful disaggrease in these two species, it has been shown that the system has developed mixed-class Hsp40 complexes combined with Hsp70 to perform protein disaggregation (92).

Hsp100 proteins belong to the AAA+ ATPase superfamily defined by a hexametric ring structure of monomers, each containing a AAA+ domain. The structure forms a tunnel-like channel allowing polypeptides to enter, while ATP hydrolysis within the AAA+ domain drives conformational changes for threading polypeptides through the channel by a mechanical action (106). Each monomer consists of 3 functional regions: N-terminal (NTD), AAA+ domain (NBD1 and NBD2), middle (MD), and C-terminal (CTD) domains (107–109) (Figure 1.13). The NTD is required for substrate interaction and for controlling substrate access to the central channel. The MD has an extended 85-90 Å long coiled-coil structure forming a propeller-like structure (107, 108, 110). Multiple groups using structural analysis have shown that the coiled-coil structure is critical for Hsp100 to interact with Hsp70 (106, 110, 111). The CTD plays a role in substrate exit and has a tetratricopeptide repeat (TPR) domain known to be a binding motif for Hsp70 (112, 113).

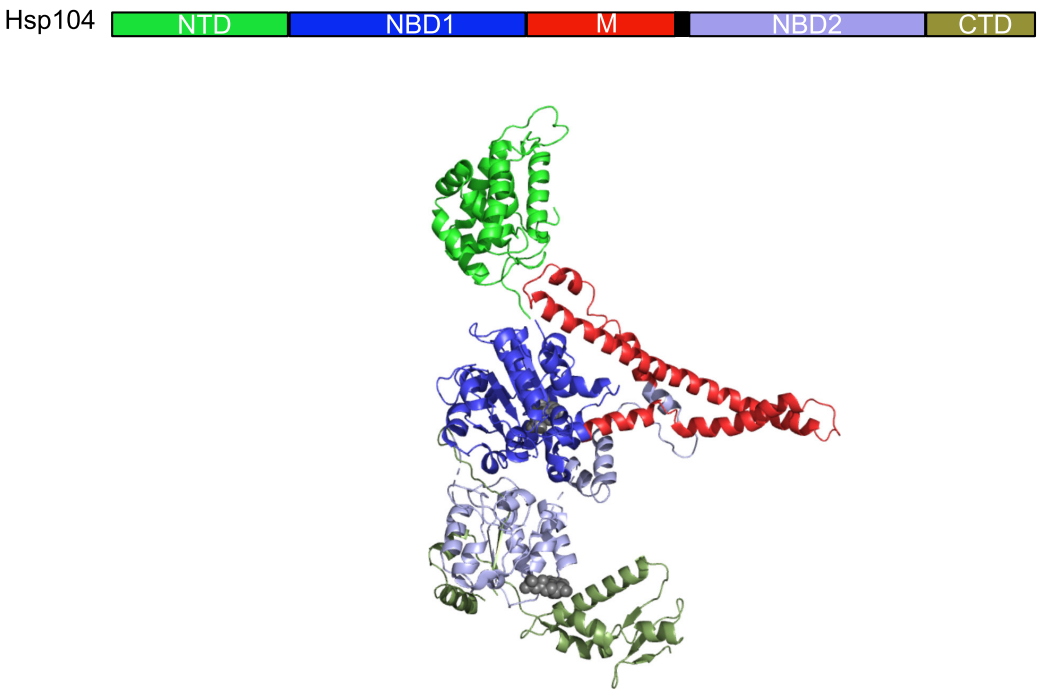

Figure 1.13 Structure and domain of monomeric Hsp104 chaperone family

Top: Schematic domain structure of yeast Hsp104. Bottom: Three-dimensional structure of Hsp104 including the NTD domain (green, PDB code: 5U2U) generated separately and NBD1 (blue), M (red), NBD2 (light blue), and CTD (smudge) domains (PDB code: 5D4W) (114, 115).

Hsp104 is an inducible yeast disaggregase under stress conditions, including heat, metal, and ethanol (116). The deletion of Hsp104 has no effect under normal growth conditions; however, it plays a critical role in coping with lethal high temperature. Previous literature demonstrated that Ssa1 together with the Hsp40 co-chaperone Ydj1, are able to refold misfolded proteins and prevent the formation of large aggregates (2, 105, 117). In addition, Hsp104 is responsible to extract polypeptides from protein aggregates by cooperating with Ssa1 and Ydj1 (106).

Hsp104 also plays an important role in the regulation of infectious proteins with amyloid structure such as prions. In yeast, there are three major prions: [*PSI*+] formed by Sup35 proteins, [*URE3*] formed by Ure2 proteins, and [*PIN*+] formed by Rnq1 proteins (118). Previous study indicates that Hsp104 directly participates in the mechanism of curing prions. Hsp104 overproduction regulated by Hsp90 and its co-factor Sti1 is able to cure [*PSI*+], regulated by the N-terminus of Hsp104 (119–121). However, [*PSI*+] seed formation for prion propagation also requires Hsp70 and Hsp40 to cooperate with Hsp104. The complex of Hsp70, Hsp40, and Hsp104 is able to extract prion monomers from the amyloid filament, which seeds new filaments and ultimately promotes prion propagation (122). The idea that misfolded proteins can form seeds that communicate misfolding to other, non aggregated protein species is common to both prions as well as the nascent proteins exposed to heavy metals (123, 124). In this sense, optimal chaperone function could be non-productive as it can generate new seeds from aggregated species and produce misfolded protein complexes at much higher rates compared to rates in the absence of chaperones.

The Proteostasis Network

A well-balanced proteostasis network is critical for functional protein maintenance, and dysregulation of this network is implicated in aging and in many human diseases (1, 2, 42). The network is composed of protein synthesis, protein folding, protein disaggregation, and protein degradation in order to regulate the quality of protein conformation. Multiple molecular chaperones and their co-chaperones cooperate with

each other and are required for a balanced proteostasis network. Cells use different classes of chaperones to maintain active protein conformations in the cytosolic environment and in specific organelles. In eukaryotes, ribosomal chaperones manage de novo folding by forming the nascent chain-associated complex (NAC)/ribosome-associated complex (RAC) (Trigger factor in bacteria) next to the exit site for nascent polypeptides on ribosomes. Proteins released from the ribosome are also maintained in a functionally active conformation by numerous cytosolic chaperones (Human Hsc70 and yeast Ssa1-2). In addition to their role in protein synthesis, molecular chaperones also participate in the removal of nonfunctional proteins, misfolded proteins, or aggregated proteins (42). In eukaryotic cells, protein aggregates with amorphous or oligomeric structures can be disaggregated by molecular chaperones and transferred to the Ubiquitin-proteosome system (UPS) for degradation. The other important degradation system is autophagy, including chaperone-mediated autophagy (CMA), endosomal microautophagy, and macroautophagy. In contrast to the proteasome in the UPS, the autophagy pathways involve lysosomal degradation and degrade long-lived protein aggregates/organelles (125). In order to regulate an increasing proteome complexity and adapt to a variety of stress conditions in mammalian cells, there are ~1400 components (including chaperones and co-chaperones) in the protein homeostasis system. Proteins are distributed within three biological pathways, including protein biogenesis (~400), conformational maintenance (~300), and degradation (~700) (1). The communication between those branches is particularly important when cells are undergoing stress responses and the unfolded protein response (UPR).

Protein Aggregation and Neurodegenerative Disease

Many neurodegenerative diseases are related to declined proteostasis, which is also associated with aging. It is still unclear how aging is able to compromise the ability of proteostasis network, yet age is a known risk factor for neurodegeneration and is associated with protein aggregation (1). Aggregated proteins are connected to neurodegenerative diseases such as amyloid and Tau in Alzheimer's disease, α-synuclin in Parkinson's disease, ataxin-1 in polyglutamine disease, and huntingtin in Huntington's disease (2, 126).

Polypeptides require proper folding to acquire unique three-dimensional structure and become functional proteins. However, polypeptides are often in a misfolded or unfolded conformation (2). These metastable proteins can easily initiate protein aggregation. The stability of protein conformations is dependent on amino acid sequence and/or environmental factors (127). Mutations from single-nucleotide polymorphisms (SNP) and/or environmental factors can increase the instability of protein conformations, and covalent modifications such as oxidation, phosphorylation, SUMOylation, and ubiquitination have also been implicated in neurodegenerative diseases (128). For instance, both oxidative and phosphorylation modifications on the α-synuclein protein have been strongly involved in aging and Parkinson's disease (129, 130). In polyglutamine-associated disease, phosphorylation of ataxin-1 has been proven to cause inclusion formation and degeneration of Purkinje neurons (131). In addition, removal of SUMOylation and ubiquitination on huntingtin protein is able to reduce the pathology in Huntington's disease (132).

Abnormal and unstable protein conformation induced by different covalent modifications initiates the complicated process of protein aggregation (128). Amorphous aggregates are formed as metastable proteins expose hydrophobic regions to aqueous environment and they are considered to be an early precursor of protein aggregates (133). Forming oligomeric β-sheet structures may stabilize these unstable precursor proteins and generate an intermediate species that has been hypothesized to be more toxic than precursor proteins or inclusions (126). With the incorporation with additional monomers, intermediate oligomers can develop into amyloid fibrils that are thermodynamically the most stable conformation (2). The fibril structure composed of aberrant β-sheet structures results in non-crystalline, insoluble aggregates (134, 135). Different forms of protein aggregates may produce abnormal three-dimensional structures and lead to different levels of toxicity (136, 137). Each stage of aggregate with different accessibility to molecular chaperones can be involved in the corresponding downstream pathways for resolving aggregates. Both amorphous aggregates and oligomers can be reversed back to metastable proteins or processed by protein degradation pathways, while insoluble amyloid fibrils can only be processed by protein degradation pathways.

Chaperone Phosphorylation

Chaperone induction during stress responses has been widely investigated since the discovery of the heat shock response (138) and also because upregulated chaperone expression is discovered in a wide variety of cancers (139). However, it is still not clear how chaperones are regulated in response to stress conditions. As mass spectrometry and biochemical tools have improved extensively in the past 10 years, more uncharacterized

PTMs on Hsp70 have been identified (10). Most of their mechanisms, however, are still unclear and only a few studies have elucidated the functional influence of specific protein modifications. Interestingly, a proposed model inspired by histone modification codes suggests that combinations of PTMs in Hsp70 might further explain its diverse functionalities (10).

Among all the different PTMs on Hsp70, phosphorylation has been identified most frequently compared to acetylation, ubiquitination, and methylation. Beltrao's group has indicated 313 phosphorylation sites on Hsp70 across 11 species by enrichment analysis and further identifies 2 phosphorylation hot spots related to canonical Hsp70 functions (11). Together with other evidence, we know that Hsp70 phosphorylation is able to regulate cell cycle progression (140–142), cellular resistance to chemotherapeutic drugs (143), control of apoptosis (144), Hsp70 dimerization (145), and Hsp70-mediated protein degradation (146). In the traditional model, Hsp70 expression level is increased under stress conditions in order to maintain protein conformation by protein folding. In addition, it is possible that different stress stimuli can alter Hsp70 phosphorylation and possibly combine different phosphorylation marks to regulate cellular responses in normal cells (139).

Hypothesis and Goals

Hsp70 dynamically folds a variety of clients and protect protein homeostasis through regulation of protein aggregation and degradation. The allosteric communication between NBD and SBD is dependent on the interaction interface between these two domains. However, it is not clear whether PTMs are required in this dynamic regulation of Hsp70.

We hypothesize that different PTMs may regulate the conformation and catalytic cycle of Hsp70 individually or collaboratively. The regulation may further affect the downstream functions of Hsp70 in co-chaperone binding, clients selection, and cooperation with other chaperone systems. Here we investigated the role of Ssa1/Hsc70 phosphorylation at S151(S153) during normal growth as well as stress conditions. We find that Ssa1 S151 phosphorylation is promoted by Cdk1 activity during logarithmic growth, and that this modification negatively regulates survival of heat exposure as well as starvation conditions. Ssa1 phosphorylation at S151 alters the interaction with Hsp40 co-chaperones that further impact the formation and function of Hsp104-dependent disaggregase complexes. Localization patterns of Ssa1 and Hsc70 in response to heat stress are also very sensitive to S151(S153) modification, as is the maintenance of the *[PSI+]* prion in budding yeast. Thus CDK1 appears to control many aspects of Ssa1/Hsc70 function, and may regulate the ability of prions to affect gene expression.

CHAPTER 2: MATERIALS AND METHODS

Yeast Strains and Plasmids

Yeast strains and plasmids used in this study are listed in Table 2.1 and Table 2.2. *S. cerevisiae* yeast cultures were grown in synthetic minimal defined media (0.67% yeast nitrogen base without amino acids, ammonium sulfate, and appropriate amino acids) with 2% glucose or YPAD media (1% yeast extract, 2% Becto peptone, 0.004% Adenine Hemisulfate) with 2% glucose. pESC-URA-GFP-Ubc9ts was a gift from Judith Frydman (Addgene plasmid # 20369 ; http://n2t.net/addgene:20369 ; RRID:Addgene_20369) (147). HSP104-b/Leu(WT) was a gift from Susan Lindquist (Addgene plasmid # 1156 ; http://n2t.net/addgene:1156 ; RRID:Addgene_1156) (148). 5787 pET28aSX104B/ pES42 was a gift from Susan Lindquist (Addgene plasmid # 1229 ; http://n2t.net/addgene:1229 ; RRID:Addgene_1229) (149). pRS315-*SSA1* and pDP122 were gifts from Daniel Masison and David Pincus, respectively.

Name	Yeast genotype	Plasmid	Source
TP5957	MH272 3f MATalpha ura3 leu2 ade2 his3 HMLa rme1 GAL+ *ssa1*::TRP1 *ssa2 ssa3 ssa4*	YCP lac33-*SSA1*	Sabine Rospert
TP8435	TP5957	YCP lac33-*SSA1* + pTP4108	this study
TP8436	TP5957	YCP lac33-*SSA1* + pTP4109	this study
TP8437	TP5957	YCP lac33-*SSA1* + pTP4110	this study
TP8724	TP5957	YCP lac33-*SSA1* + pTP4241	this study
TP8725	TP5957	YCP lac33-*SSA1* + pTP4242	this study
TP8726	TP5957	YCP lac33-*SSA1* + pTP4243	this study
TP8527	TP5957	pNH605-4xHSEpr-*YFP* (pDP122) integration	this study
TP8535	TP8527	pTP4108	this study
TP8536	TP8527	pTP4109	this study
TP8537	TP8527	pTP4110	this study
TP8761	TP8435	Yeast ORF Gal-*SIS1* (YNL007C)	this study
TP8762	TP8436	Yeast ORF Gal-*SIS1* (YNL007C)	this study
TP8763	TP8437	Yeast ORF Gal-*SIS1* (YNL007C)	this study
TP8764	TP8435	Yeast ORF Gal-*MAS5* (*YDJ1*) (YNL064C)	this study
TP8765	TP8436	Yeast ORF Gal-*MAS5* (*YDJ1*) (YNL064C)	this study
TP8766	TP8437	Yeast ORF Gal-*MAS5* (*YDJ1*) (YNL064C)	this study
TP9077	TP8724	Yeast ORF *CDK1* (YBR160W) in BG1805	this study
TP9078	TP8725	Yeast ORF *CDK1* (YBR160W) in BG1805	this study
TP9217	TP8435	pESC-URA-*GFP*-*Ubc9*ts	this study
TP9218	TP8436	pESC-URA-*GFP*-*Ubc9*ts	this study
TP9219	TP8437	pESC-URA-*GFP*-*Ubc9*ts	this study
TP9290	W303 cdc28d::cdc28-as1 ura3-1, leu2-3,112, trp1-1, his3-11,15, ade2-1, can1-100, GAL+		Gift from David Morgan
TP9372	W303 cdc28d::cdc28-as1 ura3-1, leu2-3,112, trp1-1, his3-11,15, ade2-1, can1-100, GAL+	pTP4241	this study
TP9373	W303 cdc28d::cdc28-as1 ura3-1, leu2-3,112, trp1-1, his3-11,15, ade2-1, can1-100, GAL+	pTP4242	this study
TP9301	TP8435	Yeast Gal-*HSP104*-b/Leu(WT)	this study

Table 2.1: continued next page

TP9302	TP8436	Yeast Gal-*HSP104*-b/Leu(WT)	this study
TP9303	TP8437	Yeast Gal-*HSP104*-b/Leu(WT)	this study
TP9387	TP5957 *hsp104*::KMX		this study
TP9461	TP9387	pTP4108	this study
TP9462	TP9387	pTP4109	this study
TP9463	TP9387	pTP4110	this study
TP9585	MATa kar1-1 SUQ5 ade2-1 his3Δ202 leu2Δ1 trp1Δ63 ura3-52 (1075) *ssa1*::KanMX4 *ssa2*::HIS3 *ssa3*::TRP1 *ssa4*::ura3 (1135) [PSI+]	pRDW10 (YCp50-*SSA1*)	Dan Masison
TP9613	TP9585	pRS315-*SSA1*	this study
TP9614	TP9585	pTP4698	this study
TP9615	TP9585	pTP4700	this study

Table 2.1 Yeast strains used in this study

Name	Plasmid	Source
pTP4108	pRS423-2xFlag-*SSA1*	
pTP4109	pRS423-2xFlag-*SSA1* (S151A)	
pTP4110	pRS423-2xFlag-*SSA1* (S151D)	
pTP4241	TurboGFP-2xFLAG-*SSA1*	
pTP4242	TurboGFP-2xFLAG-*SSA1* (S151A)	
pTP4243	TurboGFP-2xFLAG-*SSA1* (S151D)	
pTP4416	pFastBacHTb-2xFlag-*SSA1* (pTP4412)	
pTP4417	pFastBacHTb-2xFlag-*SSA1* S151A (pTP4413)	
pTP4418	pFastBacHTb-2xFlag-ySSA1 S151D (pTP4414)	
pTP4317	pGEX-6p-V5-*YDJ1*	
pTP4698	pRS315-*SSA1* S151A (Yeast: -Leu)	
pTP4700	pRS315-*SSA1* S151D (Yeast: -Leu)	
	pRS315-*SSA1*	Dan Masison
	pNH605-4xHSEpr-YFP (pDP122)	David Pincus
	pESC-URA-GFP-Ubc9ts	Addgene #20369
	yeast HSP104-b/Leu(WT)(Gal-inducible HSP104)	Addgene #1156
	5787 pET28aSX104B/ pES42	Addgene #1229
	Yeast ORF Gal inducible-SIS1 (YNL007C)	Dharmacon
	Yeast ORF Gal inducible-MAS5 (YDJ1) (YNL064C)	Dharmacon
	Yeast ORF CDK1 (YBR160W) in BG1805 vector	Dharmacon

Table 2.2 Plasmids used in this study

Yeast Protein Extraction and Western Blotting

Yeast cells were grown in 2 mL culture media for 2 days to stationary phase and inoculated into larger volume cultures at 0.15 O.D. $_{600}$ per ml. Cells were incubated at 30°c until log phase (0.3 – 1 O.D. $_{600}$) and collected at 4000 rpm for 5 min. Protein was extracted by bead beating in 0.3 ml lysis buffer [25 mM Tris-HCl buffer pH 7.4, 150 mM NaCl, 1 mM EDTA, 10% Glycerol, 0.5% NP40, 1 mM DTT, EDTA-free protease inhibitor mini tablets (Pierce), EDTA-free phosphatase inhibitor mini tablets (Pierce)] and 0.1ml acid-washed glass beads for 1 min at room temperature. Protein lysates were collected after 3500 rpm for 5 min at 4°c. 400 µg of protein lysates incubated with 50 µl anti-Flag- magnetic beads (MBL) for 1 hour at 4°c. Beads were collected and washed 3 times with 500 µl lysis buffer. After the third wash, the lysis buffer was removed completely and the beads were mixed with 20 µl 2.5x SDS sample buffer. The mixture was boiled at 95°c for 5 min. Boiled samples were loaded into 8% SDS-PAGE or NuPAGE 4% - 12% Bis-Tris protein gels (ThermoFisher). Specific protein targets were analyzed by immunoblot assay with specific antibodies listed in Table. S1. The S151 phospho-specific antibody was produced by PhosphoSolutions using a peptide containing the phosphorylated site.

Galactose Induction

Yeast cells were grown in 2 ml culture media with 2% glucose overnight and then inoculated into 25 ml of synthetic minimal defined media containing 2% raffinose overnight. This culture was used to inoculate cultures at 0.15 O.D. $_{600}$ 2% raffinose and

incubated at 30°c until log phase (0.3 – 1 O.D. $_{600}$). 3X YP media (3% Yeast extract, 6% Peptone with 6% Galactose) was used to induce GAL expression (or glucose-containing media as a control).

Copper Sensitivity

Δssa1-4 yeast cells expressing wild-type, S151A, or S151D Ssa1 mutants were grown to log phase in liquid culture; 11 mM $CuCl_2$ was added for 6 hrs; cells were washed with water, and plated in dilutions on YPAD plates. Colony survival was measured with 3 biological replicate experiments comparing copper exposure to control cultures.

Protein Aggregate Isolation and Analysis

The assay was performed as described previously (150). To prepare cell lysates, the pellets were resuspended in lysis buffer [20 mM Na-phosphate (pH 6.8), 10 mM DTT, 1 mM EDTA, 0.1% Tween 20, 1 mM PMSF, and EDTA-free protease inhibitor mini tablets (Pierce)]. Cells were lysed in a 4°C water bath–based sonicator (Bioruptor; eight times at level 4.5 and 50% duty cycle) and centrifuged for 20 min at 200xg at 4°C. Supernatants were adjusted to the same concentration, and protein aggregates were pelleted at 16,000x g for 20 min at 4°C. After removing supernatants, protein aggregates were washed twice with 2% NP-40 [20 mM Na-phosphate (pH 6.8), 1 mM PMSF, and EDTA-free protease inhibitor mini tablets (Pierce)], sonicated (six times at level 4.5 and 50% duty cycle), and centrifuged at 16,000 xg for 20 min at 4°C. Aggregated proteins were washed in buffer without NP-40 (sonication; four times at level 3 and 50% duty cycle), boiled in 2.5x SDS sample buffer, separated in NuPAGE 4% - 12% Bis-Tris

protein gels (ThermoFisher), and analyzed by coomassie blue staining. Levels of aggregates were quantified using Image Studio

Filter Aided Sample Preparation and Trypsin Digestion for Mass Spectrometry

Detergent-resistant aggregates or immunoprecipitated samples were resuspended in 15 µl of 10% SDS sample buffer and 50 mM beta-mercaptoethanol and boiled in 100°c for 5 minutes. The samples were diluted with 200 µl of UA buffer (8 M Urea, 0.1 M Tris-HCl pH 8.8) at room temperature. Microcon®-30 centrifugal filter units (Millipore, MRCF0R030) were equilibrated with 20% ACN, 2% formic acid solution (14,000 xg for 10 min) prior to use. Diluted samples were loaded on the filters then washed with UA buffer (8 M Urea, 0.1 M Tris-HCl pH 8.8) 3 times. After washing, samples were reduced with 50 mM DTT in UA buffer (8 M Urea, 0.1 M Tris-HCl pH 8.8) which was added to filters, incubated 5 minutes at room temperature and spun off. Then samples were alkylated with 50 mM iodoacetamide in UA buffer (8 M Urea, 0.1 M Tris-HCl pH 8.8), incubated 5 minutes at room temperature and spun off. Samples were de-salted with 40 mM ammonium bicarbonate (ABC) 3 times. 100 ul 40 mM ABC with 0.5 µl of trypsin gold (Promega, V528A) in PBS was added to samples and were incubated overnight (37°C). Trypsinized peptides were eluted by centrifugation; filters were washed with 20% ACN, 2% formic acid solution and filtrate was combined with trypsinized peptides eluted in ABC. Peptide samples were dried by lyophilization, de-salted with C18 tips (Pierce, QK224796) according to manufacturer's instructions, and resuspended in 80% ACN 2% formic acid for LC-MS-MS analysis at the Proteomics Core Facility (University

of Texas at Austin). All centrifugations were done at 14,000 xg for 20 min unless otherwise noted.

Recombinant Protein Expression

Wild-type Ssa1, Ssa1 S151A, and Ssa1 S151D proteins were expressed using the Bac-to-Bac baculovirus system (ThermoFisher). We cloned SSA1, SSA1 (S151A), and SSA1 (S151D) genes, Flag-tagged at N-terminus (pTP4416, pTP4417, and pTP4418), into pFastBac1. Recombinant bacmid DNA derived from these transfer vectors was transfected into Sf21 insect cells for recombinant baculovirus production. Ssa1 proteins were expressed in Sf21 insect cells after baculovirus infection. Cell pellets were lysed by homogenization and sonicated three times for 40 seconds in A buffer containing 0.5% tween-20, 1mM PMSF (phenylmethylsulfonyl fluoride), 12.5% ethanol, and 0.001 % 2-Mercaptoethanol. The lysate was centrifuged for 1 hr at 35000 rpm at 4°C. The supernatant was incubated with ~1mL M2 anti-Flag antibody-conjugated agarose resin (Sigma) with rotation at 4°C for 1hr. After incubation the lysate with resin was centrifuged for 3 min at 1000g. After removing the supernatant, the remaining resin was washed with 20mL of A buffer twice and was eluted with 5mL of A buffer containing 0.8mg/mL 3X Flag peptide (Sigma). The peptide was incubated with the resin for 20 min before elution. The Flag elution was then loaded onto 1mL HiTrap Q column (G.E.) and washed with buffer A then eluted with buffer A containing 500mM NaCl. The eluted protein fractions were dialyzed in A buffer and the dialyzed fractions were aliquoted frozen in liquid nitrogen, and stored at -80°C. Protein concentration was quantified by SDS-PAGE using a Licor Odyssey Imager.

V5-tagged Ydj1 proteins were purified as GST fusion proteins in BL21 *E. coli*. Starter cultures were prepared at 37°c for 16 hr. Overnight cultures were diluted 1:20 for additional 2 hr incubation at 37°c. 100 μM Isopropyl b-D-1-thiogalactopyranoside (IPTG) was used to induce protein expression for 3 hr at 37°c. Cells pellets were collected using 3400 rpm for 10 min, resuspened in phosphate buffer saline (PBS) with 1% Triton, and sonicated for 30 seconds. Cell supernatants were collected using 10000 rpm for 10 min and incubated with Glutathione sepharose 4B resin (GE Healthcare) for 2 hr at 4°c. Beads were collected and washed three times with PBS 1% Triton and three times with 50mM Tris-HCl pH8.0, 150mM NaCl, 0.01% Triton, and 2.5mM EDTA. GST fusion V5-Ydj1 was subjected to site-specific cleavage with PreScission Protease (GE Healthcare) to remove the GST tag. V5-Ydj1 was purified from beads and its protein concentration was quantified by SDS-PAGE using a Licor Odyssey Imager.

Flag-Hsp104 was purified from BL21 *E. coli*. Starter cultures were prepared at 37°C for 16 hr. Overnight cultures were diluted 1:20 for additional 2 hr incubation at 37°C. 100 μM Isopropyl b-D-1-thiogalactopyranoside (IPTG) was used to induce protein expression for 3 hr at 37°c. Cells pellets were collected using 3400 rpm for 10 min. The protein purification protocol step follows as previously described in Ssa1 protein purification.

Luciferase Refolding Assay

Firefly luciferase (Sigma L9420) was diluted in refolding buffer (20 mM Tris-HCl pH 7.4, 50 mM KCl, and 5 mM $MgCl_2$) 5-fold and denatured with 6 M Urea for 30 min at

room temperature. Denatured luciferase was then diluted 100 fold with refolding buffer and incubated with indicated chaperones, indicated co-chaperones, 10 mM ATP, and 10 mM DTT for a final volume of 25 µl. The reaction was incubated at 30°c for 30 min. 5 µl reaction were mixed with 50 µl luciferase assay substrate (Promega). A Tecan SPARK 10M plate reader was used to measure luciferase activity.

ATP Hydrolysis Measurements

Recombinant proteins were prepared in Buffer A (25mM Tris-HCl pH 8.0, 100mM NaCl, 10% Glycerol, 1mM DTT). Reactions were started by adding [α-^{32}P] ATP mixtures (25 mM Mops pH7.0, 5mM $MgCl_2$, 0.2 mM DTT, 0.1 mg/mL BSA, 50µM ATP, 50nM [α-^{32}P] ATP) to protein solutions, followed by incubation at 37°C for 1 hr. 1ul of Stop solution (2% SDS and 100 mM EDTA) was added to stop the reaction. 1 µl of each reaction was spotted onto a Plastic Backed TLC Cellulose PEI plate (Scientific Adsorbents Incorporated, #78601). The plate was dried and run in 0.75 mM KH_2PO_4 (monobasic) buffer. Percentage of hydrolyzed [α-^{32}P] ATP and ADP were quantified by Typhoon FLA 7000 biomolecular image and normalized by the reaction without proteins. Normalized percentage of hydrolyzed ATP was divided by the amount of Ssa1 proteins and further divided by the incubation time of the assay.

GFP-Ubc9^{ts} Protein Aggregate Analysis

Galactose-controlled GFP-Ubc9^{ts} was used as an indicator of the level of protein aggregation. Cells were grown overnight and re-inoculated into 2 ml of synthetic minimal defined media with 2% raffinose overnight. Cells were inculated at 0.15 O.D.$_{600}$ per ml

in 2% raffinose and incubated at 30°c until log phase (0.3 – 1 O.D. $_{600}$). Synthetic minimal defined media with 3xYP(2% Galactose) was added to induce expression of GFP-Ubc9^{ts} (or 3xYP with 2% Glucose as a control). 54°c culture media was prepared ahead and used to perform 42°c heat shock in a 1:1 ratio of culture media. Heated-cells were incubated at 42°c for 30min and then prepared for imaging. Cells with at least one focus was counted as positive and compared to the total number of cells containing GFP fluorescence.

GFP-Ssa1 Cellular Foci Analysis

For the starvation experiment, GPF-tagged wild-type Ssa1, S151A, and S151D cells were grown overnight and re-inoculated into 2 ml of synthetic minimal defined media with 2% glucose in a concentration of 0.15 O.D. 600 per ml. Cells were grown to log phase, collected by centrifugation, and then resuspended in media lacking glucose for 10 min before imaging. Cells with at least one focus was counted as positive and compared to the total number of cells containing GFP fluorescence. For the saturation phase experiment, GPF-tagged wild-type Ssa1, S151A, and S151D cells were grown for 2 days to saturation phase. Cells with at least one focus was counted as positive and compared to the total number of cells containing GFP fluorescence.

HSE-YFP Reporter Heat Shock Assays

The HSE-YFP reporter, pNH605-4xHSEpr-YFP (pDP122, a gift from David Pincus), was integrated into the genome of the Δ*ssa1-4* yeast cells (a gift from Sabine Rospert), then, cells were complemented with Flag-tagged Ssa1 (wild-type, S151A mutant, or

S151D mutant). The assay was performed essentially as described (41). Briefly, cells were prepared at a density of 0.2 O.D. 600 per ml and incubated at the indicated temperature on a thermal mixer. After 30 or 60 min, 50 µl were collected and treated with cycloheximide (Final concentration: 50 µg / mL) to stop translation. Additional 2 hr incubation at 30°c is required to mature YFP fluorophores. The Mean Fluorescence Intensity (MFI) of each cell was measured using a BD LSRFortesa™ flow cytometer and analyzed by FlowJo.

Double siRNA Knockdown in Human Cells

siRNA sequences were designed based on a previous study (151) and listed in Table S1. The transfection of siRNA into U2OS cells was perforemd with Oligofectamine transfection reagent (ThermoFisher) according to manufacturer instructions. Double knockdowns were performed with 20 µM of each siRNA.

Heat Shock and Nucleolin Staining of Human Cells

U2OS cells expressing mCherry-HSPA8 (WT, S153A, S153D) and Halo-Fibrillarin were plated into WillCo-dish® Glass Bottom dishes (cat. 14023-200) with cell culture media containing 1ug/ml doxycycline a day before the experiment. Cells were heat shocked for 45 minutes in a 43^{o}C tissue culture incubator (5% CO_2). 1 pM JF502 halotag ligand (a gift from Luke Lavis) was added to cell media for 15 minutes. Finally cells were washed with sterile PBS in room temperature then analyzed using a Zeiss Axiovert Fluorescent Light Microscope with a 64x oil immersion objective. Images were analyzed with FIJI software (ImageJ v1.52c). For quantification, at least 70 cells from several fields of view

were scored for GFP-HSC70 foci in the nucleolus (overlapping with Halo-Fibrillarin) under normal growth conditions (37^{o} C) and heat shock (43^{o} C).

Isolation of Tagged Hsc70 From Human Cells

Biotinylated, V5-tagged Hsc70 was expressed in human U2OS cells and isolated with streptavidin-coated beads under denaturing conditions. Briefly, cells were lysed with urea solution (8M Urea, 50mM Tris pH8, 5mM $CaCl_2$, 30mM NaCl, 0.1% SDS and 1:1000 PMSF/Protease Inhibitor). Lysates were sonicated for 30 sec. 3 mg of lysates were diluted to 1M Urea. 120 µL of streptavidin magnetic beads were added to each samples and rotated overnight at RT. The next day, beads were washed twice for 30 minutes each with 1M Urea solution (1M Urea, 50mM Tris pH8, 5mM $CaCl_2$, 30mM NaCl, 0.1% SDS) at RT. Then beads were washed with LiCl (500mM) for 30 minutes at RT. After, beads were washed 3 times with 0.1%SDS, 0.2%SDS and 0.5%SDS for 30 minutes at RT respectively. Finally, samples were eluted with 1% SDS with 2- mercaptoethanol at 100^{o}C. Samples were frozen in -20^{o}C until analyzed by filter-assisted sample preparation and trypsinization (see above).

CHAPTER 3: GROWTH-REGULATED HSP70 PHOSPHORYLATION REGULATES STRESS RESPONSES AND PRION MAINTENANCE

Ssa1 S151 Phosphorylation Affects Cell Growth and Thermal Stability

Multiple phosphorylated serine/threonine residues have been identified on HSP70 proteins (10, 152, 153); however, the potential functions and regulatory roles of these modifications on Hsp70 are not fully understood. To identify and characterize these sites, we analyzed Ssa1 phosphorylation in budding yeast and Hsc70 phosphorylation in human cells by quantitative mass spectrometry. In our analysis of post-translational modifications, we detected and confirmed Ssa1 and Hsc70 phosphorylation at S151 and S153 in yeast and humans, respectively, among many other modifications (154). The S151 residue is highly conserved among several Hsp70 family members in *S. cerevisiae* and higher eukaryotes (Figure 3.1). The four abundant cytosolic HSP70 proteins (Ssa1-4) and yeast mitochondrial HSP70 proteins (Ssc1 and Ssq1) all have a serine at a.a.151 in the nucleotide-binding domain (NBD) whereas most bacterial and archaeabacterial HSP70 proteins have an alanine at this position.

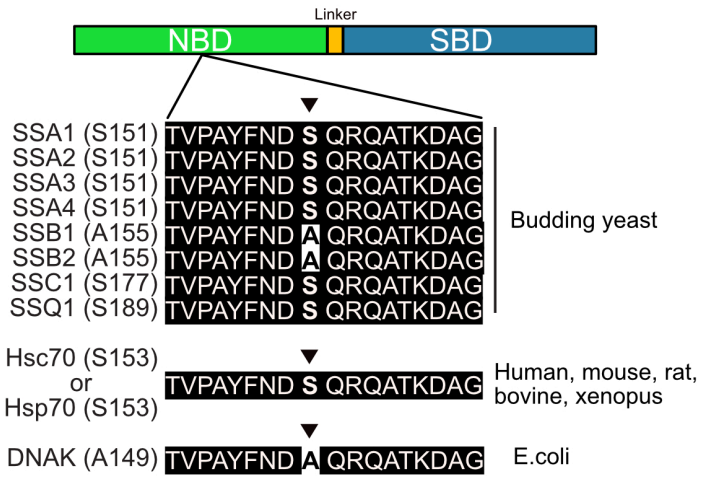

Figure 3.1 Alignment of Hsp70 protein sequences in the region surrounding S151 in the NBD in prokaryotic and eukaryotic cells.

In Hsc70/Hsp70 proteins, the substrate-binding domain (SBD) docks with the NBD in the ATP-bound state where the complex has low affinity for its clients (4, 69) (example of the ATP-bound form of DnaK (*E. coli* homologue of mammalian Hsp70) shown in Figure 3.2 (69). With ATP hydrolysis, the SBD releases from this conformation while connected to the NBD via a flexible linker in the ADP-bound state, consistent with predictions of dynamic motion of Hsp70 between different states (49, 56). Interestingly, the Alanine 149 (A149) residue of DnaK (corresponding to the S151 residue of yeast Ssa1 or S153 residue of human Hsc70/Hsp70) is located close to the interface between the NBD and SBD (Figure 3.2). Based on structures of DnaK and yeast Sse1 (67, 69), S151/153 would only be ~3Å away from Lysine 452 (K452) of the SBD in the ATP-bound state, indicating a possible role for this modification in regulating associations between the NBD and the SBD.

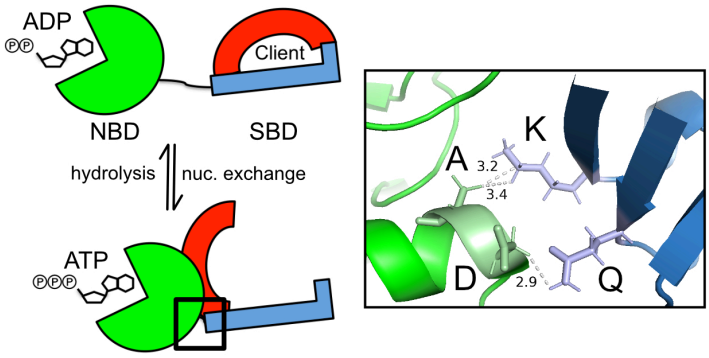

Figure 3.2 The S151 residue of Ssa1 in the NBD is located close to the interaction site with the SBD in the ATP-bound state.

Left panel: ATP hydrolysis and nucleotide exchange is postulated to regulate structural conformation changes in Hsp70 proteins. In the ADP-bound state, the NBD (green) is in an open configuration, connected to the SBD (red: alpha-helical lid; blue: beta-sheet pocket) via a flexible linker. In the ATP-bound state, NBD and SBD undergo a conformational change to interact in a closed configuration. Right panel: In DnaK, A149 and D148 of the NBD are in close contact with K452 and E442 of the SBD (PDB: 4B9Q) (69).

Interestingly, S153 in vertebrate Hsc70 orthologs is part of an (S/T)Q motif, matching the consensus for PI-3 Kinase-like Kinases (PIKK) that are targets of the ATM and ATR protein kinases in the DNA damage response (155, 156). Hsc70 S153 was also found to be phosphorylated in a global study of DNA damage-induced phosphorylation (157). In yeast, S151 in SSA1 also resides in an (S/T)Q PIKK motif; however, the role of

SSA1 S151 phosphorylation in DNA damage responses is not clear. Our observation of SSA1 S151 phosphorylation as well as previous documentation of this modification by global phosphorylation studies (11, 152) suggested that one of the PIKK kinases might use Hsp70 modification to regulate downstream DNA damage repair pathways or canonical Hsp70 functions. To investigate this possibility, we generated a custom antibody directed against phospho-S151 and monitored phosphorylation of recombinant GFP-Flag-Ssa1 expressed in budding yeast and isolated by immunoprecipitation followed by western blot of the tagged protein from normally growing cells. The result shows that the antibody recognizes wild-type Ssa1 but not Ssa1 S151A (Figure 3.3), indicating that the antibody is specific for the S151 residue and that the modification occurs during normal growth conditions. We did not observe any increase in phosphorylation with DNA damaging agents, however (data not shown), which would be expected if this modification was involved in DNA damage responses.

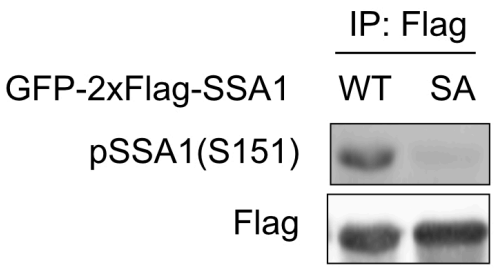

Figure 3.3 Phospho-Ssa1(S151) is detected using an antibody specific for this phosphorylation site (custom antibody made by PhosphoSolutions).
GFP-Flag-Ssa1 (WT) or GFP-Flag-Ssa1 S151A (S151A) were expressed in a *ssa1 ssa2 ssa3 ssa4* deletion (Δ*ssa1-4*) strain. GFP-Flag-Ssa1 was isolated by immunoprecipitation and analyzed by quantitative Western blotting with anti-phospho-Ssa1 S151 and anti-Flag antibodies.

In order to investigate the role of HSP70 phosphorylation at S151, we expressed Flag-tagged wild-type Ssa1, a non-phosphorylatable mutant Ssa1 (S151A) or a phospho-mimetic mutant Ssa1 (S151D) under the control of the Ssa1 natural promoter on a 2 micron plasmid in a yeast strain lacking all four Ssa proteins (158). Growth of wild-type and mutant strains were evaluated using a serial spot dilution assay on solid media (Figure 3.4A) or a growth curve in liquid culture (Figure 3.4B). Both assays indicate that the wild-type, S151A, and S151D cells grow similarly at 30°C but the S151D cells are hypersensitive to high temperature (39°C) (Figure 3.4A and Figure 3.4B). Therefore, the phospho-mimetic S151D mutant can be considered a temperature-sensitive mutant. Interestingly, we observed that the cells expressing the S151A mutant exhibit a delay in

growth as cells approach stationary phase, whereas the cells expressing S151D grow to higher density than wild-type during this period (Figure 3.4C).

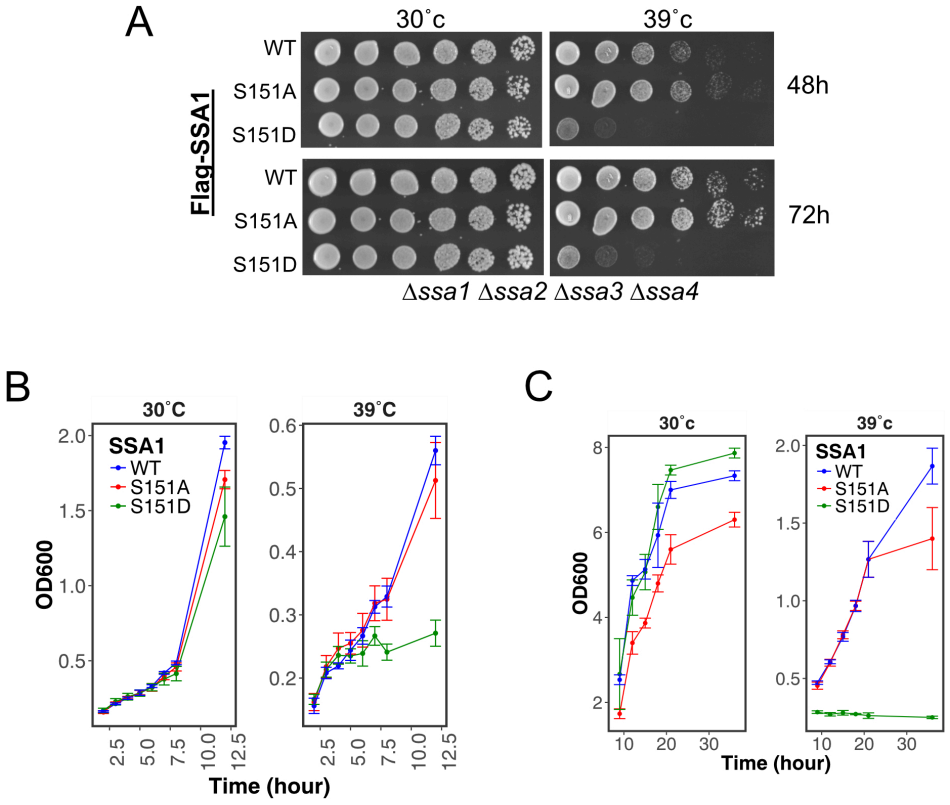

Figure 3.4 Phospho-mimetic mutant Ssa1 affects cell growth in response to heat stress (A) Δ*ssa1-4* yeast cells expressing Flag-Ssa1 (WT), Flag-Ssa1 S151A (S151A), or Flag-Ssa1 S151D (S151D) were spotted in fivefold serial dilutions and exposed to 30 or 39°C for 48 or 72 hr. (B and C) Growth of Δ*ssa1-4* yeast cells expressing Flag-Ssa1 (WT), Flag-Ssa1 S151A (S151A), or Flag-Ssa1 S151D (S151D) was monitored at 30°C or 39°C as indicated. Growth curve is measured in log (B) and stationary (C) phase by OD600. 3 biological replicates were performed and error bars represent standard deviation.

It is possible that S151D cells exhibit sensitivity to heat shock because of alterations in heat shock factor 1 (Hsf1) regulation (39). In wild-type *S. cerevisiae* cells, the transcription factor Hsf1 is repressed by Ssa1/2, which binds to Hsf1, preventing its association with heat shock elements (HSEs) (38). Heat shock generates misfolded proteins that compete with Hsf1 for the binding of Ssa1/2, which releases Hsf1 to transcribe HSE-driven genes that generate higher levels of chaperones and repress ribosomal proteins (39–41). To test whether Ssa1 S151 phosphorylation regulates HSF1 activation, we integrated a yellow fluorescence protein (YFP) reporter regulated by HSEs (41) into the genome of our strains and used flow cytometry analysis to monitor HSF1 activity. In the wild-type and S151A strains, exposure to heat (37°C and 42°C) increased the yield of YFP relative to 25°C (Figure 3.5) as previously reported (41). Cells expressing S151D Ssa1 exhibited higher HSF1 activation at high temperatures but were also elevated at 25°C compared to wild-type and S151A cells. Consistent with this finding of basal de-repression of Hsf1, cells expressing S151D Ssa1 under normal growth conditions show higher levels of expression of several other heat shock proteins (Figure 3.6) and also slight repression of ribosomal proteins (Figure 3.7).

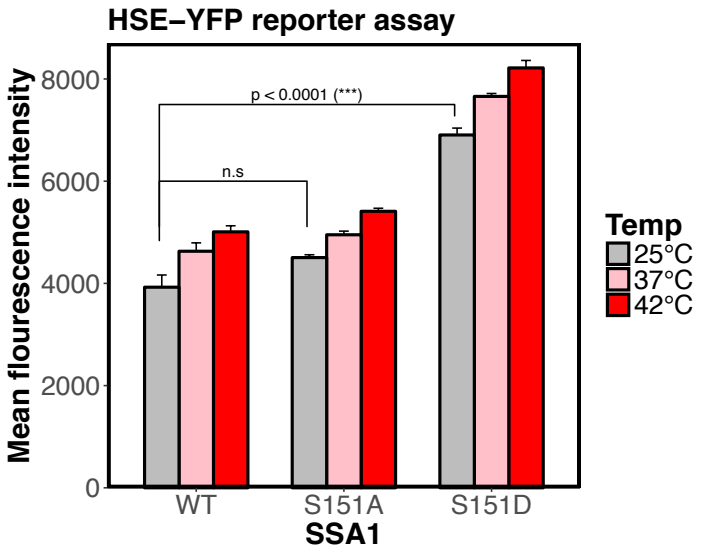

Figure 3.5 Phospho-mimetic mutant Ssa1 promotes Hsf1 hyperactivation.

Δ*ssa1-4* yeast cells with an integrated HSE-YFP reporter and expressing Flag-Ssa1 (WT), Flag-Ssa1 S151A (S151A), or Flag-Ssa1 S151D (S151D) were exposed to varying temperatures as indicated for 30 min. YFP signal was measured by flow cytometer. 3 biological replicates were performed with at least 10,000 cells per measurement; error bars represent standard deviation.

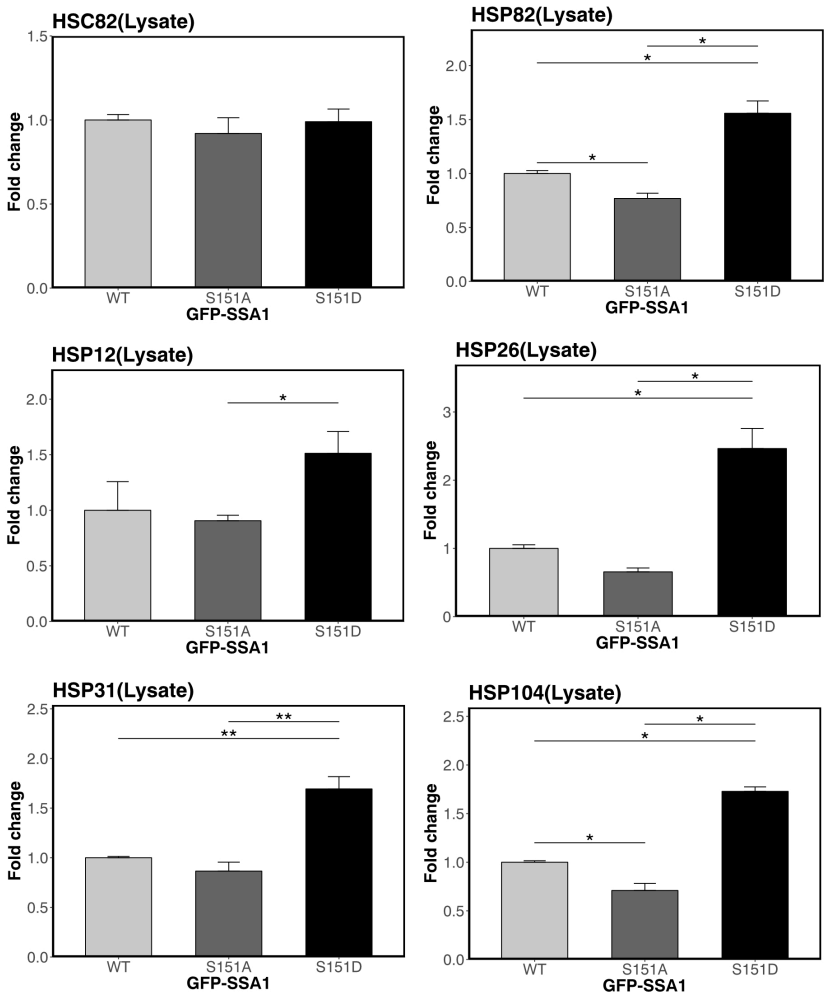

Figure 3.6 Binding of other chaperones to SSA1 is affected by S151 phosphorylation status.

Quantification of yeast Hsp90s and small chaperones binding to WT, SA, or SD forms of Ssa1 in total lysates ("Lysate") from the LC-MS analysis.

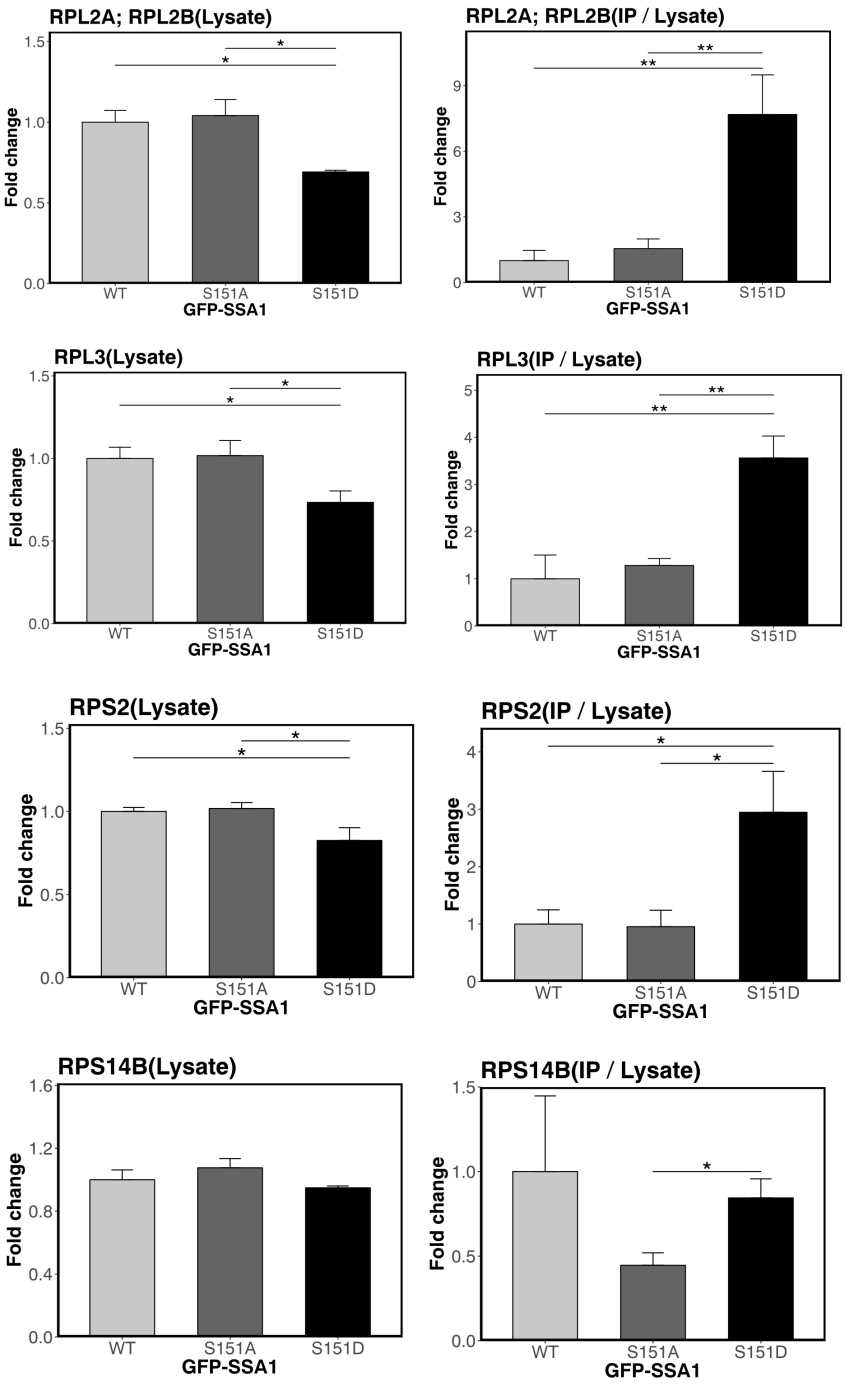

Figure 3.7 Ssa1 phosphorylation at S151 promotes higher association with ribosomal proteins.

Quantification of ribosomal proteins binding to WT, SA, or SD forms of Ssa1 in immunoprecipitations normalized by total lysates ("IP/Lysate") compared to the levels in total lysates ("Lysate") from the LC-MS analysis.

Ssa1 S151D Cells Accumulate More Heat-Induced Protein Aggregates

The impaired heat shock survival of yeast cells expressing Ssa1 S151D protein (Figure 3.4A-C) might be related to the accumulation of heat-induced protein aggregates, as Hsp70 proteins have been shown to be critical for dispersal of these toxic products (159). To test this, we collected protein aggregates by separating detergent-insoluble proteins from detergent-soluble proteins using a previously described method (150). We then compared overall levels of detergent-insoluble proteins from wild-type, S151A, and S151D cells at 30°C or 42°C by coomassie staining of the aggregates on SDS-PAGE gels (Figure 3.8). Interestingly, cells expressing Ssa1 S151D tended to form a higher basal level of total endogenous aggregates than wild-type and Ssa1 S151A cells at 30°C ("C"). Similarly, Ssa1 S151D cells produced more heat-induced total aggregates compared to wild-type and S151A cells at 42°C ("Hs", Figure 3.8). The results are consistent with the growth data above in that S151D cells accumulate more detergent-insoluble proteins than wild-type and S151A cells during heat exposure. In contrast, the S151A-expressing cells showed lower levels of protein aggregates compared to wild-type Ssa1-expressing cells, with or without heat treatment, suggesting a higher efficiency of aggregate removal compared to wild-type cells. Arsenite treatment, used here as a general form of oxidative stress, yielded similar levels of aggregates in all strains.

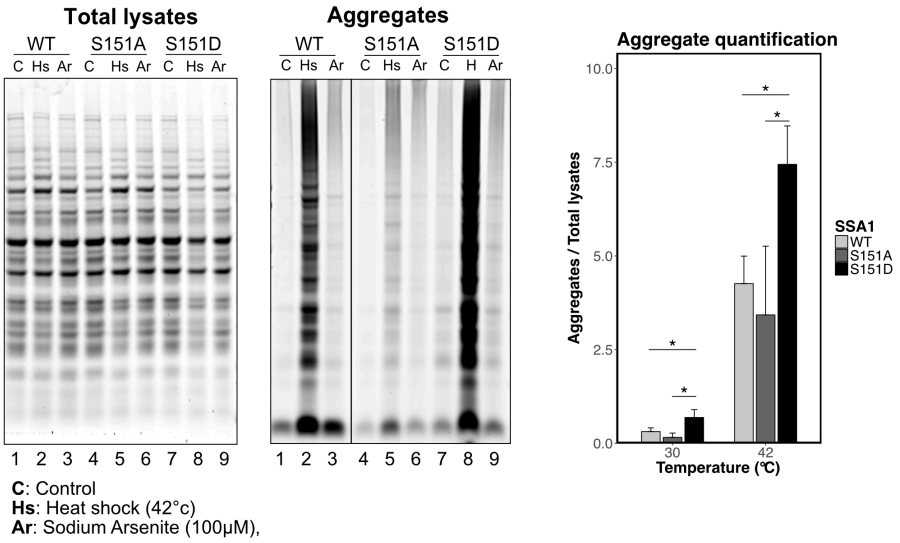

Figure 3.8 Phospho-mimetic mutant Ssa1 promotes heat-induced protein aggregation Left and middle panels: Δ*ssa1-4* yeast cells expressing Flag-Ssa1 (WT), Flag-Ssa1 S151A (S151A), or Flag-Ssa1 S151D (S151D) were treated with heat shock (42°C, "Hs"), or Sodium Arsenite (100 μM, "Ar") for 60 min. Protein aggregates were isolated (see Materials and Methods) and separated by SDS-PAGE with total lysates. Right panel: Quantification of the levels of aggregated proteins divided by the total protein levels. 3 biological replicates were performed and error bars represent standard deviation. * indicates $p < 0.05$ by student's 2-tailed T test.

We also used the well-established aggregate reporter Ubc9 Y68L, a temperature-sensitive allele of the SUMO-conjugating enzyme Ubc9 ($Ubc9^{ts}$), to measure protein aggregates in vivo (147, 160). Our results showed that cells expressing Ssa1 S151D form more endogenous GFP-Ubc9 aggregates (GFP foci) at 30°C and also show nearly 2-fold higher levels of heat-induced GFP foci compared to the wild-type and S151A cells (Figure 3.9). Taken together, these data suggest that Ssa1 S151 phosphorylation affects the cellular responses to heat and protein homeostasis stress.

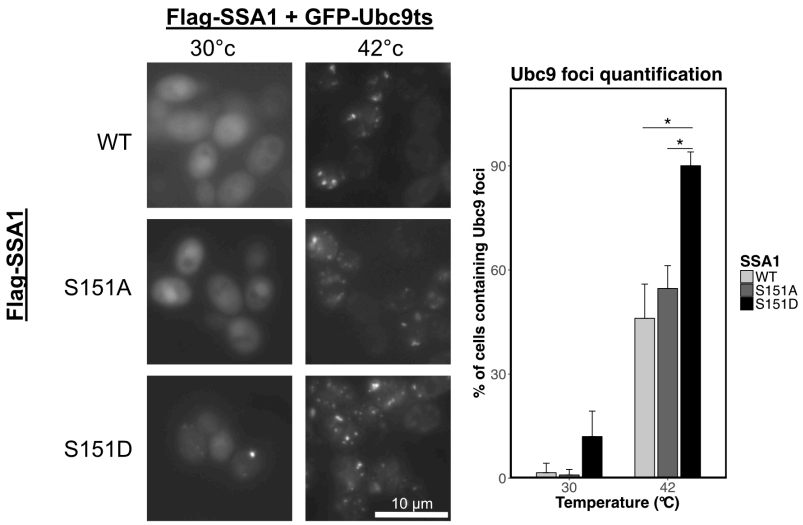

Figure 3.9. Ssa1 S151 phosphorylation promotes heat-induced Ubc9 aggregation. Left panel: Δ*ssa1-4* yeast cells expressing GFP-Ubc9ts as well as Flag-Ssa1 (WT), Flag-Ssa1 S151A (S151A), or Flag-Ssa1 S151D (S151D) were treated with 30°C or 42°C for 30 min and analyzed by immunofluorescence microscope for Ubc9 foci. Right panel: Quantification of Ubc9 foci was performed by counting the number of GFP-positive cells containing at least one GFP focus per cell divided by the total number of GFP-positive cells. 3 biological replicates were performed and error bars represent standard deviation. * indicates $p < 0.05$ by student 2-tailed T test.

Ssa1 S151 Is Phosphorylated by Cyclin-Dependent Kinase Cdk1

Although we initiated our study of S151 modification with the idea that PIKK enzymes might regulate HSP70 function, analysis of S151 phosphorylation in strains deficient in the yeast PIKK enzymes (*mec1 tel1* strains) did not support this hypothesis (data not shown). A recent study of other Ssa1 modifications showed that T36 phosphorylation on Ssa1 by yeast Cdk1 and Pho85 is important for G_1/S cell cycle control and suggested that Ssa1 is physically associated with Cdk1 and Pho85 (142). Considering this precedent, we hypothesized that cyclin-dependent kinase might phosphorylate Ssa1 S151. To determine if Cdk1 catalyzes Ssa1 S151 phosphorylation, we expressed galactose-inducible Cdk1 (Cdc28) in GFP-Flag-SSA1-expressing cells and analyzed the phosphorylation status of S151 in Ssa1 immunoprecipitated with anti-Flag antibody. The result shows that Cdk1 overexpression increases Ssa1 S151 phosphorylation signal 3-fold, with Ssa1 S151A as a negative control (Figure 3.10).

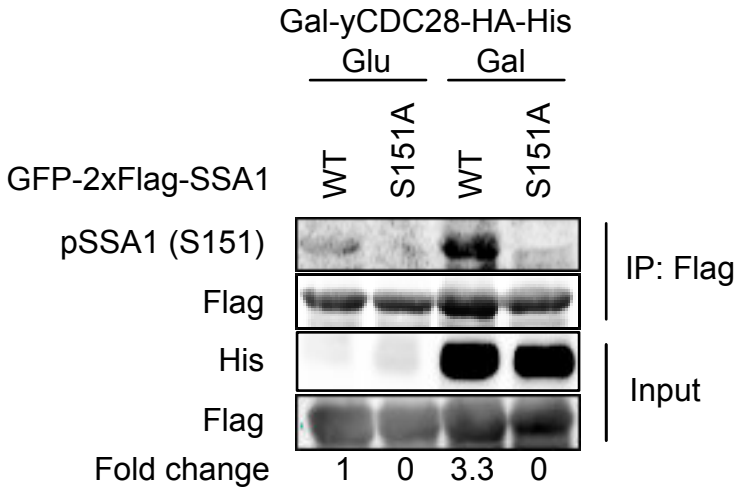

Figure 3.10 Ssa1 S151 phosphorylation is mediated by Cdk1

Δ*ssa1-4* yeast cells expressing GFP-Flag-Ssa1 (WT), or GFP-Flag-Ssa1 S151A (S151A) as well as galactose-inducible HA-His-tagged Cdk1 (Gal-yCDC28-HA-His) were grown in glucose (Glu) or galactose (Gal). Ssa1 was isolated by immunoprecipitation and analyzed by Western blotting with anti-phospho-Ssa1 S151, anti-His and anti-Flag antibodies.

We also utilized yeast cells expressing Cdk1-as1, an analog-sensitive version of Cdk1 (161), to evaluate Ssa1 S151 phosphorylation. In this strain, Cdk1 activity can be downregulated by the addition of 1-NM-PP1 analogs that uniquely block the analog-sensitive Cdk1. We overexpressed GFP-Flag-SSA1 in the Cdk1-as1 strain and immunoprecipitated Ssa1 after 1-NM-PP1 treatment, finding that Ssa1 phosphorylation at S151 was partially decreased under these conditions (Figure 3.11A). Lastly, to confirm the phosphorylation in vitro, we purified galacotose-inducible His-HA-tagged Cdk1 enzyme and evaluated its ability to phosphorylate recombinant wild-type Ssa1 purified from *E. coli*. In comparison to the purified Cdk1 from raffinose cultures, immunoprecipitated material from galactose-induced cultures produced 1.5 to 2--fold higher levels of Ssa1 S151 phosphorylation (Figure 3.11B). In addition, the S151 site was found in a global survey of Cdk1 targets in yeast, although the change in phosphorylation induced by cell cycle synchronization in this study was modest (153). Taken together, these data suggest that Cdk1 phosphorylates Ssa1 at S151 in vivo, although we cannot exclude the possibility of other kinases modifying the site in addition to Cdk1.

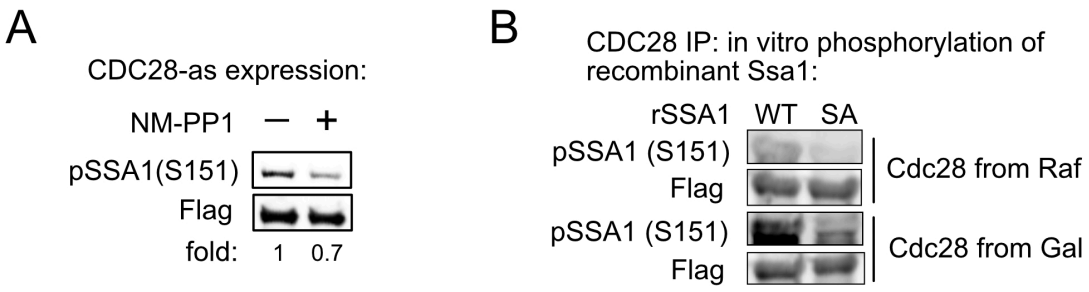

Figure 3.11 Ssa1 S151 phosphorylation is mediated by Cdk1. (A) Cdk1-as1 cells expressing GFP-Flag-Ssa1 (WT), or GFP-Flag-Ssa1 S151A (S151A) were treated with NM-PP1 (10 uM) for 3 hr. Ssa1 was isolated by immunoprecipitation and analyzed by Western blotting with anti-phospho-Ssa1 S151 and anti-Flag antibodies. (B) Recombinant Flag-tagged Ssa1 (WT) or Ssa1 S151A (S151A) was incubated with HA-His-tagged Cdk1 isolated from *ssa1-4*Δ yeast cells expressing galactose inducible HA-His-tagged Cdk1 (Gal-yCDC28-HA-His) treated with raffinose (Raf) or galactose (Gal). Phosphorylation was analyzed by Western blotting with anti-phospho-Ssa1 S151 and Flag antibodies. Arrow indicates phosphorylated species.

Starvation Conditions Reduce S151 Phosphorylation

The TOR pathway participates in protein homeostasis through the connection between TOR-mediated nutrient signaling and chaperone-mediated stress responses (162). Here we tested the effects of stationary phase, TORin (a TOR1 and TOR2 inhibitor)(163), as well as rapamycin and found that all of these treatments substantially reduce Ssa1 phosphorylation at S151 (Figure 3.12A-B). These results are consistent with our observation of CDK control of this phosphorylation since TOR inhibition blocks cell cycle progression and CDK activity is low in stationary phase (164–166).

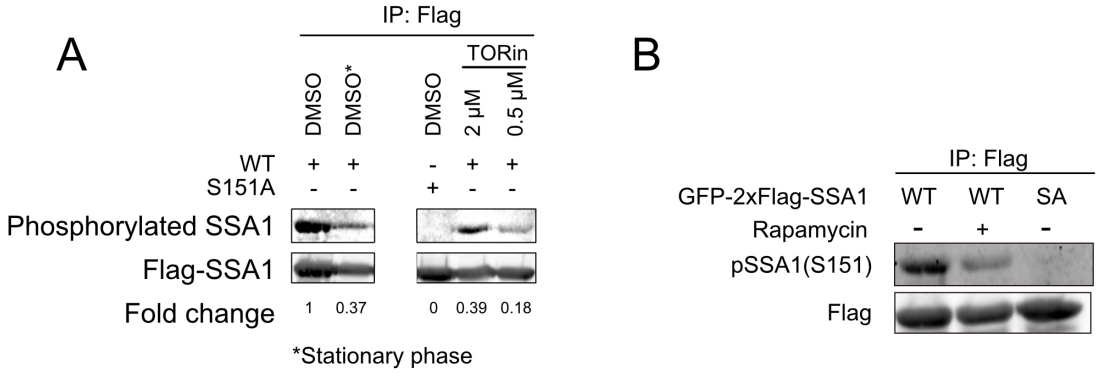

Figure 3.12 Ssa1 S151 phosphorylation is regulated by the TOR pathway.

(A) Δ*ssa1-4* yeast cells expressing GFP-Flag-Ssa1 (WT), or GFP-Flag-Ssa1 S151A (S151A) were treated with TORin (2 μM or 0.5 μM) for 30 min. Ssa1 was isolated by immunoprecipitation and analyzed by Western blotting with anti-phospho-Ssa1 S151 and anti-Flag antibodies. (B) Δ*ssa1-4* yeast cells expressing GFP-Flag-Ssa1 (WT), or GFP-Flag-Ssa1 S151A (S151A) were treated with rapamycin (200 ng/mL) for 30 min. Ssa1 was isolated by immunoprecipitation and analyzed by quantitative Western blotting with anti-phospho-Ssa1 S151 and anti-Flag antibodies.

We also tested the growth of wild-type and mutant strains under TOR inhibition conditions using a growth curve in liquid culture (Figure 3.13A) or a serial spot dilution assay on solid media (Figure 3.13B). Both assays indicated that S151D cells exhibit delayed growth in a TOR-inhibited environment, particularly in high-density cultures as cells approach stationary phase. Interestingly, S151A cells grew to higher densities than wild-type and S151D cells during long-term rapamycin treatment (Figure 3.13B). Thus, reduction of S151 phosphorylation is necessary for growth and survival under conditions of TOR inhibition.

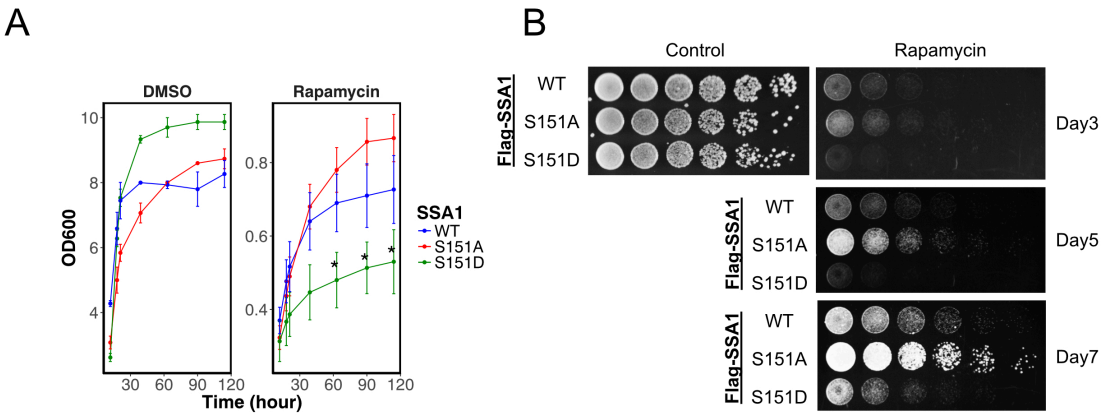

Figure 3.13 Phospho-mimetic mutant Ssa1 affects cell growth in response to TOR. inhibitor. (A) Δ*ssa1-4* yeast cells expressing Flag-Ssa1 (WT), Flag-Ssa1 S151A (S151A), or Flag-Ssa1 S151D (S151D) were monitored for growth over time in the absence or presence of rapamycin (100 ng/mL). (B) Δ*ssa1-4* yeast cells expressing Flag-Ssa1 (WT), Flag-Ssa1 S151A (S151A), or Flag-Ssa1 S151D (S151D) were spotted in fivefold serial dilution on control or rapamycin plates (100 ng/mL) as indicated.

Translation inhibition is a common response to many types of environmental stress (167). Cellular RNA-containing granules form during nutrient deprivation and during stationary phase and serve to protect mRNAs as well as to promote translation re-initiation and elongation after stress conditions are resolved. In budding yeast, Ssa proteins and Hsp40 co-chaperones are important for the formation of cytoplasmic RNA-protein (RNP) granules (stress granule and P-bodies)(168). Here we investigated the efficiency of RNP granule formation by examining GFP-SSA1 foci formation during glucose deprivation and stationary phase. The results showed that cells expressing Ssa1 S151D completely failed to form RNP granules during glucose deprivation (Figure 3.14A). We also examined the behavior of GFP-Ssa1 in stationary phase during which the chaperone also is known to form discrete foci (169). We observed a lower density of RNP granules in both S151A and S151D cells compared to wild-type cells, although S151D expression reduced foci to a greater extent than S151A (Figure 3.14B). Thus, reorganization of Ssa1 into stress granules is sensitive to the phosphorylation status of S151.

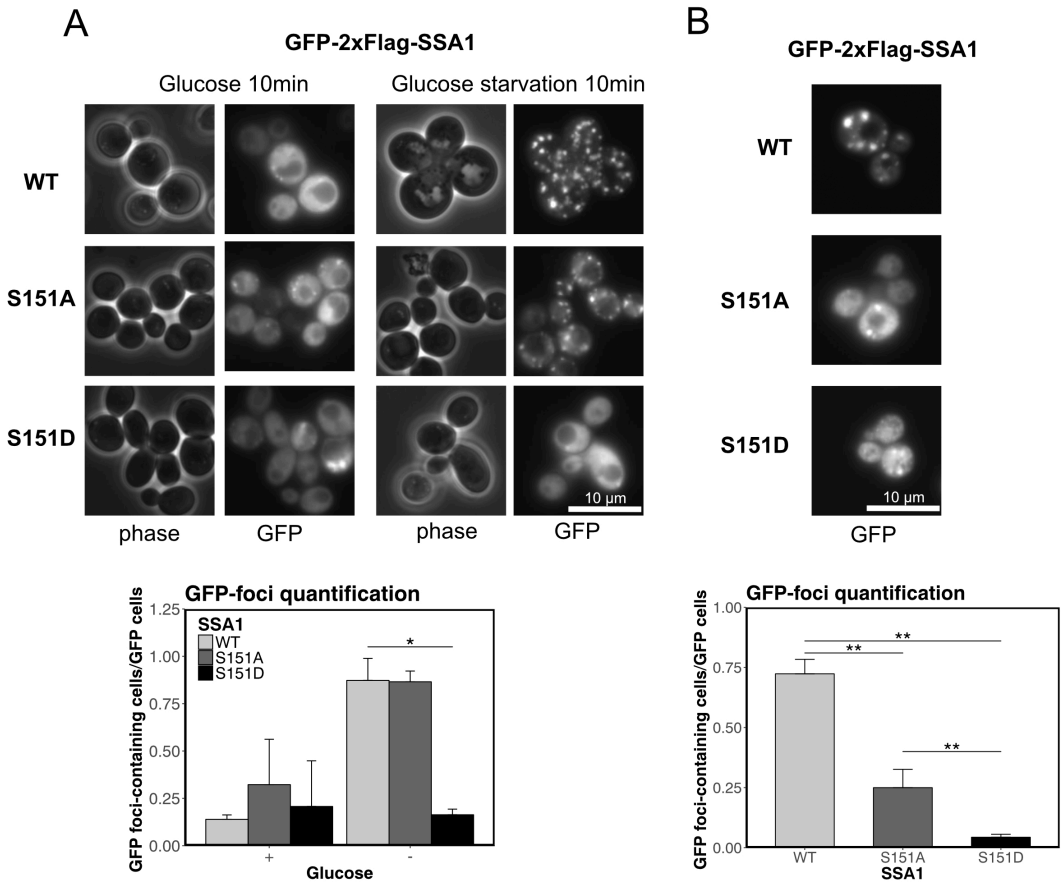

Figure 3.14 Ssa1 S151 phosphorylation regulates chaperone localization in response to stress**.** (A) Top panel: Δ*ssa1-4* yeast cells expressing GFP-Flag-Ssa1 (WT), GFP-Flag-Ssa1 S151A (S151A), or GFP-Flag-Ssa1 S151D (S151D) were incubated with or without 2% glucose for 10 min and analyzed by fluorescence microscopy. Bottom panel: Quantification of GFP foci was performed by counting the number of cells containing at least 1 GFP focus divided by the total number of GFP-positive cells. 3 biological replicates were performed with at least 50 cells counted per measurement; error bars represent standard deviation. * indicates $p < 0.05$ by student's 2-tailed T test.
(B) Top panel: Δ*ssa1-4* yeast cells expressing GFP-Flag-Ssa1 (WT), GFP-Flag-Ssa1 S151A (S151A), or GFP-Flag-Ssa1 S151D (S151D) were incubated at 30°C for 3 days to

Figure 3.14: continued
reach saturation and analyzed by fluorescence microscopy for GFP foci. Bottom panel: Quantification of GFP foci was performed by counting the number of cells containing at least 1 GFP focus divided by the total number of GFP-positive cells. 3 biological replicates were performed with at least 50 cells counted per measurement; error bars represent standard deviation. ** indicates $p < 0.05$ by student 2-tailed T test.

S151 Phosphorylation Regulates the Interactome of Ssa1

Hsp70 orthologs participate in a wide range of cellular processes through their ATP-dependent cycles of client recognition and protein folding (170). In order to investigate the impact of Ssa1 S151 phosphorylation on the global interactome of Ssa1, we purified GFP-Flag-tagged Ssa1 wild-type, Ssa1 (S151A), and Ssa1 (S151D) proteins from yeast cells during exponential growth and compared their binding partners by quantitative liquid chromatography-tandem mass spectrometry (LC-MS/MS). We detected 2006 proteins in lysates and immunoprecipitates and used untagged Ssa1 for immunoprecipitation as a negative control. The bound proteins included known co-chaperones and chaperone-associated factors as well as other proteins that may be clients. We identified 46 proteins significantly altered in their binding to S151A compared to wild-type chaperone, while 57 proteins are altered in cells expressing S151D, comparing 3 biological replicates from each strain (Figure 3.15A-C) These results suggested that the Ssa1 S151 phosphorylation broadly influences the binding between Ssa1 and cellular factors.

A

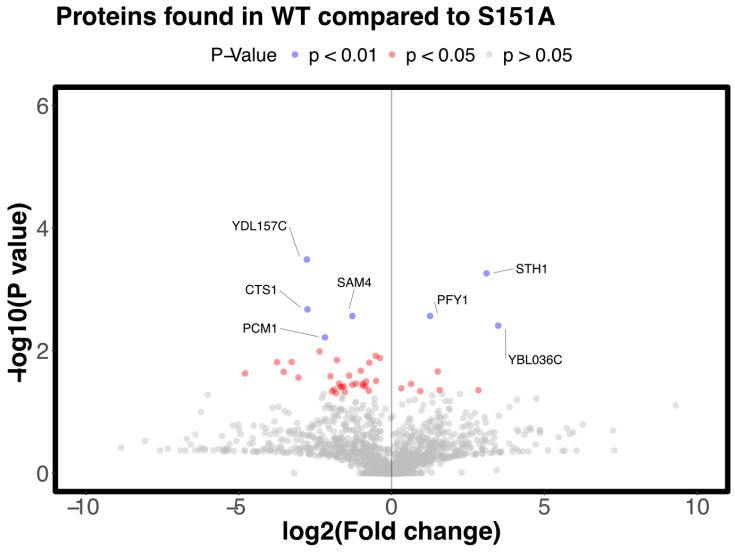

B

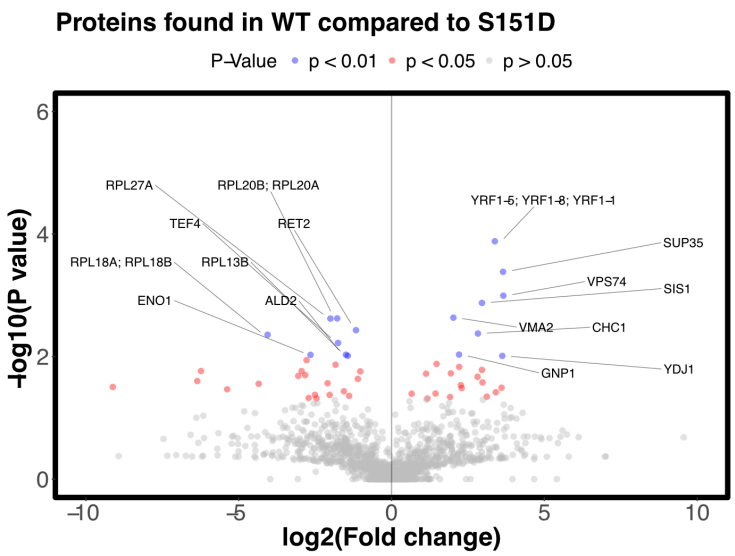

C

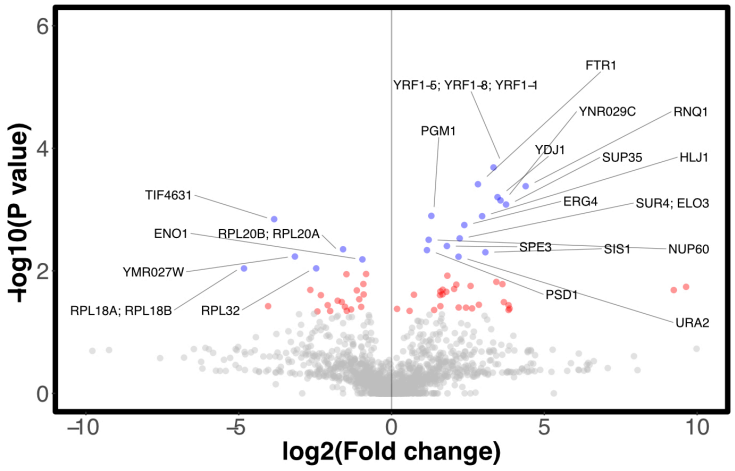

Figure 3.15: continued next page

Figure 3.15 S151 phosphorylation regulates the interactome of Ssa1. Δ*ssa1-4* yeast cells expressing GFP-Flag-Ssa1 (WT), GFP-Flag-Ssa1 S151A (S151A), or GFP-Flag-Ssa1 S151D (S151D) were grown to exponential phase. Ssa1 was isolated by immunoprecipitation and binding partners were analyzed by label-free quantitative LC-MS/MS from 3 biological replicates. (A-C) Volcano plot comparison of Ssa1 binding partners between WT and SA (A), WT and SD (B), and SA and SD (C) summarizing results of t tests by showing log2 ratios of the fold change between comparisons (X axis) and the -log10 of p values (Y axis) for each binding partner identified. Values were normalized by levels of Ssa1 recovered from each immunoprecipitation. Error bars represent standard deviation. * indicates $p < 0.05$ by student 2-tailed T test.

J-domain containing proteins (Hsp40s) and nucleotide-exchange factors (NEFs) are the major regulators of Hsp70 in its catalytic cycle (4). Both co-chaperones dynamically interact with Hsp70 and carry out diverse functions. Hsp40 proteins transfer substrates to Hsp70 and promote ATP hydrolysis by Hsp70, which transforms Hsp70 into an ADP-bound closed conformation in which the substrate is tightly bound (171). To complete the Hsp70 conformational cycle, NEFs promote the exchange of ADP for ATP and transform Hsp70 back to an ATP-bound open conformation which releases the folded client (172). Two of the primary Hsp40 enzymes in S. *cerevisiae* are Ydj1 (Type I) and Sis1 (Type II), each of which independently direct Hsp70 to execute different cellular functions (89, 168, 173). In our co-immunoprecipitation analysis, both Ydj1 and Sis1 are detected with wild-type Ssa1 and the S151A mutant, but show significantly lower association with Ssa1 S151D (Figure 3.16A-B). In addition, we found that several known Hsp70 binding partners including endoplasmic reticulum (ER)-specific co-chaperone (HLJ1), mitochondria-specific ATPase (MCX1), and prion-associated factors (SUP35 and RNQ1) exhibited higher association with Ssa1 S151A compared to Ssa1 S151D (Figure 3.15C). In contrast, several ribosomal proteins (both small and large subunit) exhibited higher association with Ssa1 S151D compared to Ssa1 S151A (Figure 3.15C.

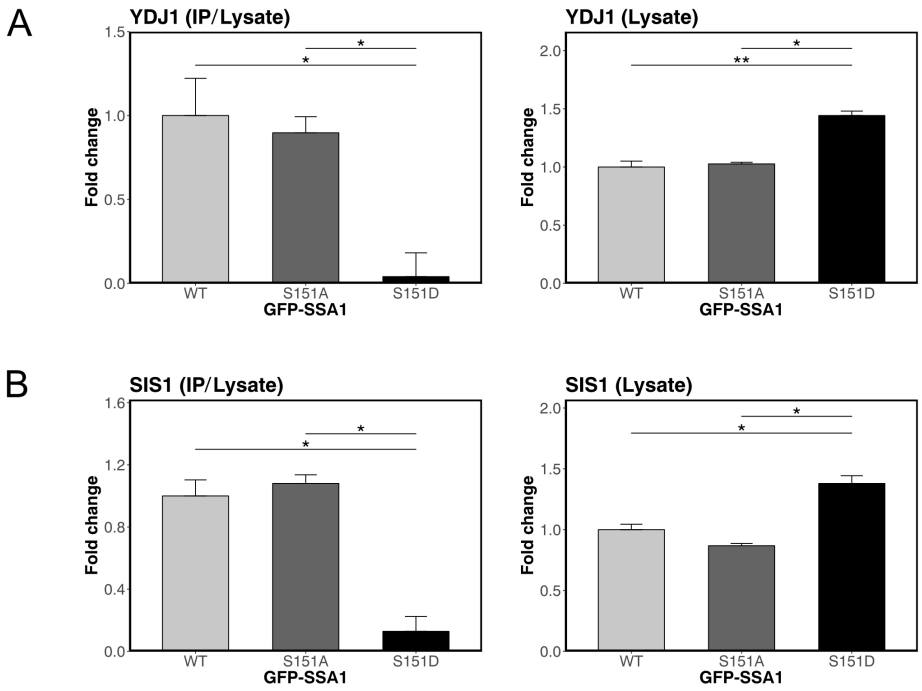

Figure 3.16 Phospho-mimetic mutant Ssa1 fails to associate with Type I and Type II Hsp40s in budding yeast. (A) Quantification of Ydj1 binding to WT, SA, or SD forms of Ssa1 in immunoprecipitations normalized by total lysates ("IP/Lysate") compared to the levels in total lysates ("Lysate"). (B) Quantification of Sis1 binding to WT, SA, or SD forms of Ssa1 in immunoprecipitations normalized by total lysates ("IP/Lysate") compared to the levels in total lysates ("Lysate"). Error bars represent standard deviation. * and ** indicate $p < 0.05$ and $p<0.01$, respectively, by student 2-tailed T test.

The binding defect between Ssa1 S151D and the Hsp40 factors could underlie the growth and heat survival deficits observed with this mutant. One possibility we considered was that the S151D phenotype might be suppressed by overexpression of the Hsp40 factors that exhibit lower levels of binding. To test this, we overexpressed Ydj1 and Sis1 with an inducible GAL promoter in cells expressing wild-type, S151A, or S151D Ssa1 genes at 30°C (Figure 3.17). Instead of rescuing the S151D growth defect, we found that the S151D-expressing cells were nearly inviable with galactose induction of Ydj1 and Sis1. Thus the reduction in Ydj1 and Sis1 binding cannot be functionally overcome by overexpression.

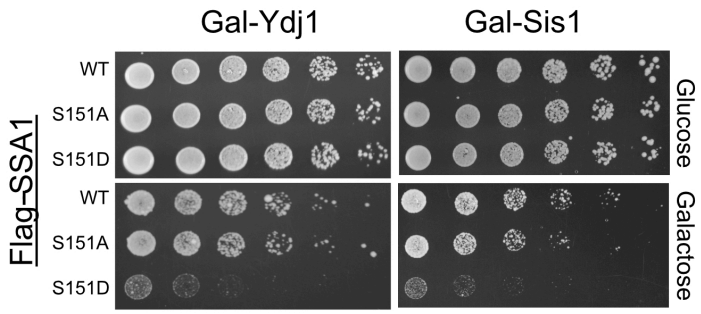

Figure 3.17 Overexpression of Type I and Type II Hsp40s fail to complement the phenotype of phospho-mimetic mutant Ssa1. Δ*ssa1-4* yeast cells expressing Flag-Ssa1 (WT), Flag-Ssa1 S151A (S151A), or Flag-Ssa1 S151D (S151D) as well as galactose-inducible Ydj1 (Gal-Ydj1) or Sis1 (Gal-Sis1) were spotted on glucose or galactose-containing plates in fivefold serial dilution and grown for 3 days.

In addition to facilitating client binding by Hsp70 proteins, Ydj1 also promotes association between Ssa1 and Hsp104 as well as with small chaperones such as Hsp12, Hsp26, and Hsp31 to promote disaggregation and refolding of aggregated proteins (174–176). Perhaps relevant to this function, we observed that Hsp104 and small chaperones have higher protein expression in cells expressing Ssa1 S151D. HSP82 (yeast HSP90), known to bind directly to Ssa1, is also present at higher levels in S151D-expressing cells (177). Combined with the observation that HSF1 is hyperactive in cells expressing Ssa1 S151D, these observations suggest that Ssa1 phosphorylation may have broad effects on many clients through altered co-chaperone binding properties.

Ssa1 S151 Phosphorylation Regulates Disaggregation by Ssa1, Ydj1, And Hsp104

Previous studies have demonstrated that Ssa1 together with the Hsp40 co-chaperone Ydj1 are able to refold misfolded proteins and to prevent the formation of large aggregates from misfolded proteins (2, 117). Budding yeast also have the Hsp104 chaperone, which cooperates with Hsp70 and Hsp40 proteins to generate an efficient protein disaggregation assembly (105). Hsp104 is a critical protein disaggregase for yeast cell survival of severe stress conditions, and has been shown to be responsible for extracting polypeptides from protein aggregates in cooperation with Ssa1 and Ydj1 (106).

To directly measure the effects of Ssa1 on protein folding, we established an in vitro luciferase-refolding assay with purified recombinant components (Figure 3.18A-C).

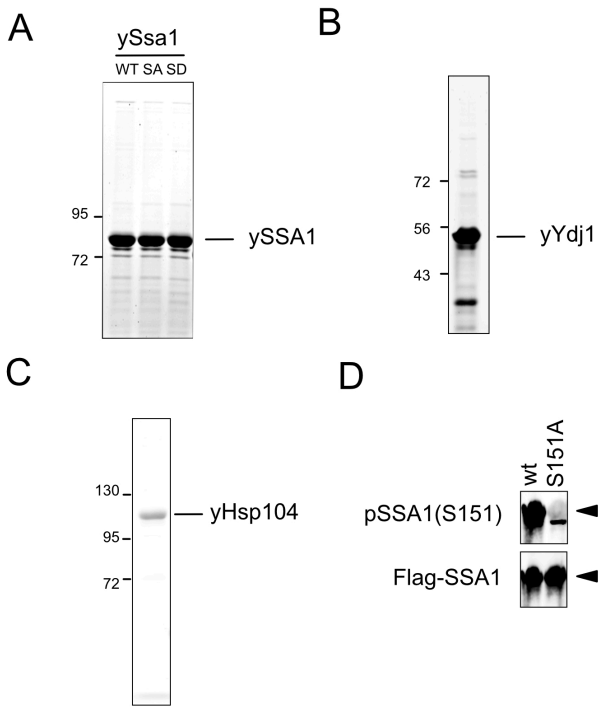

Figure 3.18 Recombinant proteins used in this study.

(A-C) Ssa1, Ssa1 (S151A), Ssa1 (S151D), Hsp104, and Ydj1 were separated by SDS-PAGE and stained with Coomassie Blue. (D) Ssa1 phosphorylation at S151 of recombinant Ssa1 proteins were analyzed by quantitative Western blotting with anti-phospho-Ssa1 S151 and anti-Flag antibodies.

We tested purified wild-type Ssa1, Ssa1 S151A, and Ssa1 S151D proteins in vitro with urea-denatured luciferase and found that purified Ssa1 S151D has poor luciferase reactivation efficiency compared to wild-type Ssa1 whereas the S151A mutant is more active than wild-type protein (Figure 3.19). In this case the Ssa1 proteins were produced in insect cells and the wild-type protein does have S151 phosphorylation (Figure 3.18D) so it is expected that the wild-type would show an intermediate level of activity compared

to the S151A and S151D mutants. Based on our co-immunoprecipitation observations, Ssa1 S151A and Ssa1 S151D mutants associate with Ydj1 differently, so Ydj1 might play a critical role in controlling refolding or disaggregation functions of Ssa1 in a manner that is controlled by S151 phosphorylation. We found that the combination of purified wild-type Ssa1 and Ydj1 was more efficient in reactivation of urea-denatured luciferase than reactions containing purified wild-type Ssa1 or purified Ydj1 only (Figure 3.19), consistent with previous reports (105). Both wild-type and S151A proteins were significantly more efficient in luciferase reactivation with Ydj1 present while the activity of the S151D protein did not improve at all with Ydj1 addition (Figure 3.19), consistent with our binding results in Figure 3.15 showing Ssa1 S151D has extremely reduced binding affinity for Ydj1.

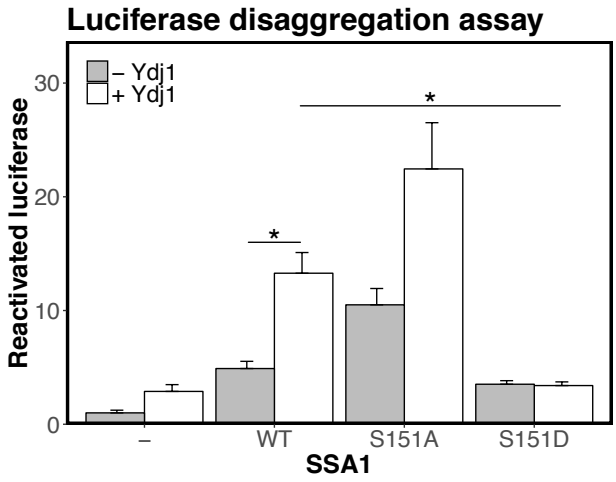

Figure 3.19 Ssa1 S151 phosphorylation regulates disaggregation by Ssa1 and Ydj1 *in vitro*. Recombinant wild-type Ssa1, Ssa1 S151A, and Ssa1 S151D proteins (2.5 μM) were incubated with denatured luciferase (3.3 x 10^4 units) in the presence or absence of Ydj1 (0.4 μM) and steady-state luciferase activity was measured. 3 biological replicates were performed and error bars represent standard deviation. * indicates $p < 0.05$ by student's 2-tailed T test.

Although Ssa1 and Ydj1 are able to perform a modest level of refolding, previous work has shown that Hsp104 can increase the level of luciferase reactivation by Ssa1 and Ydj1 (105). With purified Ssa1 and Ydj1 in the reaction, we thus compared the efficiency of the reaction with recombinant Hsp104 present (Figure 3.20). Consistent with previous results, we also observed that the addition of Hsp104 to wild-type Ssa1 and Ydj1 generated significantly higher levels of reactivated luciferase compared to reactions without Hsp104 (Figure 3.20A). This cooperative effect was also observed with Ssa1 S151A and Ydj1, but Ssa1 S151D and Ydj1 fail to cooperate with Hsp104 in reactivation of aggregated luciferase (Figure 3.20A). Without purified Ydj1, we observed that Ssa1 and Hsp104 failed to increase the level of luciferase reactivation although wild-type Ssa1 and Ssa1 S151A still showed more efficient luciferase reactivation than Ssa1 S151D (Figure 3.20B). The results indicate that purified Ssa1 S151D fails to form an efficient and functional disaggregase complex with Hsp104 in vitro, at least in part due to lack of productive binding to Ydj1.

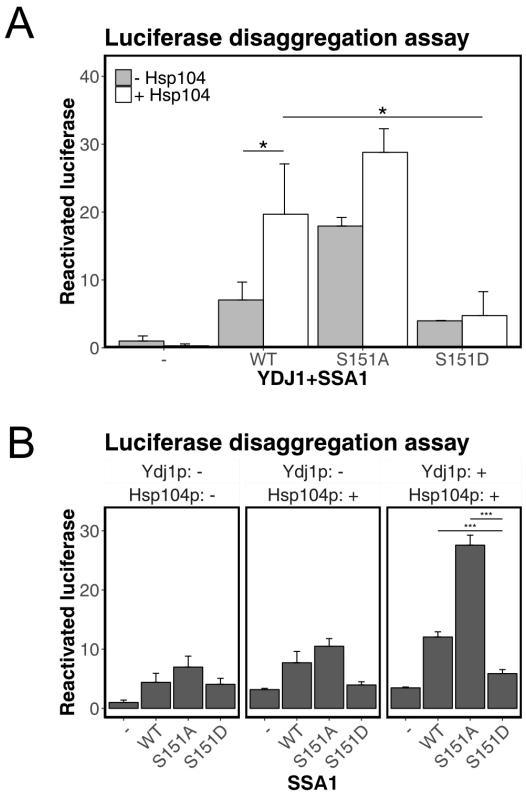

Figure 3.20 Ssa1 S151 phosphorylation regulates disaggregation by Ssa1, Ydj1, and Hsp104 *in vitro*. (A) Recombinant wild-type Ssa1, Ssa1 S151A, Ssa1 S151D, and Ydj1 were tested for luciferase reactivation as in Figure 3.16 but also in the presence of Hsp104 (1 μM) as indicated. (B) Comparative summary of luciferase assay results from Figure 3.19 and Figure 3.20A.

This deficiency is not due to a lack of ATPase activity, as measurements of ATP hydrolysis with purified S151D protein show approximately 2-fold higher rates of hydrolysis compared with wild-type or S151A protein in vitro (Figure 3.21).

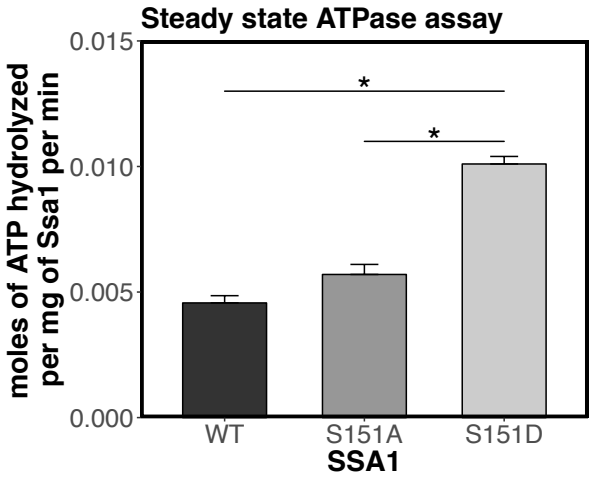

Figure 3.21 Steady-state levels of ATP hydrolysis activity of recombinant wild-type Ssa1 (WT), Ssa1 S151A (S151A), and Ssa1 S151D (S151D). 3 technical replicates were performed and error bars represent standard deviation. * indicates $p < 0.05$ by student's 2-tailed T test.

To determine if the effects of Ssa1 S151 phosphorylation are dependent on HSP104-dependent activities in vivo, we deleted the *HSP104* gene in our *Δssa1/2/3/4* yeast strain complemented by wild-type, S151A, or S151D *SSA1*. The cells were analyzed by serial dilutions on solid media and also exposed to heat shock at 39°C. The results show that Ssa1 S151D cells exhibit slow growth at elevated temperature compared to wild-type Ssa1-expressing cells while the Ssa1 S151A-expressing cells are even more

resistant than wild-type cells (Figure 3.22). Thus, the phosphorylation of S151 (as it occurs in the wild-type strain) yields greater functional deficiencies in the absence of HSP104 than in its presence.

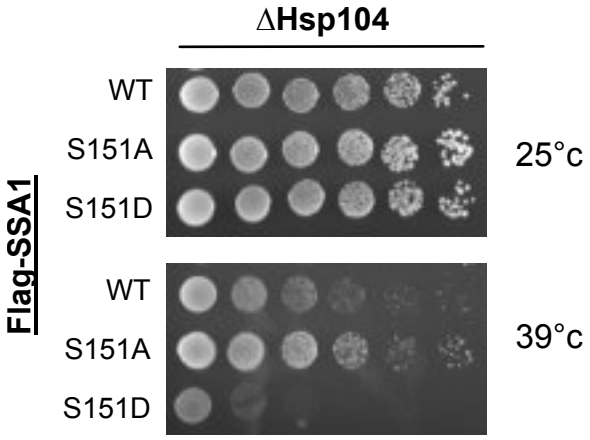

Figure 3.22 Ssa1 S151 phosphorylation are dependent on HSP104-dependent activities in vivo. Δ*ssa1-4 Hsp104*Δ yeast cells expressing Flag-Ssa1 (WT), Flag-Ssa1 S151A (S151A), or Flag-Ssa1 S151D (S151D) were spotted in fivefold serial dilutions and exposed to 30 or 39°C for 120 hr.

To test whether additional Hsp104 can recover the heat sensitivity of the S151D mutant strain, we introduced galactose-inducible Hsp104 into the *Δssa1/2/3/4* strain. Our results showed that additional Hsp104 expression did not affect growth of wild-type, Ssa1 S151A, or Ssa1 S151D cells at 30°C (Figure 3.23). Interestingly, Ssa1 S151D cells with endogenous levels of Hsp104 (glucose) were sensitive to the heat shock at 37°C in a short-term incubation (3 days), although recovered similar to wild-type cells after a long-term incubation (6 days). However, Ssa1 S151D cells with additional Hsp104 expression

in the presence of galactose lost the ability to recover (Figure 3.23). The result indicates that additional Hsp104 might create incomplete or dominant negative disaggregase complexes in the presence of Ssa1 S151D that not only are non-functional but can block protein refolding.

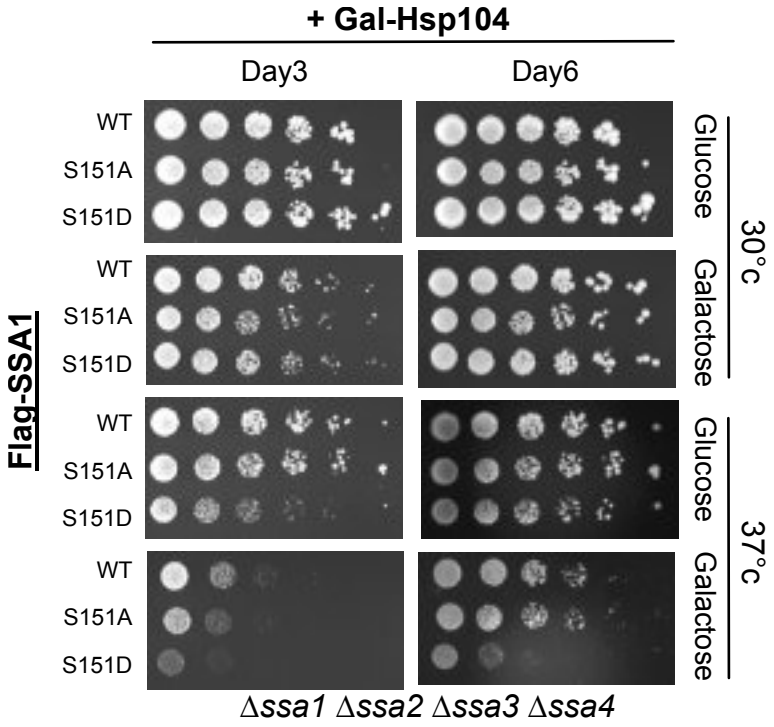

Figure 3.23 Additional Hsp104 can recover the heat sensitivity of the S151D mutant strain. Δ*ssa1-4* yeast cells expressing Flag-Ssa1 (WT), Flag-Ssa1 S151A (S151A), or Flag-Ssa1 S151D (S151D) as well as galactose-inducible Hsp104 (Gal-Hsp104) were spotted in fivefold serial dilutions and grown on glucose (Glu) or galactose (Gal) containing plates which were incubated at 30°C or 37°C for 3 days or 6 days as indicated.

S151 Phosphorylation Regulates Sup35 Prion Function

In our co-immunoprecipitation analysis, we observed that Ssa1 is associated with two prion-associated proteins, Rnq1 and Sup35, and that the S151D form of Ssa1 exhibits significantly lower binding to these proteins (Figure 3.24). The *S. cerevisiae [PSI$^+$]* prion is an inheritable, amyloid form of the Sup35 translation termination factor that is deficient in termination function (178). Formation of the amyloid form occurs spontaneously but is promoted by Hsp70 function, specifically Ssa1, as well by the Hsp104 disaggregation machinery, which is required to convert large prion assemblies into smaller units that "seed" new fibers (120, 122, 149, 179, 180). Rnq1 has a prion-like domain that can functionally substitute for Sup35 and is required for the de novo appearance of *[PSI$^+$]*(181, 182). To test whether Ssa1 phosphorylation plays a role in prion propagation, we monitored [*PSI*$^+$] using *Δssa1/2/3/4* yeast strain containing an *ade2-1* mutation as a color-based reporter for nonsense codon read-through (Figure 3.25)(183). In short, [*PSI*$^+$] propagation leads to the generation of functional ADE2 protein (white) due to partial loss of Sup35 termination activity, whereas [*psi*$^-$] cells have normal Sup35 activity and have a red pigment due to lack of ADE2 function

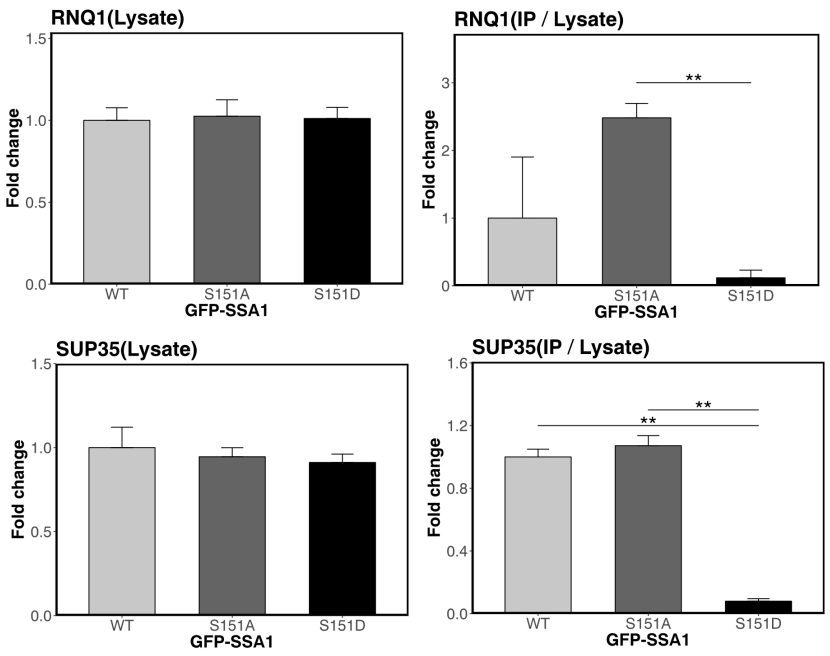

Figure 3.24 Dephosphorylation of Ssa1 at S151 exhibited higher association with prion proteins. Quantification of SUP35, and RNQ1 binding to WT, SA, or SD forms of Ssa1 in immunoprecipitations normalized by total lysates ("IP/Lysate") compared to the levels in total lysates ("Lysate") from the LC-MS analysis.

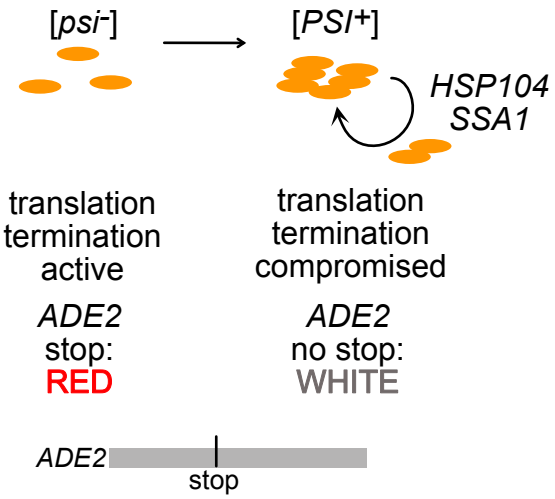

Figure 3.25 Schematic diagram of *[PSI+]* Sup35 prion formation and propagation through Ssa1/Hsp104-dependent generation of seeds that form new aggregates. Red or white colonies are formed depending on the level of Sup35 function, as indicated

Expression of wild-type, S151A, and S151D versions of *SSA1* in a [*PSI*$^+$] strain showed that [*PSI*$^+$] propagation is maximal (white colonies) with S151A, while it is slightly less efficient in wild-type SSA1-expressing cells (slightly pink colonies) after long-term incubation (5 days)(Figure 3.26). In contrast, cells expressing Ssa1 S151D show no apparent [*PSI*$^+$] activity (red colonies)(Figure 3.26). These results are consistent with our finding that Ssa1 S151A exhibits higher disaggregation efficiency in vitro whereas Ssa1 S151D fails to promote disaggregation under these conditions.

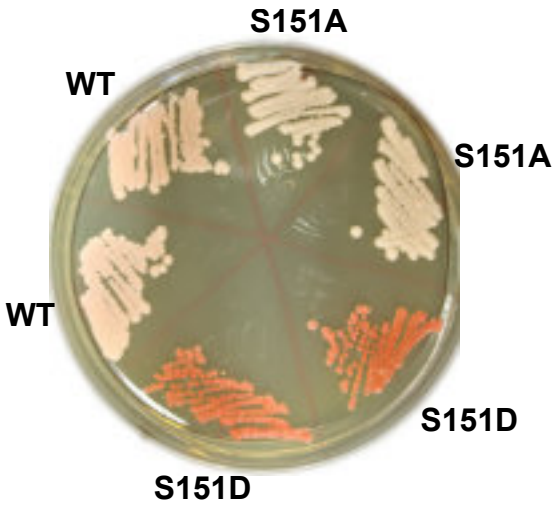

Figure 3.26 Prion propagation and heavy metal sensitivity are regulated by S151 Ssa1 phosphorylation. *[PSI+]* Δ*ssa1-4* yeast cells expressing full-length Ssa1 WT, S151A, or S151D from a CEN plasmid were streaked on YPD plates for 5 days to show the level of *ade2-1* nonsense read-through.

S151 Phosphorylation Regulates Survival of Heavy Metal Exposure

An early report of Δ*hsp104* phenotypes by Lindquist and colleagues showed that cells lacking this chaperone are dramatically resistant to heavy metal exposure (cadmium and copper) compared to wild-type cells (116). More recent work suggests that cadmium and copper compounds directly generate misfolding of nascent proteins in budding yeast, and that these and other heavy metals generate metal-protein aggregates that seed the formation of new aggregates (123, 124). In this sense, metal-induced misfolding intermediates may be analogous to prion intermediates in their ability to communicate protein misfolding states (Figure 3.27).

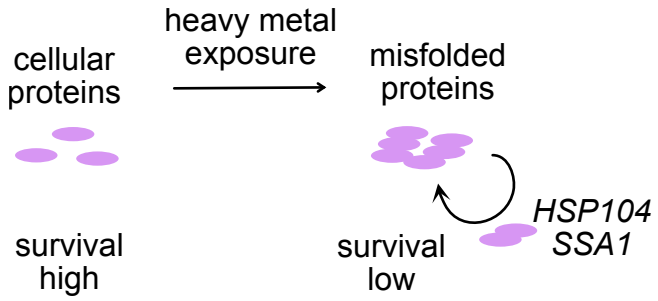

Figure 3.27 Schematic diagram of heavy metal-induced protein aggregation and propagation through Ssa1/Hsp104-dependent generation of seeds that form new aggregates.

To test if Ssa1 S153 phosphorylation may have a similar effect as Δ*hsp104*, we exposed yeast cells expressing wild-type, S151A, or S151D Ssa1 to copper (II) chloride and measured viability. It is clear that the phospho-mimic S151D allele promotes survival of copper exposure under these conditions at a level significantly higher than either S151A or wild-type Ssa1 expression (Figure 3.28), similar to the report for Δ*hsp104* (116).

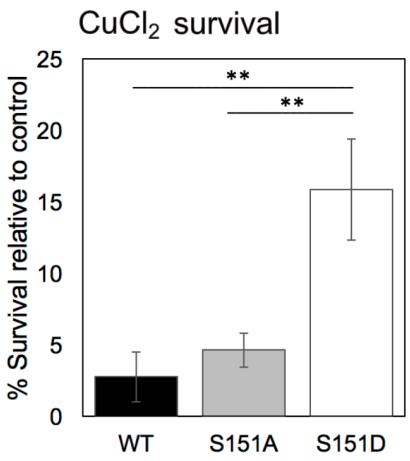

Figure 3.28 Ssa1 S151 phosphorylation may have a similar effect as Δ*hsp104* under exposure to copper (II) chloride. Δ*ssa1-4* yeast cells expressing full-length Ssa1 WT, S151A, or S151D from a CEN plasmid were exposed to $CuCl_2$ (11 mM) for 6 hrs, followed by washing out of copper and plating on non-selective plates to determine viability. Survival relative to controls are shown for each strain. ** indicates t test p value < 0.01.

S151 Phosphorylation Regulates Chaperone Function in Mammalian Cells

As discussed above, Ssa1 S151 is highly conserved in eukaryotes including humans, where S153 is the corresponding residue in the constitutive Hsc70 as well as heat-induced HSP70 (Figure 3.1). Hsc70/Hsp70 phosphorylation at S153 was observed previously in a study of global SQ/TQ phosphorylation sites in human cells (157), and we found this phosphorylation site in human U2OS osteosarcoma cells as well. To confirm that phosphorylation occurs during normal growth, we expressed V5-tagged wild-type HSC70 and a S153A mutant in U2OS cells, isolated the protein by immunoprecipitation,

followed by western blotting with the phospho-specific antibody. The results confirm that S153 phosphorylation does occur in these cells, although residual signal is still present with the S153A mutant, perhaps due to cross-reacting phosphorylation elsewhere in the protein (Figure 3.29).

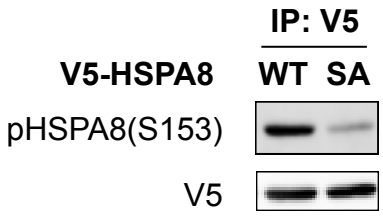

Figure 3.29 S151 phosphorylation occurs in mammalian cells and regulates heat-induces relocalization of Hsc70. V5-HSPA8 (WT) or V5-HSPA8 S153A (SA) were expressed in U2OS cells with concurrent HSPA8 and HSPA1A depletion. HSPA8 was isolated by immunoprecipitation and analyzed by Western blotting with anti-phospho-Ssa1 S151 and anti-V5 antibodies.

To investigate the role of Hsc70 phosphorylation at S153 we depleted endogenous Hsc70 using siRNA; however, in human cells, depletion of Hsc70 generates a dramatic induction of Hsp70 (HSPA1A/B) expression (Figure 3.30A) (151). To alleviate this overexpression we also depleted Hsp70, as previously described (151), resulting in 4-fold lower levels of Hsc70 with approximately 3-fold higher levels of Hsp70 relative to untreated cells. In these double-depleted cells we expressed V5-tagged wild-type Hsc70, the non-phosphorylatable mutant Hsc70 (S153A) or the phospho-mimetic mutant Hsc70 (S151D) from a stably-integrated doxycyline-inducible promoter (Figure 3.30B).

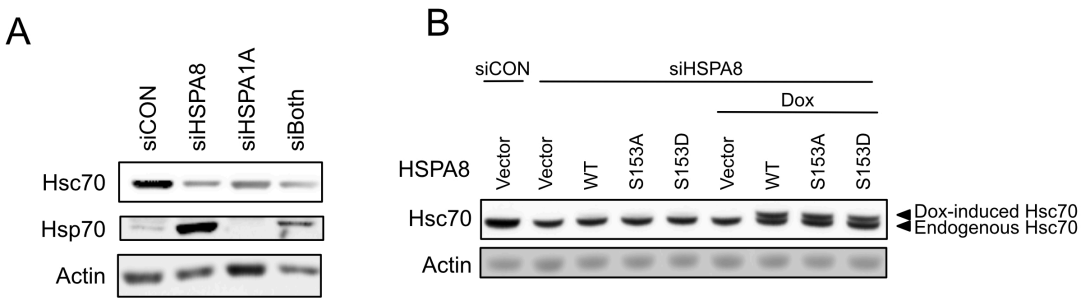

Figure 3.30 Complementation of U2OS cells depleted of endogenous Hsc70 and Hsp70. (A) U2OS cells were transfected with HSPA8 or HSPA1A-specific siRNA as indicated. After 72 hr, cell lysates were analyzed by Western blotting with anti-Hsc70 and anti-Hsp70 antibodies. (B) U2OS cells inducibly expressing V5-HSPA8 (WT), V5-HSPA8 S153A (S153A), or V5-HSPA8 S153D (S153D) were transfected with control siRNA or HSPA8-specific siRNA. Exogenous HSPA8 (white arrow) is induced by dox addition and compared to the level of endogenous HSPA8 (black arrow).

We tested for the effect of S153 phosphorylation status on survival of 39°C heat exposure and observed that cells expressing the phospho-mimetic S153D mutant were hypersensitive to heat shock (Figure 3.31), consistent with the results we observed in yeast cells (Figure 3.4). Therefore, Hsc70 S153 phosphorylation also acts in a dominant negative way during heat shock in human cells.

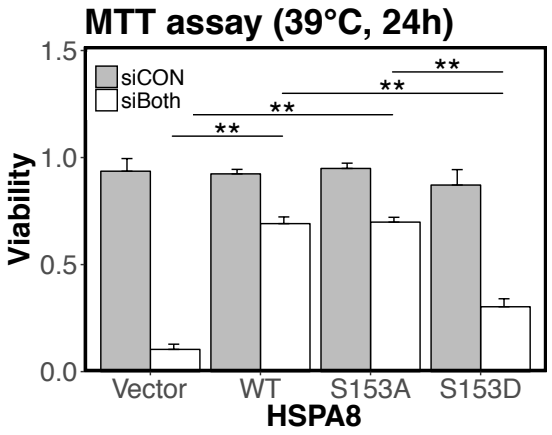

Figure 3.31 S153 phosphorylation regulates cell survival in response to heat shock. U2OS cells expressing V5-HSPA8 (WT), V5-HSPA8 S153A (S153A), or V5-HSPA8 S153D (S153D) were transfected with control siRNA (siCON) or both HSPA8 and HSPA1A siRNAs (siBoth) and seeded in 96-wells plates. Cells were treated with doxycylin to induce recombinant HSPA8 expression and incubated at 39°C for 24 hr. Cell viability was measured by MTT assay (Thermo Fisher Scientific). 3 biological replicates were performed and error bars represent standard deviation. * indicates $p < 0.05$ by student's 2-tailed T test.

Hsc70/Hsp70 proteins are critical in the nucleolus for ribosome biogenesis, stress responses, and cell signaling (184). In mammalian cells during heat shock, Hsc70 rapidly accumulates in nucleoli, a response which is important for counteracting damage and protein misfolding during heat stress (185, 186). We tested nucleoli accumulation of GFP-tagged wild-type, S153A, or S153D Hsc70 in U2OS cells during heat shock and found that Hsc70 S153D completely failed to accumulate in nucleoli compared to wild-type and Hsc70 S153A cells (Figure 3.32). Thus, S153 phosphorylation regulates Hsc70

relocalization in response to heat in a similar manner in humans as it does in budding yeast.

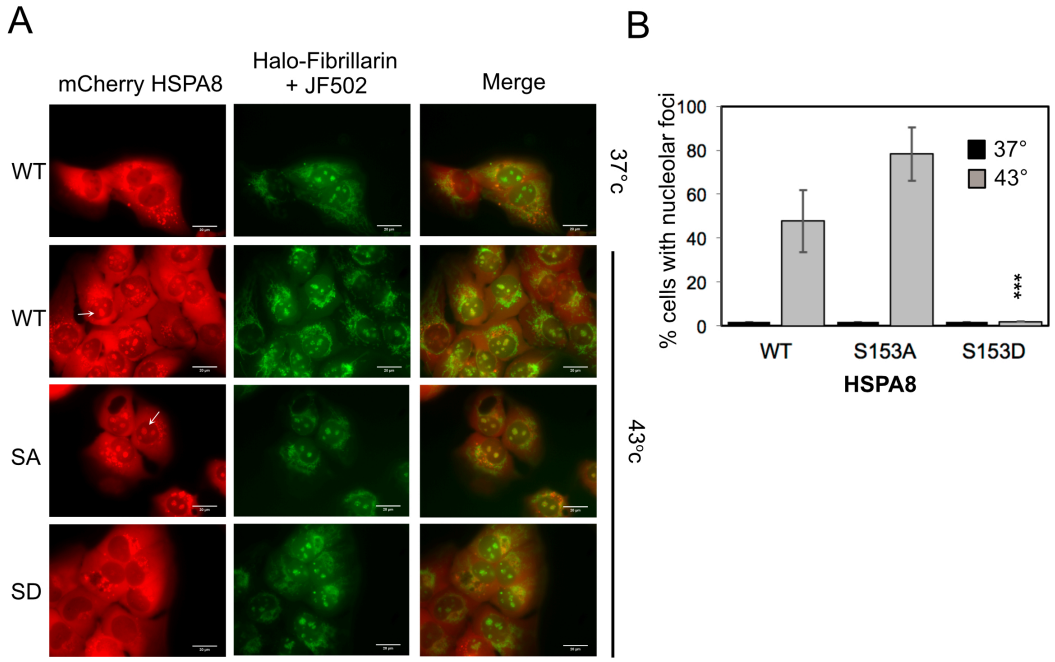

Figure 3.32 S153 phosphorylation regulates heat-induces relocalization of Hsc70. (A) mCherry-tagged WT, S153A, or S153D Hsc70 was expressed in U2OS cells expressing Halo-Fibrillarin and also treated with the JF502 halotag ligand. Cells were exposed to heat shock (43°C) for 60 min and analyzed by fluorescence microscopy. White arrows indicate nucleolar Hsc70. (B) Quantification of results from (A) showing percentage of cells with overlap between mCherry-Hsc70 and Halo-Fibrillarin. *** indicates t test p value < 0.0001 comparing S153D to either wild-type or S153A.

CHAPTER 4: DISCUSSION AND FUTURE DIRECTIONS

Here we investigated the role of Ssa1/HSC70 phosphorylation at S151(S153) during normal growth as well as stress conditions. We found that Ssa1 S151 phosphorylation is promoted by Cdk1 activity during logarithmic growth, and that this modification negatively regulates survival of heat exposure as well as starvation conditions. Ssa1 phosphorylation at S151 alters the interaction with Hsp40 co-chaperones that further impact the formation and function of Hsp104-dependent disaggregase complexes. Localization patterns of Ssa1 and Hsc70 in response to heat stress are also very sensitive to S151(S153) modification, as is survival of heavy metals and the maintenance of the *[PSI+]* prion in budding yeast. Thus Cdk1 appears to control many aspects of Ssa1/HSC70 function, and may regulate the ability of prions to affect gene expression.

The Effect of Chaperone Phosphorylation on Ssa1 Function

Hsp70 includes 3 major domains: the N-terminal nucleotide binding domain (NBD), a linker region, and the C-terminal substrate binding domain (SBD)(171). The ATPase activity of Hsp70 is mainly dependent on the NBD, a globular structure composed of four coordinated subdomains, each of which is responsible for specific interactions with ATP. However, previous studies of bacterial DnaK and DnaJ show that NBD ATPase activity is also tightly coupled to SBD interactions as well as to the binding of co-chaperone and peptide clients (187–189). Based on DnaK strutures as well as the Hsp70 ortholog Sse1, serine 151 of Ssa1 is predicted to be in a surface-exposed loop of the NBD, juxtaposed against the SBD (67, 69). Taken together, this data suggests that S151 phosphorylation

may not only play a regulatory role in domain interaction between NBD and SBD, but also in co-chaperone interactions.

Consistent with this prediction, we found that the phospho-mimetic version of S151, Ssa1 S151D, exhibits very low levels of binding to Ydj1 and Sis1: co-chaperones in the Hsp40 family responsible for escorting clients to Hsp70 and accelerating HSP70 ATP hydrolysis (75–77). Results with recombinant Ssa1 and Ydj1 in an *in vitro* luciferase refolding assay showed that non-phosphorylated Ssa1 (the S151A phospho-blocking mutant) exhibits even higher refolding efficiency than the wild-type Ssa1 protein and that addition of Ydj1 cooperatively increases this activity, as reported previously for Ssa1/Ydj1 (105). In contrast, the S151D mutant failed to promote any co-chaperone-mediated refolding, and expression of the Ssa1 S151D phospho-mimic allele *in vivo* results in accumulation of higher levels of more protein aggregates in vivo (Figure 3.6).

The Hsp104 chaperone is an important disaggregase in budding yeast, functioning cooperatively with Hsp70 and Hsp40 proteins to recognize aggregated proteins and extract individual polypeptides (105, 106). Here we found that the S151D phospho-mimic Ssa1 failed to cooperate with Hsp104 in luciferase refolding assays in vitro and also exhibited more severe heat shock sensitivity in a *Δhsp104* background in vivo. Under these conditions, the S151A form of Ssa1 was remarkably more efficient than wild-type Ssa1 in promoting heat shock survival, suggesting that the unphosphorylated form of Ssa1 can partially compensate for chaperone function normally provided by Hsp104. Expressing higher levels of Hsp104, Ydj1, and Sis1 in Ssa1 S151D strains failed to improve heat shock survival, thus the functional defect with S151D Ssa1 is not simply

a lower affinity of Ssa1 for the co-chaperones but more likely involves a conformational change that is incompatible with co-chaperone function. A similar combination of attributes was reported with Cdk1 phosphorylation of Ssa1 on T36, also in the NBD (142). In this case, the phospho-mimic version of Ssa1 (T36E) exhibited higher levels of nucleotide binding *in vitro*, low survival of heat shock, reduced binding to Ydj1 (although in this case no effect on Sis1 binding), and altered cell cycle progression (142). The T36 residue is adjacent to the ATP-binding pocket in Ssa1, unlike S151, probably explaining the change in nucleotide binding affinity, but similarly illustrates dominant negative effects of Cdk1 phosphorylation on Ssa1 functional interactions.

Ssa1 S151 Phosphorylation Occurs under Conditions of Rapid Growth

Although Ssa1 S151 does not conform to the S/T-P consensus phosphorylation motif that is normally found for Cdk1 substrates, our data from *in vitro* as well as *in vivo* assays indicates that Cdk1 participates in Ssa1 phosphorylation at S151 (Figure 3.8 and 3.9). Non-S/T-P sites for Cdk kinases have been reported in other biological contexts (190–195). Ssa1 S151 was also identified in a phosphorylation screen for Cdk1 targets, although the extent of cell cycle dependence was not very high compared to other targets, suggesting that there could also be other kinases responsible for this modification (153). Our results are not inconsistent with this conclusion as we do not see an absolute dependence on Cdk1 *in vivo*. We do observe a strong reduction in S151 phosphorylation with Tor inhibition and in stationary phase (Figure 3.10), suggesting that if there are other kinases involved they are likely also subject to growth regulation.

Consistent with the idea that S151 is generally unphosphorylated during conditions of growth inhibition, we found that cells expressing Ssa1 S151A exhibit significantly better growth in the presence of the Tor inhibitor rapamycin compared to cells expressing either wild-type or S151D Ssa1 (Figure 3.10). Previous proteomic analysis of yeast cells grown in the presence of rapamycin indicated that cells with activated Hsf1 are hypersensitive to rapamycin (196). Our finding that Ssa1 S151D-expressing cells show high levels of Hsf1 activation (Figure 3.5) is consistent with this, and suggests that regulation of S151 modifications contribute to survival during nutrient limitation. Ssa1 S151D also exhibits lower levels of binding to ribosomal subunits (Figure 3.7), a deficit that appears not to be growth-limiting under normal conditions but may be important for viability during starvation.

Negative Functional Effects of S151 Phosphorylation

The S151D phospho-mimic allele of Ssa1, as well as the S153D form of human HSC70, have mostly negative-acting functional effects on survival of stress conditions and growth. The S151A allele, on the other hand, exhibits either similar or higher activity than the wild-type S151 in these assays, with higher activity associated with Tor inhibition or Hsp104 deficiency. Most prokaryotes have an alanine at this position, so it is puzzling that eukaryotes have stably inherited and maintained a version of the chaperone that can be inactivated by a kinase that is active during normal growth.

One possibility is that the multiplication of Hsp70 orthologs in eukaryotes has selected for a diversification of functions and binding partners (197). In *S. cerevisiae*, the *SSA* subfamily (Ssa1, Ssa2, Ssa3, Ssa4) is important for protein folding, membrane

translocation, nuclear import, and transcriptional responses to a variety of stress conditions, while the *SSB* subfamily (Ssb1 and Ssb2) are key components of the ribosome-associated complex (RAC) that assists the de novo folding of newly synthesized polypeptides (158, 198–203). Ssb1 and Ssb2 have an alanine at the 151 position, while all 4 of the Ssa proteins have a serine. It could be that the ability to phosphorylate Ssa proteins, which is predicted to block Ydj1 and Sis1 binding, could promote associations that are beneficial in other environmental conditions. These alterations are likely tolerated because of the presence of the ubiquitously expressed, non-phosphorylatable Ssb proteins. Although most prokaryotes have an alanine at the equivalent position and most eukaryotes have a serine, the NCBI database shows approximately 120 bacterial and ascomycete species with an aspartate. How the Hsp70 proteins with this sequence function in concert with their respective DnaJ(Hsp40) co-chaperones is unknown.

Prions and Metal-Induced Misfolded Proteins as Targets of Hsp70 Activity

We show in this work that the *[PSI$^+$]* prion can be regulated by modification of S151 of Ssa1. Hsp70 is well-known for its role in prion dynamics, as many laboratories have documented the necessity of Hsp70, Hsp40, and Hsp104 protein families for propagation of the amyloid structures that constitute the infectious and heritable species (122, 178, 183, 204). Previous studies of Hsp70 mutants showed that an L483W change in Ssa1 generates higher rates of ATP hydrolysis, reduced co-chaperone binding, and reduced protein refolding efficiency in comparison to wild-type Ssa1, as well as dramatically

reduced ability of the protein to promote Sup35-dependent prion propagation (179, 205), all very similar to the Ssa1 S151D mutant described here.

The idea that misfolded proteins can form seeds that communicate misfolding to other, non aggregated protein species is common to both prions as well as to nascent proteins exposed to heavy metals (123, 124). In this sense, optimal chaperone function could be non-productive as it can generate new seeds from aggregated species and produce misfolded protein complexes at much higher rates compared to rates in the absence of chaperones. The higher viability conferred by S151D Ssa1 in the presence of copper suggests that there could be selection for phosphorylation due to pervasive heavy metals in the environment (206) that directly induce protein misfolding.

Our finding that Cdk1 is involved in phosphorylation of S151 suggests that *[PSI$^+$]* prion as well as metal-induced misfolded protein species would tend to be repressed by phospho(S151)-Ssa1 in actively growing cultures. *[PSI$^+$]* and other related prions in yeast affect translation read-through - a phenomenon proposed to increase the diversity of expressed proteins by translation of 3′ UTR regions and other normally untranslated sequences (204). It is attractive to consider the possibility that serine 151 phosphorylation is a mechanism by which this evolutionary diversification could be controlled, in effect a switch regulating the appearance of novel polypeptides that is dependent on stress conditions and growth rate. The evolutionary maintenance of S151 in eukaryotic Hsp70 orthologs, perhaps driven by metal exposure, could ultimately regulate diversification advantages through prion regulation of gene expression in a fluctuating environment.

Concluding Remarks and Future Work

The studies described here reveal the role of Hsp70 phosphorylation at S151/153 in yeast and human cells. Interestingly, the site is located in NBD and closed to the interaction interface between NBD and SBD. The distance between S151 from NBD and SBD is only ~3A, potentially indicating that S151 phosphorylation participates in the dynamic conformational changes of Hsp70. This is consistent with the effects of Hsp70 phosphorylation at S151 on the binding and releasing states of Hsp70 regulated by ATP/ADP exchange and co-chaperone binding. In order to confirm our hypothesis, a structural analysis is required to further understand the mechanistic regulation of phosphorylation on Hsp70. The next step of my current study would be compare the structure of wild-type Ssa1, non-phosphorylable version of Ssa1 (S151A), and phospho-mimetic version of Ssa1 (S151D) under the condition with or without co-chaperones and substrates. Among all cytosolic Hsp70s, Sse1 has glutamic acid (E) in a corresponding site to serine 151 in Ssa1-4 and the structure of Sse1 is similar to the structure of Ssa1 in an open state (67). It is possible that the phosphorylated and phosphomimetic versions of Ssa1 (S151D) might be a "holdase" similar to Sse1.

Although our studies have shown that Cdk1 and Tor are related to Hsp70 phosphorylation at S151 in yeast cells, we do not rule out the possibility of other kinases phosphorylating this site since only partial dependence on Cdk1 was observed (Figure 3.10 and 3.11). Further investigation of this issue using a kinase screen may be beneficial to understand the roles of different kinases from different signaling pathways in this regulation. Regarding other phosphorylation sites in Hsp70, we can also further evaluate

the potential combinatorial effects of S151 phosphorylation with other phosphorylation sites on Hsp70 functions.

Recent studies indicate that the TOR signaling pathway is connected to chaperone-mediated protein homeostasis (14, 15). TOR inhibition has been shown to be related to proteotoxic stress reduction by several related pieces of evidence: increased autophagy and decreased mRNA translation speed (16–18). TOR has tied to the formation of pre-atuophagosome by the regulation of Atg1, a critical upstream kinase in autophagy pathway (207, 208). As Tor plays a critical role in the autophagy and Ssa1 is partially regulated by Tor, we further tested whether Ssa1 phosphorylation at S151 affects autophagy by expressing a GFP-conjugated Atg8 reporter in wild-type Ssa1, Ssa1 S151, and Ssa1 S151D expressing cells. Cleavage of GFP from Atg8 was previously shown to be an accurate indicator for autophagy efficiency (209). However, we did not observe a significant difference in autophagy efficiency between wild-type and the mutants under rapamycin treatment (data not shown).

mRNA translation speed can also be a direct link between Tor inhibition and protein homeostasis. Translation is one of the sources of proteotoxic stress as nearly 10% of newly synthesized polypeptides are mistranslated in normally growing cells (19). Chaperone networks also participate in the maintenance of translation error by co-translational folding and the proteasome system. The TOR pathway is directly linked to translation speed through the regulation of ribosomal genes expression (20). Uncontrolled protein synthesis from a hyperactive form of TOR generates such high levels of translation that the chaperone system to maintain proper protein folding (162). In contrast, slower translation speed induced by rapamycin exposure can increase the

capacity for luciferase protein folding (162). Our data shows that wild-type and Ssa1 S151A both form stress granules and stall translation initiation under glucose deprivation and saturated culture conditions. This finding may suggest that Ssa1 phosphorylation at S151 affects translation speed, which would be consistent with a previous study indicating that Ssa1 is required for translation by associating with Sis1 and Pab1 (21). Previous investigation of the Ssa1 interactome has shown that Ssa1 associate with multiple ribosomal subunits (22), consistent with our data (Figure 3.7). Our results also indicated that Ssa1 S151A mutant has lower association with several ribosomal subunits compared to Ssa1 S151D mutant (Figure 3.7). Future directions may focus on evaluating the role of Hsp70 phosphorylation at S151 in co-translational folding.

The protein sequence alignment between different Hsp70 proteins indicates that mitochondria-specific HSP70 proteins (Ssc1 and Ssq1) have a serine residue at the site equivalent to S151 in Ssa1-4 whereas bacterial HSP70 protein (DnaK) and ribosomal HSP70 protein (Ssb1 and Ssb2) have an alanine at this position. We are interested in further understanding how phosphorylation could affect the function of Ssc1 and Ssq1 in mitochondria and whether this affects their interaction between mitochondria-specific co-chaperones and substrates. Also, we are interested in whether a phospho-mimic of this residue might compromise the functions of Ssb1 and Ssb2 in translation.

Taken together, our observations further characterize the functions of Hsp70 and their regulation by post-translational modifications. The fundamental functions of Hsp70 are related to the phosphorylation at S151 by modifying the Hsp70 catalytic cycle, co-chaperone binding, and ribosomal subunit association. The modified functions of phosphorylated Hsp70 further affect the Hsp104 disaggregase complex which determines

how Hsp70 regulates protein aggregation, prion propagation, and metal-induced misfolded proteins.

REFERENCES

1. Y. E. Kim, M. S. Hipp, A. Bracher, M. Hayer-Hartl, F. U. Hartl, Molecular chaperone functions in protein folding and proteostasis. *Annu. Rev. Biochem.* **82**, 323–355 (2013).

2. D. Balchin, M. Hayer-Hartl, F. U. Hartl, In vivo aspects of protein folding and quality control. *Science* **353**, aac4354 (2016).

3. C. Soto, Unfolding the role of protein misfolding in neurodegenerative diseases. *Nat. Rev. Neurosci.* **4**, 49–60 (2003).

4. H. Saibil, Chaperone machines for protein folding, unfolding and disaggregation. *Nat. Rev. Mol. Cell Biol.* **14**, 630–642 (2013).

5. H. H. Kampinga, E. A. Craig, The HSP70 chaperone machinery: J proteins as drivers of functional specificity. *Nat. Rev. Mol. Cell Biol.* **11**, 579–592 (2010).

6. M. Daugaard, M. Rohde, M. Jäättelä, The heat shock protein 70 family: Highly homologous proteins with overlapping and distinct functions. *FEBS Lett.* **581**, 3702–3710 (2007).

7. J. Verghese, J. Abrams, Y. Wang, K. A. Morano, Biology of the heat shock response and protein chaperones: budding yeast (Saccharomyces cerevisiae) as a model system. *Microbiol. Mol. Biol. Rev.* **76**, 115–158 (2012).

8. M. Werner-Washburne, D. E. Stone, E. A. Craig, Complex interactions among members of an essential subfamily of hsp70 genes in Saccharomyces cerevisiae. *Mol. Cell. Biol.* **7**, 2568–2577 (1987).

9. N. Hasin, S. A. Cusack, S. S. Ali, D. A. Fitzpatrick, G. W. Jones, Global transcript and phenotypic analysis of yeast cells expressing Ssa1, Ssa2, Ssa3 or Ssa4 as sole source of cytosolic Hsp70-Ssa chaperone activity. *BMC Genomics* **15**, 194 (2014).

10. P. Cloutier, B. Coulombe, Regulation of molecular chaperones through post-translational modifications: decrypting the chaperone code. *Biochim. Biophys. Acta* **1829**, 443–454 (2013).

11. P. Beltrao, *et al.*, Systematic functional prioritization of protein posttranslational modifications. *Cell* **150**, 413–425 (2012).

12. F. Ritossa, A new puffing pattern induced by temperature shock and DNP in drosophila. *Experientia* **18**, 571–573 (1962).

13. F. Ritossa, Discovery of the heat shock response. *Cell Stress Chaperones* **1**, 97–98 (1996).

14. S. L. McKenzie, S. Henikoff, M. Meselson, Localization of RNA from heat-induced polysomes at puff sites in Drosophila melanogaster. *Proc. Natl. Acad. Sci. U.S.A.* **72**, 1117–1121 (1975).

15. M. P. Scott, M. L. Pardue, Translational control in lysates of Drosophila melanogaster cells. *Proc. Natl. Acad. Sci. U.S.A.* **78**, 3353–3357 (1981).

16. J. M. Velazquez, S. Sonoda, G. Bugaisky, S. Lindquist, Is the major Drosophila heat shock protein present in cells that have not been heat shocked? *J. Cell Biol.* **96**, 286–290 (1983).

17. W. J. Gong, K. G. Golic, Loss of Hsp70 in Drosophila is pleiotropic, with effects on thermotolerance, recovery from heat shock and neurodegeneration. *Genetics* **172**, 275–286 (2006).

18. L. Nover, Ed., *Heat shock response* (CRC Press, 1991).

19. S. Lindquist, E. A. Craig, The heat-shock proteins. *Annu. Rev. Genet.* **22**, 631–677 (1988).

20. K. Watson, R. Cavicchioli, Acquisition of ethanol tolerance in yeast cells by heat shock. *Biotechnol Lett* **5**, 683–688 (1983).

21. , *Changes in Eukaryotic Gene Expression in Response to Environmental Stress* (Elsevier, 1985) https:/doi.org/10.1016/B978-0-12-066290-6.X5001-3 (July 31, 2019).

22. J. Plesset, C. Palm, C. S. McLaughlin, Induction of heat shock proteins and thermotolerance by ethanol in Saccharomyces cerevisiae. *Biochem. Biophys. Res. Commun.* **108**, 1340–1345 (1982).

23. F. C. Neidhardt, Stress proteins in biology and medicine. *Cell* **63**, 865–866 (1990).

24. G. M. Hahn, G. C. Li, Thermotolerance and Heat Shock Proteins in Mammalian Cells. *Radiation Research* **92**, 452 (1982).

25. H. H. Kampinga, *et al.*, Guidelines for the nomenclature of the human heat shock proteins. *Cell Stress Chaperones* **14**, 105–111 (2009).

26. E. A. Craig, K. Jacobsen, Mutations in cognate genes of Saccharomyces cerevisiae hsp70 result in reduced growth rates at low temperatures. *Mol. Cell. Biol.* **5**, 3517–3524 (1985).

27. R. J. Nelson, T. Ziegelhoffer, C. Nicolet, M. Werner-Washburne, E. A. Craig, The translation machinery and 70 kd heat shock protein cooperate in protein synthesis. *Cell* **71**, 97–105 (1992).

28. M. Gautschi, *et al.*, RAC, a stable ribosome-associated complex in yeast formed by the DnaK-DnaJ homologs Ssz1p and zuotin. *Proc. Natl. Acad. Sci. U.S.A.* **98**, 3762–3767 (2001).

29. C. Pfund, *et al.*, The molecular chaperone Ssb from Saccharomyces cerevisiae is a component of the ribosome-nascent chain complex. *EMBO J.* **17**, 3981–3989 (1998).

30. J. Rassow, *et al.*, Mitochondrial protein import: biochemical and genetic evidence for interaction of matrix hsp70 and the inner membrane protein MIM44. *J. Cell Biol.* **127**, 1547–1556 (1994).

31. G. Pareek, M. Samaddar, P. D'Silva, Primary Sequence That Determines the Functional Overlap between Mitochondrial Heat Shock Protein 70 Ssc1 and Ssc3 of *Saccharomyces cerevisiae*. *J. Biol. Chem.* **286**, 19001–19013 (2011).

32. M. Lussier, *et al.*, Large scale identification of genes involved in cell surface biosynthesis and architecture in Saccharomyces cerevisiae. *Genetics* **147**, 435–450 (1997).

33. B. Schilke, *et al.*, The cold sensitivity of a mutant of Saccharomyces cerevisiae lacking a mitochondrial heat shock protein 70 is suppressed by loss of mitochondrial DNA. *J. Cell Biol.* **134**, 603–613 (1996).

34. T. Lutz, B. Westermann, W. Neupert, J. M. Herrmann, The mitochondrial proteins Ssq1 and Jac1 are required for the assembly of iron sulfur clusters in mitochondria. *J. Mol. Biol.* **307**, 815–825 (2001).

35. B. Schilke, C. Voisine, H. Beinert, E. Craig, Evidence for a conserved system for iron metabolism in the mitochondria of Saccharomyces cerevisiae. *Proc. Natl. Acad. Sci. U.S.A.* **96**, 10206–10211 (1999).

36. J. Nieto-Sotelo, G. Wiederrecht, A. Okuda, C. S. Parker, The yeast heat shock transcription factor contains a transcriptional activation domain whose activity is repressed under nonshock conditions. *Cell* **62**, 807–817 (1990).

37. P. K. Sorger, H. R. Pelham, Purification and characterization of a heat-shock element binding protein from yeast. *EMBO J.* **6**, 3035–3041 (1987).

38. P. K. Sorger, H. R. Pelham, Yeast heat shock factor is an essential DNA-binding protein that exhibits temperature-dependent phosphorylation. *Cell* **54**, 855–864 (1988).

39. E. W. Trotter, L. Berenfeld, S. A. Krause, G. A. Petsko, J. V. Gray, Protein misfolding and temperature up-shift cause G1 arrest via a common mechanism dependent on heat shock factor in Saccharomycescerevisiae. *Proc. Natl. Acad. Sci. U.S.A.* **98**, 7313–7318 (2001).

40. A. Rowley, G. C. Johnston, B. Butler, M. Werner-Washburne, R. A. Singer, Heat shock-mediated cell cycle blockage and G1 cyclin expression in the yeast Saccharomyces cerevisiae. *Mol. Cell. Biol.* **13**, 1034–1041 (1993).

41. X. Zheng, *et al.*, Dynamic control of Hsf1 during heat shock by a chaperone switch and phosphorylation. *Elife* **5** (2016).

42. M. R. Fernández-Fernández, J. M. Valpuesta, Hsp70 chaperone: a master player in protein homeostasis. *F1000Res* **7** (2018).

43. A. Arakawa, *et al.*, The C-terminal BAG domain of BAG5 induces conformational changes of the Hsp70 nucleotide-binding domain for ADP-ATP exchange. *Structure* **18**, 309–319 (2010).

44. H. Sondermann, *et al.*, Structure of a Bag/Hsc70 complex: convergent functional evolution of Hsp70 nucleotide exchange factors. *Science* **291**, 1553–1557 (2001).

45. Y. Shomura, *et al.*, Regulation of Hsp70 function by HspBP1: structural analysis reveals an alternate mechanism for Hsp70 nucleotide exchange. *Mol. Cell* **17**, 367–379 (2005).

46. Z. Dragovic, S. A. Broadley, Y. Shomura, A. Bracher, F. U. Hartl, Molecular chaperones of the Hsp110 family act as nucleotide exchange factors of Hsp70s. *EMBO J.* **25**, 2519–2528 (2006).

47. C. J. Harrison, M. Hayer-Hartl, M. Di Liberto, F. Hartl, J. Kuriyan, Crystal structure of the nucleotide exchange factor GrpE bound to the ATPase domain of the molecular chaperone DnaK. *Science* **276**, 431–435 (1997).

48. P. Bork, C. Sander, A. Valencia, An ATPase domain common to prokaryotic cell cycle proteins, sugar kinases, actin, and hsp70 heat shock proteins. *Proc. Natl. Acad. Sci. U.S.A.* **89**, 7290–7294 (1992).

49. K. M. Flaherty, C. DeLuca-Flaherty, D. B. McKay, Three-dimensional structure of the ATPase fragment of a 70K heat-shock cognate protein. *Nature* **346**, 623–628 (1990).

50. J. N. Rao, Y. Madasu, R. Dominguez, Mechanism of actin filament pointed-end capping by tropomodulin. *Science* **345**, 463–467 (2014).

51. M. Vogel, M. P. Mayer, B. Bukau, Allosteric regulation of Hsp70 chaperones involves a conserved interdomain linker. *J. Biol. Chem.* **281**, 38705–38711 (2006).

52. A. Zhuravleva, L. M. Gierasch, Allosteric signal transmission in the nucleotide-binding domain of 70-kDa heat shock protein (Hsp70) molecular chaperones. *Proc. Natl. Acad. Sci. U.S.A.* **108**, 6987–6992 (2011).

53. J. F. Swain, *et al.*, Hsp70 chaperone ligands control domain association via an allosteric mechanism mediated by the interdomain linker. *Mol. Cell* **26**, 27–39 (2007).

54. E. R. P. Zuiderweg, *et al.*, Allostery in the Hsp70 chaperone proteins. *Top Curr Chem* **328**, 99–153 (2013).

55. M. R. Fernández-Fernández, M. Gragera, L. Ochoa-Ibarrola, L. Quintana-Gallardo, J. M. Valpuesta, Hsp70 - a master regulator in protein degradation. *FEBS Lett* **591**, 2648–2660 (2017).

56. X. Zhu, *et al.*, Structural analysis of substrate binding by the molecular chaperone DnaK. *Science* **272**, 1606–1614 (1996).

57. R. C. Morshauser, *et al.*, High-resolution solution structure of the 18 kDa substrate-binding domain of the mammalian chaperone protein Hsc70. *J. Mol. Biol.* **289**, 1387–1403 (1999).

58. K. M. Flaherty, S. M. Wilbanks, C. DeLuca-Flaherty, D. B. McKay, Structural basis of the 70-kilodalton heat shock cognate protein ATP hydrolytic activity. II. Structure of the active site with ADP or ATP bound to wild type and mutant ATPase fragment. *J. Biol. Chem.* **269**, 12899–12907 (1994).

59. M. Pellecchia, *et al.*, Structural insights into substrate binding by the molecular chaperone DnaK. *Nat. Struct. Biol.* **7**, 298–303 (2000).

60. J. Osipiuk, M. A. Walsh, B. C. Freeman, R. I. Morimoto, A. Joachimiak, Structure of a new crystal form of human Hsp70 ATPase domain. *Acta Crystallogr. D Biol. Crystallogr.* **55**, 1105–1107 (1999).

61. E. B. Bertelsen, H. Zhou, D. F. Lowry, G. C. Flynn, F. W. Dahlquist, Topology and dynamics of the 10 kDa C-terminal domain of DnaK in solution. *Protein Sci.* **8**, 343–354 (1999).

62. Y.-W. Chang, Y.-J. Sun, C. Wang, C.-D. Hsiao, Crystal structures of the 70-kDa heat shock proteins in domain disjoining conformation. *J. Biol. Chem.* **283**, 15502–15511 (2008).

63. M. Revington, Y. Zhang, G. N. B. Yip, A. V. Kurochkin, E. R. P. Zuiderweg, NMR investigations of allosteric processes in a two-domain Thermus thermophilus Hsp70 molecular chaperone. *J. Mol. Biol.* **349**, 163–183 (2005).

64. J. Jiang, K. Prasad, E. M. Lafer, R. Sousa, Structural basis of interdomain communication in the Hsc70 chaperone. *Mol. Cell* **20**, 513–524 (2005).

65. E. B. Bertelsen, L. Chang, J. E. Gestwicki, E. R. P. Zuiderweg, Solution conformation of wild-type E. coli Hsp70 (DnaK) chaperone complexed with ADP and substrate. *Proc. Natl. Acad. Sci. U.S.A.* **106**, 8471–8476 (2009).

66. J. F. Swain, E. G. Schulz, L. M. Gierasch, Direct comparison of a stable isolated Hsp70 substrate-binding domain in the empty and substrate-bound states. *J. Biol. Chem.* **281**, 1605–1611 (2006).

67. Q. Liu, W. A. Hendrickson, Insights into Hsp70 chaperone activity from a crystal structure of the yeast Hsp110 Sse1. *Cell* **131**, 106–120 (2007).

68. D. P. Easton, Y. Kaneko, J. R. Subjeck, The hsp110 and Grp1 70 stress proteins: newly recognized relatives of the Hsp70s. *Cell Stress Chaperones* **5**, 276–290 (2000).

69. R. Kityk, J. Kopp, I. Sinning, M. P. Mayer, Structure and dynamics of the ATP-bound open conformation of Hsp70 chaperones. *Mol. Cell* **48**, 863–874 (2012).

70. R. Qi, *et al.*, Allosteric opening of the polypeptide-binding site when an Hsp70 binds ATP. *Nat. Struct. Mol. Biol.* **20**, 900–907 (2013).

71. A. Zhuravleva, E. M. Clerico, L. M. Gierasch, An interdomain energetic tug-of-war creates the allosterically active state in Hsp70 molecular chaperones. *Cell* **151**, 1296–1307 (2012).

72. A. L. Lai, *et al.*, Key features of an Hsp70 chaperone allosteric landscape revealed by ion-mobility native mass spectrometry and double electron-electron resonance. *J. Biol. Chem.* **292**, 8773–8785 (2017).

73. A. Zhuravleva, L. M. Gierasch, Substrate-binding domain conformational dynamics mediate Hsp70 allostery. *Proc Natl Acad Sci USA* **112**, E2865–E2873 (2015).

74. J. Yang, M. Nune, Y. Zong, L. Zhou, Q. Liu, Close and Allosteric Opening of the Polypeptide-Binding Site in a Human Hsp70 Chaperone BiP. *Structure* **23**, 2191–2203 (2015).

75. M. E. Cheetham, A. J. Caplan, Structure, function and evolution of DnaJ: conservation and adaptation of chaperone function. *Cell Stress Chaperones* **3**, 28–36 (1998).

76. M. K. Greene, K. Maskos, S. J. Landry, Role of the J-domain in the cooperation of Hsp40 with Hsp70. *Proc. Natl. Acad. Sci. U.S.A.* **95**, 6108–6113 (1998).

77. J. Jiang, *et al.*, Structural basis of J cochaperone binding and regulation of Hsp70. *Mol. Cell* **28**, 422–433 (2007).

78. B. A. Schilke, *et al.*, Broadening the functionality of a J-protein/Hsp70 molecular chaperone system. *PLoS Genet.* **13**, e1007084 (2017).

79. J. Tsai, M. G. Douglas, A conserved HPD sequence of the J-domain is necessary for YDJ1 stimulation of Hsp70 ATPase activity at a site distinct from substrate binding. *J. Biol. Chem.* **271**, 9347–9354 (1996).

80. R. Kityk, J. Kopp, M. P. Mayer, Molecular Mechanism of J-Domain-Triggered ATP Hydrolysis by Hsp70 Chaperones. *Molecular Cell* **69**, 227-237.e4 (2018).

81. C. Sahi, E. A. Craig, Network of general and specialty J protein chaperones of the yeast cytosol. *Proceedings of the National Academy of Sciences* **104**, 7163–7168 (2007).

82. S. Ghaemmaghami, *et al.*, Global analysis of protein expression in yeast. *Nature* **425**, 737–741 (2003).

83. M. Reidy, *et al.*, Hsp40s specify functions of Hsp104 and Hsp90 protein chaperone machines. *PLoS Genet.* **10**, e1004720 (2014).

84. J. C. Silva, J. C. Borges, D. M. Cyr, C. H. Ramos, I. L. Torriani, Central domain deletions affect the SAXS solution structure and function of yeast Hsp40 proteins Sis1 and Ydj1. *BMC Struct. Biol.* **11**, 40 (2011).

85. J. C. Borges, *et al.*, Identification of Regions Involved in Substrate Binding and Dimer Stabilization within the Central Domains of Yeast Hsp40 Sis1. *PLoS ONE* **7**, e50927 (2012).

86. A. J. Caplan, M. G. Douglas, Characterization of YDJ1: a yeast homologue of the bacterial dnaJ protein. *J. Cell Biol.* **114**, 609–621 (1991).

87. D. W. Summers, P. M. Douglas, C. H. I. Ramos, D. M. Cyr, Polypeptide transfer from Hsp40 to Hsp70 molecular chaperones. *Trends Biochem. Sci.* **34**, 230–233 (2009).

88. N. Lopez, R. Aron, E. A. Craig, Specificity of Class II Hsp40 Sis1 in Maintenance of Yeast Prion [RNQ^{+}]. *MBoC* **14**, 1172–1181 (2003).

89. C.-Y. Fan, S. Lee, H.-Y. Ren, D. M. Cyr, Exchangeable chaperone modules contribute to specification of type I and type II Hsp40 cellular function. *Mol. Biol. Cell* **15**, 761–773 (2004).

90. J. C. Borges, H. Fischer, A. F. Craievich, C. H. I. Ramos, Low resolution structural study of two human HSP40 chaperones in solution. DJA1 from subfamily A and DJB4 from subfamily B have different quaternary structures. *J. Biol. Chem.* **280**, 13671–13681 (2005).

91. C. H. I. Ramos, C. L. P. Oliveira, C.-Y. Fan, I. L. Torriani, D. M. Cyr, Conserved central domains control the quaternary structure of type I and type II Hsp40 molecular chaperones. *J. Mol. Biol.* **383**, 155–166 (2008).

92. N. B. Nillegoda, *et al.*, Crucial HSP70 co-chaperone complex unlocks metazoan protein disaggregation. *Nature* **524**, 247–251 (2015).

93. S. Laloraya, B. D. Gambill, E. A. Craig, A role for a eukaryotic GrpE-related protein, Mge1p, in protein translocation. *Proc. Natl. Acad. Sci. U.S.A.* **91**, 6481–6485 (1994).

94. S. Polier, Z. Dragovic, F. U. Hartl, A. Bracher, Structural basis for the cooperation of Hsp70 and Hsp110 chaperones in protein folding. *Cell* **133**, 1068–1079 (2008).

95. L. Shaner, A. Trott, J. L. Goeckeler, J. L. Brodsky, K. A. Morano, The function of the yeast molecular chaperone Sse1 is mechanistically distinct from the closely related hsp70 family. *J. Biol. Chem.* **279**, 21992–22001 (2004).

96. A. P. Gasch, *et al.*, Genomic expression programs in the response of yeast cells to environmental changes. *Mol. Biol. Cell* **11**, 4241–4257 (2000).

97. A. Y.-W. Yam, V. Albanèse, H.-T. J. Lin, J. Frydman, Hsp110 cooperates with different cytosolic HSP70 systems in a pathway for de novo folding. *J. Biol. Chem.* **280**, 41252–41261 (2005).

98. L. Shaner, H. Wegele, J. Buchner, K. A. Morano, The Yeast Hsp110 Sse1 Functionally Interacts with the Hsp70 Chaperones Ssa and Ssb. *J. Biol. Chem.* **280**, 41262–41269 (2005).

99. L. Shaner, R. Sousa, K. A. Morano, Characterization of Hsp70 binding and nucleotide exchange by the yeast Hsp110 chaperone Sse1. *Biochemistry* **45**, 15075–15084 (2006).

100. J. P. Schuermann, *et al.*, Structure of the Hsp110:Hsc70 nucleotide exchange machine. *Mol. Cell* **31**, 232–243 (2008).

101. H. Raviol, H. Sadlish, F. Rodriguez, M. P. Mayer, B. Bukau, Chaperone network in the yeast cytosol: Hsp110 is revealed as an Hsp70 nucleotide exchange factor. *EMBO J.* **25**, 2510–2518 (2006).

102. M. Kabani, C. McLellan, D. A. Raynes, V. Guerriero, J. L. Brodsky, HspBP1, a homologue of the yeast Fes1 and Sls1 proteins, is an Hsc70 nucleotide exchange factor. *FEBS Lett.* **531**, 339–342 (2002).

103. M. Kabani, J.-M. Beckerich, J. L. Brodsky, Nucleotide Exchange Factor for the Yeast Hsp70 Molecular Chaperone Ssa1p. *Molecular and Cellular Biology* **22**, 4677–4689 (2002).

104. A. K. Ho, G. A. Raczniak, E. B. Ives, S. R. Wente, The integral membrane protein snl1p is genetically linked to yeast nuclear pore complex function. *Mol. Biol. Cell* **9**, 355–373 (1998).

105. J. R. Glover, S. Lindquist, Hsp104, Hsp70, and Hsp40: a novel chaperone system that rescues previously aggregated proteins. *Cell* **94**, 73–82 (1998).

106. J. Lee, *et al.*, Heat shock protein (Hsp) 70 is an activator of the Hsp104 motor. *Proc. Natl. Acad. Sci. U.S.A.* **110**, 8513–8518 (2013).

107. S. Lee, B. Sielaff, J. Lee, F. T. F. Tsai, CryoEM structure of Hsp104 and its mechanistic implication for protein disaggregation. *Proc. Natl. Acad. Sci. U.S.A.* **107**, 8135–8140 (2010).

108. S. Lee, *et al.*, The structure of ClpB: a molecular chaperone that rescues proteins from an aggregated state. *Cell* **115**, 229–240 (2003).

109. D. A. Parsell, A. S. Kowal, M. A. Singer, S. Lindquist, Protein disaggregation mediated by heat-shock protein Hsp104. *Nature* **372**, 475–478 (1994).

110. F. Seyffer, *et al.*, Hsp70 proteins bind Hsp100 regulatory M domains to activate AAA+ disaggregase at aggregate surfaces. *Nat. Struct. Mol. Biol.* **19**, 1347–1355 (2012).

111. R. Rosenzweig, S. Moradi, A. Zarrine-Afsar, J. R. Glover, L. E. Kay, Unraveling the mechanism of protein disaggregation through a ClpB-DnaK interaction. *Science* **339**, 1080–1083 (2013).

112. A. G. Cashikar, *et al.*, Defining a pathway of communication from the C-terminal peptide binding domain to the N-terminal ATPase domain in a AAA protein. *Mol. Cell* **9**, 751–760 (2002).

113. R. G. Mackay, C. W. Helsen, J. M. Tkach, J. R. Glover, The C-terminal extension of Saccharomyces cerevisiae Hsp104 plays a role in oligomer assembly. *Biochemistry* **47**, 1918–1927 (2008).

114. P. Wang, J. Li, C. Weaver, A. Lucius, B. Sha, Crystal structures of Hsp104 N-terminal domains from Saccharomyces cerevisiae and Candida albicans suggest the mechanism for the function of Hsp104 in dissolving prions. *Acta Crystallogr D Struct Biol* **73**, 365–372 (2017).

115. A. Heuck, *et al.*, Structural basis for the disaggregase activity and regulation of Hsp104. *Elife* **5** (2016).

116. Y. Sanchez, J. Taulien, K. A. Borkovich, S. Lindquist, Hsp104 is required for tolerance to many forms of stress. *EMBO J.* **11**, 2357–2364 (1992).

117. J. Becker, W. Walter, W. Yan, E. A. Craig, Functional interaction of cytosolic hsp70 and a DnaJ-related protein, Ydj1p, in protein translocation in vivo. *Mol. Cell. Biol.* **16**, 4378–4386 (1996).

118. R. B. Wickner, *et al.*, Yeast Prions: Structure, Biology, and Prion-Handling Systems. *Microbiol. Mol. Biol. Rev.* **79**, 1–17 (2015).

119. B. Moosavi, J. Wongwigkarn, M. F. Tuite, Hsp70/Hsp90 co-chaperones are required for efficient Hsp104-mediated elimination of the yeast [PSI(+)] prion but not for prion propagation. *Yeast* **27**, 167–179 (2010).

120. G.-C. Hung, D. C. Masison, N-terminal domain of yeast Hsp104 chaperone is dispensable for thermotolerance and prion propagation but necessary for curing prions by Hsp104 overexpression. *Genetics* **173**, 611–620 (2006).

121. M. Reidy, D. C. Masison, Sti1 Regulation of Hsp70 and Hsp90 Is Critical for Curing of Saccharomyces cerevisiae [PSI+] Prions by Hsp104. *Molecular and Cellular Biology* **30**, 3542–3552 (2010).

122. Y. O. Chernoff, S. L. Lindquist, B. Ono, S. G. Inge-Vechtomov, S. W. Liebman, Role of the chaperone protein Hsp104 in propagation of the yeast prion-like factor [psi+]. *Science* **268**, 880–884 (1995).

123. T. Jacobson, *et al.*, Cadmium Causes Misfolding and Aggregation of Cytosolic Proteins in Yeast. *Molecular and Cellular Biology* **37** (2017).

124. M. Tamás, S. Sharma, S. Ibstedt, T. Jacobson, P. Christen, Heavy Metals and Metalloids As a Cause for Protein Misfolding and Aggregation. *Biomolecules* **4**, 252–267 (2014).

125. A. Lilienbaum, Relationship between the proteasomal system and autophagy. *Int J Biochem Mol Biol* **4**, 1–26 (2013).

126. C. A. Ross, M. A. Poirier, Protein aggregation and neurodegenerative disease. *Nat. Med.* **10 Suppl**, S10-17 (2004).

127. V. N. Uversky, Protein folding revisited. A polypeptide chain at the folding ? misfolding ? nonfolding cross-roads: which way to go? *Cellular and Molecular Life Sciences (CMLS)* **60**, 1852–1871 (2003).

128. N. Sahni, *et al.*, Widespread macromolecular interaction perturbations in human genetic disorders. *Cell* **161**, 647–660 (2015).

129. T. Iwatsubo, *et al.*, Purification and characterization of Lewy bodies from the brains of patients with diffuse Lewy body disease. *Am. J. Pathol.* **148**, 1517–1529 (1996).

130. K. A. Conway, J. C. Rochet, R. M. Bieganski, P. T. Lansbury, Kinetic stabilization of the alpha-synuclein protofibril by a dopamine-alpha-synuclein adduct. *Science* **294**, 1346–1349 (2001).

131. T. Iwatsubo, Aggregation of alpha-synuclein in the pathogenesis of Parkinson's disease. *J. Neurol.* **250 Suppl 3**, III11-14 (2003).

132. J. S. Steffan, *et al.*, SUMO modification of Huntingtin and Huntington's disease pathology. *Science* **304**, 100–104 (2004).

133. M. Stefani, S. Rigacci, Protein folding and aggregation into amyloid: the interference by natural phenolic compounds. *Int J Mol Sci* **14**, 12411–12457 (2013).

134. L. C. Serpell, J. Berriman, R. Jakes, M. Goedert, R. A. Crowther, Fiber diffraction of synthetic alpha-synuclein filaments shows amyloid-like cross-beta conformation. *Proc. Natl. Acad. Sci. U.S.A.* **97**, 4897–4902 (2000).

135. L. C. Serpell, C. C. Blake, P. E. Fraser, Molecular structure of a fibrillar Alzheimer's A beta fragment. *Biochemistry* **39**, 13269–13275 (2000).

136. W. F. A. Den Dunnen, Trinucleotide repeat disorders. *Handb Clin Neurol* **145**, 383–391 (2017).

137. F. U. Hartl, A. Bracher, M. Hayer-Hartl, Molecular chaperones in protein folding and proteostasis. *Nature* **475**, 324–332 (2011).

138. K. Richter, M. Haslbeck, J. Buchner, The Heat Shock Response: Life on the Verge of Death. *Molecular Cell* **40**, 253–266 (2010).

139. null Nitika, A. W. Truman, Cracking the Chaperone Code: Cellular Roles for Hsp70 Phosphorylation. *Trends Biochem. Sci.* **42**, 932–935 (2017).

140. L. O'Regan, *et al.*, Hsp72 is targeted to the mitotic spindle by Nek6 to promote K-fiber assembly and mitotic progression. *J. Cell Biol.* **209**, 349–358 (2015).

141. Y.-J. Chen, *et al.*, HSP70 colocalizes with PLK1 at the centrosome and disturbs spindle dynamics in cells arrested in mitosis by arsenic trioxide. *Arch. Toxicol.* **88**, 1711–1723 (2014).

142. A. W. Truman, *et al.*, CDK-dependent Hsp70 Phosphorylation controls G1 cyclin abundance and cell-cycle progression. *Cell* **151**, 1308–1318 (2012).

143. T. Liu, *et al.*, Identification and characterization of a 66-68-kDa protein as a methotrexate-binding protein in murine leukemia L1210 cells. *Cell Stress Chaperones* **18**, 223–234 (2013).

144. C.-L. Ding, *et al.*, Anchoring of both PKA-RIIα and 14-3-3θ regulates retinoic acid induced 16 mediated phosphorylation of heat shock protein 70. *Oncotarget* **6**, 15540–15550 (2015).

145. N. Morgner, *et al.*, Hsp70 forms antiparallel dimers stabilized by post-translational modifications to position clients for transfer to Hsp90. *Cell Rep* **11**, 759–769 (2015).

146. P. Muller, *et al.*, C-terminal phosphorylation of Hsp70 and Hsp90 regulates alternate binding to co-chaperones CHIP and HOP to determine cellular protein folding/degradation balances. *Oncogene* **32**, 3101–3110 (2013).

147. D. Kaganovich, R. Kopito, J. Frydman, Misfolded proteins partition between two distinct quality control compartments. *Nature* **454**, 1088–1095 (2008).

148. E. C. Schirmer, O. R. Homann, A. S. Kowal, S. Lindquist, Dominant Gain-of-Function Mutations in Hsp104p Reveal Crucial Roles for the Middle Region. *Molecular Biology of the Cell* **15**, 2061–2072 (2004).

149. J. Shorter, S. Lindquist, Hsp104 catalyzes formation and elimination of self-replicating Sup35 prion conformers. *Science* **304**, 1793–1797 (2004).

150. A. Koplin, *et al.*, A dual function for chaperones SSB-RAC and the NAC nascent polypeptide-associated complex on ribosomes. *J. Cell Biol.* **189**, 57–68 (2010).

151. M. V. Powers, P. A. Clarke, P. Workman, Dual targeting of HSC70 and HSP72 inhibits HSP90 function and induces tumor-specific apoptosis. *Cancer Cell* **14**, 250–262 (2008).

152. C. P. Albuquerque, *et al.*, A multidimensional chromatography technology for in-depth phosphoproteome analysis. *Mol. Cell Proteomics* **7**, 1389–1396 (2008).

153. L. J. Holt, *et al.*, Global analysis of Cdk1 substrate phosphorylation sites provides insights into evolution. *Science* **325**, 1682–1686 (2009).

154. C.-H. Kao, *et al.*, "Growth-regulated Hsp70 phosphorylation regulates stress responses and prion maintenance" (Molecular Biology, 2019) https:/doi.org/10.1101/759241 (October 29, 2019).

155. S.-T. Kim, D.-S. Lim, C. E. Canman, M. B. Kastan, Substrate Specificities and Identification of Putative Substrates of ATM Kinase Family Members. *Journal of Biological Chemistry* **274**, 37538–37543 (1999).

156. T. O'Neill, *et al.*, Utilization of Oriented Peptide Libraries to Identify Substrate Motifs Selected by ATM. *Journal of Biological Chemistry* **275**, 22719–22727 (2000).

157. S. Matsuoka, *et al.*, ATM and ATR substrate analysis reveals extensive protein networks responsive to DNA damage. *Science* **316**, 1160–1166 (2007).

158. H. Jaiswal, *et al.*, The chaperone network connected to human ribosome-associated complex. *Mol. Cell. Biol.* **31**, 1160–1173 (2011).

159. A. Mogk, B. Bukau, H. H. Kampinga, Cellular Handling of Protein Aggregates by Disaggregation Machines. *Molecular Cell* **69**, 214–226 (2018).

160. J. Betting, W. Seufert, A yeast Ubc9 mutant protein with temperature-sensitive in vivo function is subject to conditional proteolysis by a ubiquitin- and proteasome-dependent pathway. *J. Biol. Chem.* **271**, 25790–25796 (1996).

161. A. C. Bishop, *et al.*, A chemical switch for inhibitor-sensitive alleles of any protein kinase. *Nature* **407**, 395–401 (2000).

162. C. S. Conn, S.-B. Qian, mTOR signaling in protein homeostasis: less is more? *Cell Cycle* **10**, 1940–1947 (2011).

163. H. Huang, *et al.*, Two mTOR inhibitors, rapamycin and Torin 1, differentially regulate iron-induced generation of mitochondrial ROS. *Biometals* **30**, 975–980 (2017).

164. N. C. Barbet, *et al.*, TOR controls translation initiation and early G1 progression in yeast. *Mol. Biol. Cell* **7**, 25–42 (1996).

165. L. H. Hartwell, J. Culotti, J. R. Pringle, B. J. Reid, Genetic control of the cell division cycle in yeast. *Science* **183**, 46–51 (1974).

166. M. D. Mendenhall, C. A. Jones, S. I. Reed, Dual regulation of the yeast CDC28-p40 protein kinase complex: cell cycle, pheromone, and nutrient limitation effects. *Cell* **50**, 927–935 (1987).

167. V. Cherkasov, *et al.*, Coordination of translational control and protein homeostasis during severe heat stress. *Curr. Biol.* **23**, 2452–2462 (2013).

168. R. W. Walters, D. Muhlrad, J. Garcia, R. Parker, Differential effects of Ydj1 and Sis1 on Hsp70-mediated clearance of stress granules in Saccharomyces cerevisiae. *RNA* **21**, 1660–1671 (2015).

169. R. Narayanaswamy, *et al.*, Widespread reorganization of metabolic enzymes into reversible assemblies upon nutrient starvation. *Proceedings of the National Academy of Sciences* **106**, 10147–10152 (2009).

170. E. M. Clerico, J. M. Tilitsky, W. Meng, L. M. Gierasch, How hsp70 molecular machines interact with their substrates to mediate diverse physiological functions. *J. Mol. Biol.* **427**, 1575–1588 (2015).

171. M. P. Mayer, Hsp70 chaperone dynamics and molecular mechanism. *Trends Biochem. Sci.* **38**, 507–514 (2013).

172. S. K. Sharma, P. De los Rios, P. Christen, A. Lustig, P. Goloubinoff, The kinetic parameters and energy cost of the Hsp70 chaperone as a polypeptide unfoldase. *Nat. Chem. Biol.* **6**, 914–920 (2010).

173. S. Rüdiger, J. Schneider-Mergener, B. Bukau, Its substrate specificity characterizes the DnaJ co-chaperone as a scanning factor for the DnaK chaperone. *EMBO J.* **20**, 1042–1050 (2001).

174. C.-Y. Fan, S. Lee, D. M. Cyr, Mechanisms for regulation of Hsp70 function by Hsp40. *Cell Stress Chaperones* **8**, 309–316 (2003).

175. A. G. Cashikar, M. Duennwald, S. L. Lindquist, A chaperone pathway in protein disaggregation. Hsp26 alters the nature of protein aggregates to facilitate reactivation by Hsp104. *J. Biol. Chem.* **280**, 23869–23875 (2005).

176. M. L. Duennwald, A. Echeverria, J. Shorter, Small Heat Shock Proteins Potentiate Amyloid Dissolution by Protein Disaggregases from Yeast and Humans. *PLoS Biology* **10**, e1001346 (2012).

177. A. N. Kravats, *et al.*, Functional and physical interaction between yeast Hsp90 and Hsp70. *Proc. Natl. Acad. Sci. U.S.A.* **115**, E2210–E2219 (2018).

178. S. W. Liebman, Y. O. Chernoff, Prions in Yeast. *Genetics* **191**, 1041–1072 (2012).

179. P. G. Needham, D. C. Masison, Prion-impairing mutations in Hsp70 chaperone Ssa1: effects on ATPase and chaperone activities. *Arch. Biochem. Biophys.* **478**, 167–174 (2008).

180. D. Sharma, D. C. Masison, Hsp70 structure, function, regulation and influence on yeast prions. *Protein Pept. Lett.* **16**, 571–581 (2009).

181. N. Sondheimer, S. Lindquist, Rnq1: an epigenetic modifier of protein function in yeast. *Mol. Cell* **5**, 163–172 (2000).

182. I. L. Derkatch, M. E. Bradley, J. Y. Hong, S. W. Liebman, Prions Affect the Appearance of Other Prions. *Cell* **106**, 171–182 (2001).

183. G. Jung, G. Jones, R. D. Wegrzyn, D. C. Masison, A role for cytosolic hsp70 in yeast [PSI(+)] prion propagation and [PSI(+)] as a cellular stress. *Genetics* **156**, 559–570 (2000).

184. P. Bański, M. Kodiha, U. Stochaj, Chaperones and multitasking proteins in the nucleolus: networking together for survival? *Trends Biochem. Sci.* **35**, 361–367 (2010).

185. S. Kose, M. Furuta, N. Imamoto, Hikeshi, a nuclear import carrier for Hsp70s, protects cells from heat shock-induced nuclear damage. *Cell* **149**, 578–589 (2012).

186. F. Frottin, *et al.*, The nucleolus functions as a phase-separated protein quality control compartment. *Science* **365**, 342–347 (2019).

187. G. Flynn, T. Chappell, J. Rothman, Peptide binding and release by proteins implicated as catalysts of protein assembly. *Science* **245**, 385–390 (1989).

188. A. Buchberger, *et al.*, Nucleotide-induced Conformational Changes in the ATPase and Substrate Binding Domains of the DnaK Chaperone Provide Evidence for Interdomain Communication. *Journal of Biological Chemistry* **270**, 16903–16910 (1995).

189. B. Bukau, A. L. Horwich, The Hsp70 and Hsp60 Chaperone Machines. *Cell* **92**, 351–366 (1998).

190. K. Suzuki, *et al.*, Identification of non-Ser/Thr-Pro consensus motifs for Cdk1 and their roles in mitotic regulation of C2H2 zinc finger proteins and Ect2. *Scientific Reports* **5** (2015).

191. M. Kusubata, *et al.*, cdc2 Kinase Phosphorylation of Desmin at Three Serine/Threonine Residues in the Amino-Terminal Head Domain. *Biochemical and Biophysical Research Communications* **190**, 927–934 (1993).

192. L. L. Satterwhite, Phosphorylation of myosin-II regulatory light chain by cyclin-p34cdc2: a mechanism for the timing of cytokinesis. *The Journal of Cell Biology* **118**, 595–605 (1992).

193. S. L. Harvey, A. Charlet, W. Haas, S. P. Gygi, D. R. Kellogg, Cdk1-Dependent Regulation of the Mitotic Inhibitor Wee1. *Cell* **122**, 407–420 (2005).

194. M. Isoda, *et al.*, Dynamic Regulation of Emi2 by Emi2-Bound Cdk1/Plk1/CK1 and PP2A-B56 in Meiotic Arrest of Xenopus Eggs. *Developmental Cell* **21**, 506–519 (2011).

195. D. McCusker, *et al.*, Cdk1 coordinates cell-surface growth with the cell cycle. *Nature Cell Biology* **9**, 506–515 (2007).

196. S. Bandhakavi, *et al.*, Hsf1 activation inhibits rapamycin resistance and TOR signaling in yeast revealed by combined proteomic and genetic analysis. *PLoS ONE* **3**, e1598 (2008).

197. V. Albanèse, A. Y.-W. Yam, J. Baughman, C. Parnot, J. Frydman, Systems analyses reveal two chaperone networks with distinct functions in eukaryotic cells. *Cell* **124**, 75–88 (2006).

198. W. R. Boorstein, T. Ziegelhoffer, E. A. Craig, Molecular evolution of the HSP70 multigene family. *J. Mol. Evol.* **38**, 1–17 (1994).

199. S. Kim, B. Schilke, E. A. Craig, A. L. Horwich, Folding in vivo of a newly translated yeast cytosolic enzyme is mediated by the SSA class of cytosolic yeast Hsp70 proteins. *Proc. Natl. Acad. Sci. U.S.A.* **95**, 12860–12865 (1998).

200. M. Oka, *et al.*, Loss of Hsp70-Hsp40 chaperone activity causes abnormal nuclear distribution and aberrant microtubule formation in M-phase of Saccharomyces cerevisiae. *J. Biol. Chem.* **273**, 29727–29737 (1998).

201. N. Shulga, *et al.*, In vivo nuclear transport kinetics in Saccharomyces cerevisiae: a role for heat shock protein 70 during targeting and translocation. *J. Cell Biol.* **135**, 329–339 (1996).

202. M. P. Mayer, B. Bukau, Hsp70 chaperone systems: diversity of cellular functions and mechanism of action. *Biol. Chem.* **379**, 261–268 (1998).

203. D. E. Stone, E. A. Craig, Self-regulation of 70-kilodalton heat shock proteins in Saccharomyces cerevisiae. *Mol. Cell. Biol.* **10**, 1622–1632 (1990).

204. J. Shorter, S. Lindquist, Prions as adaptive conduits of memory and inheritance. *Nature Reviews Genetics* **6**, 435–450 (2005).

205. G. W. Jones, D. C. Masison, Saccharomyces cerevisiae Hsp70 mutations affect [PSI+] prion propagation and cell growth differently and implicate Hsp40 and tetratricopeptide repeat cochaperones in impairment of [PSI+]. *Genetics* **163**, 495–506 (2003).

206. P. B. Tchounwou, C. G. Yedjou, A. K. Patlolla, D. J. Sutton, "Heavy Metal Toxicity and the Environment" in *Molecular, Clinical and Environmental Toxicology*, A. Luch, Ed. (Springer Basel, 2012), pp. 133–164.

207. A. Matsuura, M. Tsukada, Y. Wada, Y. Ohsumi, Apg1p, a novel protein kinase required for the autophagic process in Saccharomyces cerevisiae. *Gene* **192**, 245–250 (1997).

208. Y. Kamada, *et al.*, Tor-mediated induction of autophagy via an Apg1 protein kinase complex. *J. Cell Biol.* **150**, 1507–1513 (2000).

209. D. J. Klionsky, For the last time, it is GFP-Atg8, not Atg8-GFP (and the same goes for LC3). *Autophagy* **7**, 1093–1094 (2011).